Università degli Studi di Ferrara

DOTTORATO DI RICERCA IN

FARMACOLOGIA E ONCOLOGIA MOLECOLARE

CICLO XVIII

COORDINATORE Prof. Antonio Cuneo

P2X7 expression modulates mitochondrial metabolism

Settore Scientifico Disciplinare MED/05

Dottoranda

Dott. Alba Clara Sarti

Tutore

Prof. Francesco Di Virgilo

Cotutori

Prof. Paolo Pinton

Dott. Massimo Bonora

Anni 2013/2015

CONTENTS

ABSTRACT

P2X7 expression modulates mitochondrial metabolism.

The P2X7 receptor is a trimeric ATP-gated cation channel best known for its ability to cause plasma membrane permeabilization and cell death after prolonged exposure to extracellular ATP. However, recent data show that its brief activation triggers rapid inward cation currents and intracellular signalling pathways associated with a multiplicity of physiological processes such as induction of the inflammatory cascade, cell proliferation and survival. Recently, there has been an increased effort to understand the mechanism by which P2X7 supports energy-requiring cell functions. We previously showed that basal P2X7 expression has a trophic effect on cellular energetics as it increases mitochondrial potential and ATP synthesis, while on the contrary pharmacological P2X7 stimulation causes mitochondrial potential collapse and fragmentation. These findings point to major role for P2X7 in the modulation of mitochondrial metabolism. In the present study we show that P2X7 localizes to the mitochondria especially following activation. Furthermore P2X7 genetic deletion severely impairs mitochondrial respiration, mitochondrial membrane potential and ability to produce ROS. Decreased energy generation impacts negatively on key cell functions such as migration. These observations demonstrate the central role played by P2X7 in the modulation of cellular energy homeostasis and energy-requiring processes.

1. INTRODUCTION

1.1 Purinergic Receptors

The first definition of purinergic receptors was put forward in 1976 (1) followed 2 years later by a proposed basis for distinguish- ing two types of purinoceptor, identified as P1 and P2 (for adenosine and ATP/adenosine diphosphate [ADP], respectively) (2). The purinergic signalling, mediated by multiple receptors called P1 and P2 purinoreceptors upon extracellular stimulation by adenine nucleoside or nucleotide di- or triphosphates respectively, represents very dynamic and plastic mechanisms for controlling a diversity of crucial biological functions of cells and tissues such as cell-to-cell communications, secretory exocytosis, membrane excitability, cell proliferation, cell differentiation, cell adhesion and migration, and cell death. P1 and P2 receptors are expressed in a large number of eukaryotes and particularly at the plasma membrane of virtually every mammalian cell. P1 receptors are seven-transmembrane spanning, (7TM) G-protein coupled receptors and commonly termed adenosine receptors because nanomolar levels of extracellular adenosine physiologically activate them.

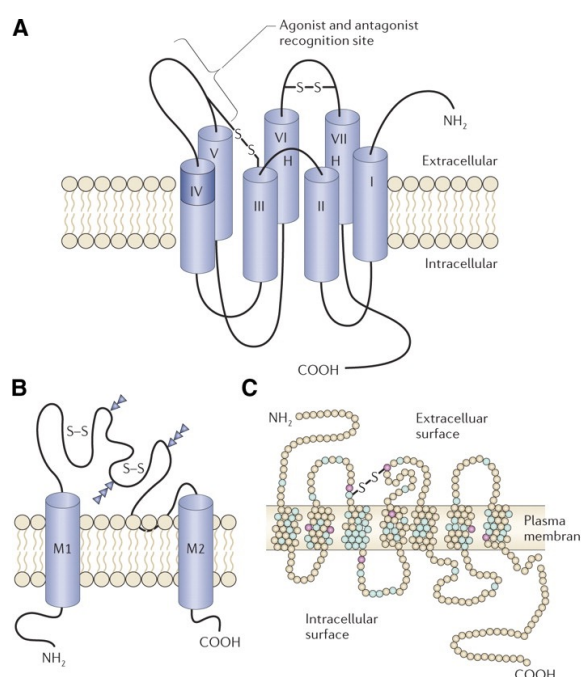**Fig. 1. Membrane receptors for extracellular adenosine and ATP**. **A**: the P1 family of receptors for extracellular adenosine are G protein-coupled receptors (S-S; disulfide bond). **B**: the P2X family of receptors are ligand-gated ion channels (S-S; disulfide bond; M1 and M2, transmembrane domains). **C**: the P2Y family of receptors are G protein-coupled receptors (S-S; disulfide bond). Adopted from Burnstock (2007).

P2 receptor

P2 receptors can be divided into two subfamilies, P2X and P2Y receptors, based on their pharmacology and the different downstream signalling pathways with they are associated (3,4).

P2Y receptors

P2YR belongs to the G-protein-coupled receptor (GPCR) family and contains an extracellular amino terminus, an intracellular carboxy terminus and seven transmembrane-spanning motifs. At present, eight distinct mammalian P2YRs have been cloned and characterized (P2Y1/2/4/6/11/12/13/14R). According to their phylogenetic and sequence divergence, two distinct P2YR subgroups have been proposed. The first group includes the P2Y1/2/4/6/11R subtypes, activates heterotrimeric G proteins of the Gq family, thereby activating phospholipase C and promoting inositol lipid-dependent signaling (**5**). In addition to activating Gq, the P2Y11 receptor also activates Gs and therefore stimulates adenylyl cyclase activity. The second group contains

P2Y12/13/14 receptors, activates Gi/o, thereby promoting inhibition of adenylyl cyclase activity (**6**). The most abundant and best-characterized endogenous ligand for P2YR is the nucleotide ATP. ATP binds to all P2YRs except P2Y6R and P2Y14R. Its binding characteristics exemplify the complexity of P2YR signalling: at low concentrations it is the only native agonist for P2Y11R, but at higher concentrations it functions as a partial agonist for P2Y1R and P2Y13R, or as an antagonist for human P2Y4R or P2Y12R. Other nucleotides, such as ADP, UTP, UDP or UDP-glucose, exhibit more specificity for individual P2YRs. For example, ADP (adenosine 5′-diphosphate) is a better agonist at $P2Y_1$, $P2Y_{12}$ and $P2Y_{13}$ and UDP-glucose (uridine 5'-diphosphate-glucose) activates $P2Y_{14}$ (7,8,9).

P2X receptors

The P2X receptor family is composed of seven members (P2X1, P2X2, P2X3, P2X4, P2X5, P2X6 and P2X7) that are capable to form trimeric ion channels activated by to extracellular adenosine triphosphate (ATP). P2X receptors are formed of two-transmembrane segments (TM1 and TM2) separated by a large extracellular loop including the ATP-binding site. Both the N-terminal and C-terminal ends are cytoplasmic (10,11). P2X receptors constitute functional non-selective cation channels and their activation mediates very rapid cellular effects, generally resulting in a depolarizing inward current due to a large influx of Na^+ and Ca^{2+} into the cytosol at physiological membrane potential and a concomitant efflux of K^+. Besides this direct effect on the membrane

potential, P2X receptors cause large increases in the intracellular Ca^{2+} concentration by activation of voltage gated Ca^{2+} channels as a result of membrane depolarisation (12) and therefore activate intracellular Ca^{2+}-dependent signalling pathways that can have longer-term effects (13). In addition, other signalling pathways may be generated following K^+ efflux (14). Some P2X receptors have also been identified in intracellular compartments, such as the P2X4, which is also localised in the lysosomes of some cells such as macrophages, microglia and endothelial cells (15).

1.2 P2X7 receptor

The P2X7 receptor is very unique member of P2X family by multiple features, from its molecular structure, to its biophysical and pharmacological properties. The P2X7 subunit is a 595 amino acid long with an intracellular N- terminus, two hydrophobic transmembrane domains, an extracellular loop and an intracellular C-terminus (16) (Fig.2). The N- and C-termini of P2X7 comprise amino acids 1-25 and 356-595 respectively. The first and second transmembrane domains comprise amino acids 26-46 and 335-355, repectively.
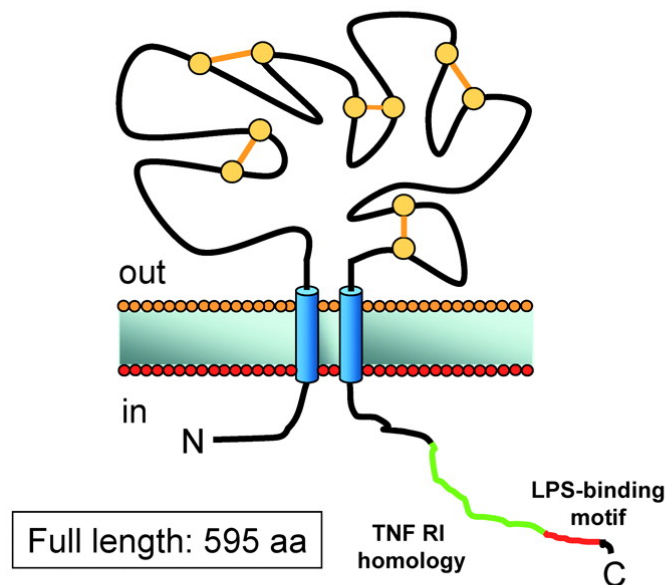
Fig.2. Schematic representation of the P2X7 subunit. The P2X7 protein is a 595 amino acid sequence consisting of an intracellular N-terminus, two hydrophobic transmembrane domains, an extracellular loop and an intracellular C-terminus. Adapted from Adinolfi et al (2006).

The extracellular loop (amino acids 47- 334) comprises the main binding site for ATP and also contains five *N*-glycosylation sites (17), of which Asn^{187}, Asn^{213} and Asn^{241} have been proposed to contribute to P2X7 function (18;19). The most striking difference between the P2X7 receptor and other P2X receptors is the long intracellular COOH terminal (fig. 3A), that endows P2X7 with the ability to generate a non selective membrane pore that allows transmembrane fluxes to cations, nucleotides and other small hydrophilic molecules of MW up to 900 Da (fig 3B). Channel-to-pore transition is hastened by prolonged stimulation with ATP or by stimulation with high (hundred micromolar) ATP concentrations. ATP removal or hydrolysis causes the pore to close. Sustained stimulation of P2X7 receptor by high ATP concentration can lead to cellular death by prolonged pore opening (20). The C-terminus of P2X7 has been implicated in regulating receptor function, sub-cellular localisation, and the initiation of intracellular signalling cascades (21) also through protein–protein interactions, with several membrane proteins including β-actin, receptor-like tyrosine phosphatase and heat shock proteins (22). Truncation of the cytoplasmic tail prevents the channel-to-pore transition (23).
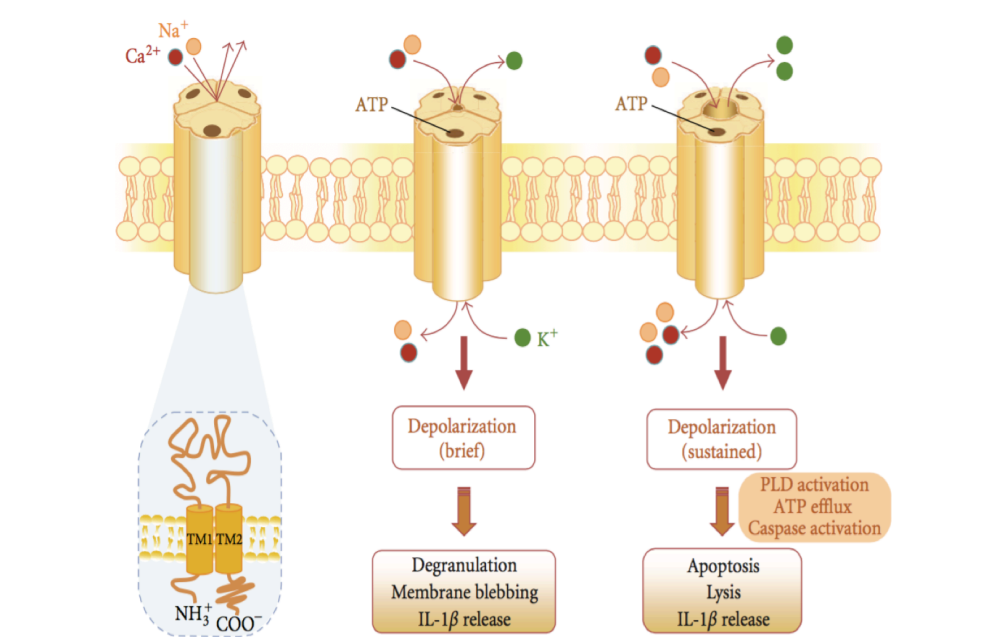
Fig.3 Structure and signaling functions of the P2X7receptor. Each functional P2X receptor is a trimer, with the three protein subunits arranged around a cation-permeable channel pore. Brief ATP activation (<10 seconds) of the P2X7receptor results in rapid and reversible channel opening that is permeable to Na^+, K^+, and Ca^{2+}. Continued stimulation results in the formation of a larger plasma membrane pore, which facilitates the uptake of cationic molecules up to900 Da. Further activation of the receptor in some cell types results in the induction of apoptosis/cell lysis. Adapted from Skaper et al; (2009).

Distribution

P2X7 Receptor was originally cloned from a rat cervical ganglion cDNA library (24), but later work revealed that P2X7 are widely distributed across animal species and ubiquitously present on both excitable and nonexcitable mammalian cell with high expression level in immune cells, such as monocytes, macrophages, dendritic cells, B and T lymphocytes, mast cells and epidermal Langerhans cells (25,26,27,28,29). In particular, the participation of P2X7 is critical in inflammation as this receptor triggers inflammasome and caspase-1 activation with the subsequent releases of the pro-inflammatory IL-1β from Pathogens Associated Molecular Patterns (PAMPs)-primed macrophages and microglial cells (30,31). P2X7 receptors are also found abundantly in brain glial cells (microglia, astrocytes, and Muller cells), bone cells (osteoblasts, osteoclasts, and osteocytes), epithelial cells and endothelial cells (32,33,34,35,36,37), in central and spinal cord neurons (38,39,40), in cells originating from the small intestine, kidney, urinary tract, uterus, and liver (41,42,43), and quite importantly in a variety of tumor cell lines and primary tumors (44) including myeloid leukemic and carcinomas.

Gene, splicing variants and single nucleotide polymorphisms (SNPs)

The human P2X7 is encoded by the *P2RX7* gene located on the locus 12q24.31. The *P2RX7* gene comprises 13 exons. Ten naturally occurring alternative splicing variants have been identified in humans and have been named P2X7A to J. The P2X7A variant is the well-characterised full-length receptor. Among the ten, five splice variants (P2X7B, P2X7C, P2X7E, P2X7G and P2X7J) lack the extended C-terminal intracellular tail typical of P2X7A. The truncated P2X7B seems to display the same pharmacological properties, towards both agonists and antagonists, as the P2X7A and to be functional as an ion channel but it is unable to trigger membrane permeabilisation to large hydrophilic molecules. The P2X7I variant is generated by a 5-intronic splice site and is responsible for a null allele, unable to promote membrane permeabilization. The P2X7J variant consists of 258 amino acid residues and compared to the full-length variant lacks the distal 337 amino acids corresponding to the entire intracellular carboxyterminal end, the second transmembrane domain and the distal part of the extra-cellular loop. This variant, which is unable to induce pore formation, has been shown to oligomerise with the full-length P2X7A receptor and to act as in dominant negative fashion (45,46). This variant was identified in cervical cancer cells and proposed to be a new marker for cervical cancer (47).

Splice variants have also been identified in rodents. The first identified was termed P2X7k, resulting from alternative exon 1 usage in the rodent P2X7 gene. This variant is fully functional and

bears a different N-terminal and first transmembrane domain conferring an increased sensitivity to agonists and slower deactivation kinetics compared to the human variants (48). There are also two variants, P2X7 13B and P2X7 13C, that are truncated in the C-terminus due to an alternative splicing in the exon 13. These two variants displayed a low plasma membrane expression, low channel function and no membrane permeabilisation (49).

Therefore, depending on the given splice variant, the biophysical properties, its surface expression, as well as interacting molecules and downstream signalling pathways, functional responses could be quite different, with relevant pathophysiological implications.

The human P2X7 receptor is highly polymorphic, and numerous single nucleotide polymorphisms (SNPs) have been identified in the recent years. About 150 non-synonymous SNPs (NS-SNPs) have been reported. Some of these SNPs have been the focus of attention following genetic association studies suggesting for their possible role in conferring susceptibility to a variety of diseases (50,51).

P2X7 receptor pharmacology and ligands

Agonist:
ATP is the physiological P2X7R ligand. Ten- to 100-fold higher ATP concentrations for P2X7 activation are needed compared to the other P2X receptors. The half-effective ATP concentration (EC$_{50}$) required to activate the P2X7 receptor is ~100 μM, with maximal activation obtained at 300 μM ATP (52). The ATP analog, 2',3'-(4-benzoil)-benzoil-ATP (BzATP), is 10-30 times more potent than ATP, and currently is the most widely used P2X7 receptor agonist. However, BzATP is not absolutely selective for P2X7 as it can also activate P2X1 and P2X3 receptors (53).

Antagonist:
The first generation of antagonist for P2X7 receptor were generally non-specific as they also inhibited other member of P2X family and in some case P2Y receptors as well. These early compound include Reactive Blu2, surmarin and Brilliant Blu (BBG) and pyridoxal phosphate-6-azophenyl-2-4-disulfonic acid (PPADS), periodate-oxidized ATP (oATP), and 1-[N,O-bis(5-isoquinolinesulfonyl)-N-methyl-l-tyrosyl]-4-phenylpiperazine (KN-62) (54,55,56).

Oxidized ATP (oATP) is widely used as a P2X7 antagonist, but it may also inhibit other P2X receptors. In fact oATP bears a highly reactive aldehide group that can form a Schiff base with unprotonated lysine close to any accessible ATP-binding site. Thus, oATP causes a covalent, irreversible, modification of the receptor. (57,58,59).

1-[N,O-bis(5-isoquinolinesulfonyl)-N-methyl-L-tyrosyl]-4- phenylpiperazine (KN-62), is a potent, non-competitive, human P2X7 antagonist (60) initially identified as calmodulin-kinase II inhibitor. KN-62 was characterised as the first potent human P2X7 inibitor with an IC50 of 40-100 nM. (61). KN-62 is inactive at the rat P2X7 homolog (62). More recently, a family of highly selective and potent KN-62 pharmacologic analogs with a strong interleukin-1β (IL-1β)-blocking activity has been synthesized (63).

Second generation P2X7 antagonists resolved many problems typical of first generation compounds, such as rapid degradation when used in vivo or predicted poor pharmacokinetics (64,65). The tetrazolylmethylpyridine based compounds *A- 438079* (66), a competitive antagonist with in vivo antinociceptive activity in neurophatich pain, and the adamantyl derivative *AZ10606120*, are recent, potent, and selective P2X7 competitive antagonists active at both the human and rat P2X7 receptor.

Recently, *A740003*, a cyanoguanidine derivate, was shown to have antinociceptive activity in neurophatic pain and inflammatory animal models (67,68), and to prevent invasiveness and metastatic spreading in models of MDA-MB-435 breast cancer and A549 lung cancer (69,70). Pharmacological studies are made more difficult by the different species specificity of P2X7 antagonists (Tab.1).

TABLE 2
Antagonist profiles of mammalian P2X7

Species	IC$_{50}$									References
	PPADS	BBG	Reactive Blue	KN-62	A438079	A740003	AZ10606120	AZ11645373	JNJ-47965567	
						μM				
Human	1.2	1.9	5.4	0.2	0.9	0.09	0.003	0.05	0.005	Donnelly-Roberts et al., 2009; Michel et al., 2009; Roman et al., 2009; Bhattacharya et al., 2013
Rhesus macque	N.D.	N.D.	N.D.	0.1	0.3	N.D.	0.004	0.02	0.003	Bradley et al., 2011b; Bhattacharya et al., 2013
Dog	N.D.	0.05	N.D.	0.01	3.9	N.D.	0.06	0.04	0.005	Michel et al., 2009; Roman et al., 2009; Bhattacharya et al., 2013
Rat	1.2	0.6	2.8	>100	0.1	0.1	0.03	>20	0.063	Donnelly-Roberts et al., 2009; Michel et al., 2009; Bhattacharya et al., 2013
Mouse (BALB/c)	4.9	0.2	21	0.2	0.6	0.7	0.6^a	1.6^a	0.03^a	Donnelly-Roberts et al., 2009; Michel et al., 2009; Bhattacharya et al., 2013
Mouse (C57BL/6)	40	0.5	18	0.6	0.6	1.7	0.6^a	1.6^a	0.03^a	Donnelly-Roberts et al., 2009; Michel et al., 2009; Bhattacharya et al., 2013
Guinea pig	0.2	0.02	N.D.	0.1	N.D.	N.D.	N.D.	1.2	N.D.	Fonfria et al., 2008; Michel et al., 2009

N.D., not determined.
^{a}Mouse strain not disclosed.

Tab. 1 Antagonist profiles of mammalian P2X7. Bartlett et al; (2014)

P2X7 can also be inhibited by various cations, such Ca^{2+} and Mg^{2+}, Zn Cu and protons (71,72), either directly acting on the receptor, or indirectly via the chelation of the free acid form of ATP (or ATP^{4-}) by Ca^{2+} and Mg^{2+}, thus limiting the amount of available ATP (73). The mechanism of inhibition by the other divalent cations remains unclear. Extracellular Na^{2+} ions can also reduce P2X7 receptor function. Michel *et al*. (74) have shown that the potency of BzATP for human P2X7 is approximately 20-fold higher in sucrose medium (containing nominal amounts of Na^{2+}) compared to NaCl medium. Similarly, maximal response and efflux rates of P2X7 to ATP and BzATP are higher in KCl medium compared to NaCl medium (75,76).

Several major pharmaceutical companies, such as Pfizer (77) GlaxoSmithKline (78) and Abbott have active programs for the development of novel and potent drug-like P2X7 antagonists. P2X7 antagonists are in Phase I/II clinical trials for treatment of rheumatoid arthritis, osteoarthritis, chronic obstructive pulmonary disease and inflammatory bowel disease.

Molecular and cellular consequence of P2X7 Activation on cells

Activation of the P2X7 request high concentration of extracellular ATP ($EC_{50} \approx 100$ μM) in contrasts with much lower activation thresholds of the other six members of the P2X family($EC_{50} \approx$ 10 μM) (79). Under physiological conditions, such high concentrations are seldom if ever found. On the contrary, increasing evidence show that at sites of trauma, infection, inflammation or at tumor sites extracellular ATP concentrations as high as 100-300 uM are often reached. P2X7 receptor activation is associated with two different membrane permeability states: a small non-selective monovalent and divalent cation conductance, activated by brief agonist stimulation, and an increased non-selective membrane permeability to high MW aqueous solutes activatd after prolonged and repetitive agonist stimulation (80). Fluorescent dyes such as ethidium bromide (EthBr) (314 Da) and YO-PRO-1 (375 Da) are routinely used to assay the increase in the plasma membrane permeability, and therefore the pore properties of the receptor (81). Pore formation has also been measured electrophysiologically as a progressive increase in the permeability of the large cation NMDG (82). The molecular basis of this bifunctional behaviour is not clear. Two different models have been proposed:

Model 1 Single structure: The large pore might be intrinsic to the receptor, which initially forms a channel that undergoes a dilatation and, therefore, a "channel-to-pore" transition, upon sustained activation. Different studies underline the importance of P2X7 carboxyl tail in the formation of large pore, Adinolfi and colleagues showed that a naturally-occurring truncated P2X7 splice variant, isoform B (P2X7B) is able to form a channel after ATP stimulation, but is unable to switch

to pore formation (83). In this model, single structure, channel and pore are part of the same structure and many agents, for example Brilliant Blu G, block both for example Brilliant Blu G (84).
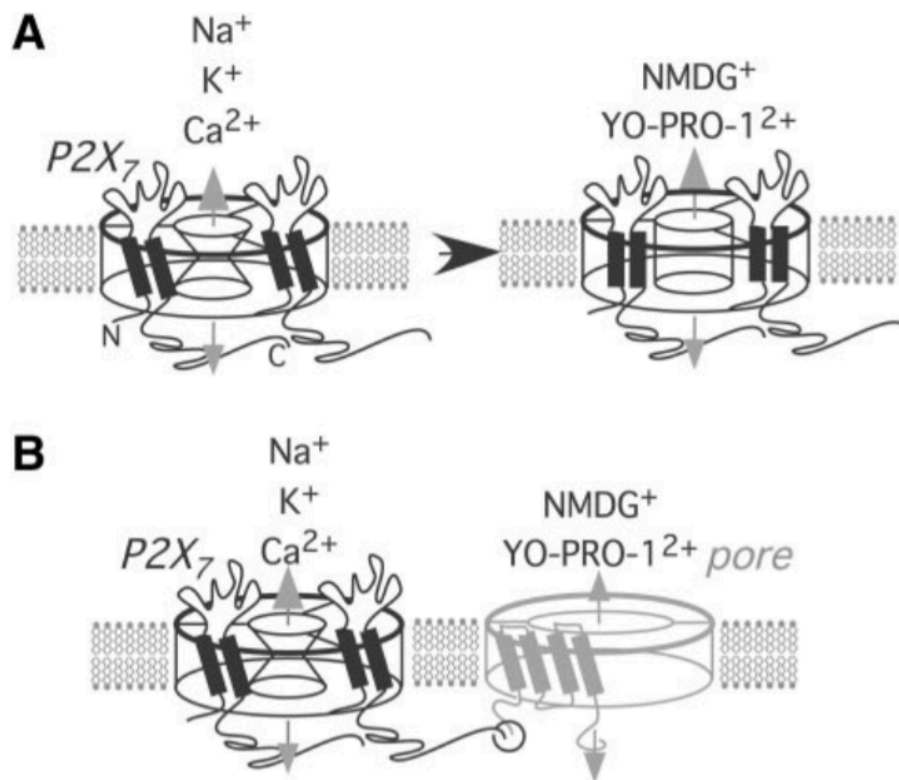
Fig. 4. Schematic illustration of two contrasting mechanisms for the time-dependent increase in permeability observed for P2X7 receptors. **A**: pore dilatation. Several subunits (two indicated) form a channel permeable to small cations. This opens within milliseconds after binding ATP but undergoes a conformational change (arrow) that is associated with dilatation of the ion-conducting pathway. **B**: activation of a distinct channel protein. The P2X7 receptor (left) forms a channel permeable to small cations, as in A. The activated receptor interacts with (directly, as indicated by circle, or through further intermediate proteins) and opens a distinct channel protein (shown in gray), which is permeable to larger cations including fluorescent dyes. Adapted from North (2002).

Model 2 Channel and large pore: In this case the "channel" and the "pore" are separate molecular entities. P2X7 Receptor is the "channel", which allows small cation fluxes, and after its activation initiates the formation of separate pore-forming protein complexes in the membrane. The hemichannels pannexin-1 (Panx1) was proposed to be the "pore" responsible for permeability to larger molecules (85). At present, there is little evidence supporting the "channel and large pore" mechanism as P2X7-mediated pore formation alos occurs in cells from pannexin$^{-/-}$ mice. Whatever is the mechanism, P2X7 receptor activation by high ATP concentrations generally leads to dramatic cellular events such as membrane permeabilisation and blebbing, loss of asymmetric distribution in

13

phosphatidyl serine, cell swelling, increase of intracellular Ca^{2+}, loss of mitochondrial potential. These changes are reversible if agonist application is short lasting (less than 30 min), while prolonged stimulation leads to cell death (86).

P2X7 activation induces downstream signalling events

The P2X7 receptor is associated with different signalling pathways. These events including the release of metalloproteases, proinflammatory cytokine, such as IL-1β, reactive oxygen and nitrogen species, formation of phagolysosomes intracellular pathogen killing, apoptosis, cell proliferation, differentiation and production of IL-2, activation of innate immune responses, regulation of bone resorption and mineralization, fast synaptic transmission, pain (87,88,89,90). Maturation and release of IL-1β is one of the most thoroughly investigated P2X7-dependent responses, and P2X7-dependent K^+ efflux is commonly accepted as the most important signal activating the NLRP3 inflammasome complex. P2X7 receptor is generally known for its ability to induce cell death when overstimulated, however low-level stimulation generates a trophic stimulus that promote cell proliferation. In fact its activation has been correlated with the aggressive form of B-cell chronic lymphocytic leukemia, where a several-fold higher P2X7 expression level is found compared to a lymphocytes from healthy subjects. Furthermore Verderio and co-workers (91) showed that P2X7 support growth in microglia cell clones and in primary microglia and Monif and coworkers (92) provided evidence that the trophic effect of P2X7 is mediated only by functional receptor expressing the pore function, and not by a P2X7R mutant (P2X7R-G345Y) with intact channel but altered pore function. For this dual role, cell death or cell, the P2X7 receptor is attracting interest in normal and neoplastic cell growth (93,94).

P2X7 activation induces cell proliferation

Since the P2X7 receptor is generally known for its ability to trigger cell death (95,96,97), a role in cell proliferation would seem a nonsense, but there is clear evidence to support this claim. Early proof to support a trophic role for P2X7 was generated in P2X7-transfected leukemic K562 and LG14 cell lines, normal and leukemic T- and B-lymphocytes and P2X7-transfected human HEK293 cells. (98,99,100,101). The molecular basis underlying this process is under investigation. Our laboratory (105) showed that HEK-293 cells transfected with the P2X7 receptor exibited higher resting concentrations of mitochondrial Ca^{2+} and larger releasable intracellular Ca^{2+} stores. The elevated intramitochondrial Ca^{2+} stimulated NADH oxidation and ATP production via oxidative phosphorylation. This increased intracellular ATP content facilitated cell survival and growth. In a

second study we showed that P2X7 expression in HEK-293 cells increased endoplasmic reticulum Ca^{2+} and activated the nuclear factor of activated T-cells (NFATc1) to enhance cell survival and protect cells from apoptosis (106). These findings pointed to a link between P2X7 and mitochondria. Close scrutiny of the effects of P2X7 expression on mitochondrial physiology revealed that mitochondrial membrane potential was 20-30 mV more negative in P2X7- than in mock-transfected or wt control cells. The hyperpolarized mitochondrial potential was entirely dependent of $P2X_7$ function as it returned to control values following addition of oATP or apyrase, or chelation of extracellular Ca^{2+}. Mitochondrial Ca^{2+} in P2X7-transfected cells turns out to be at least twice as high as in mock-transfected or wt cells. Higher intramitochondrial Ca^{2+} is fully dependent on influx across the plasma membrane as it reverts to normal level upon chelation of extracellular Ca^{2+} or addition of apyrase . This finding, together with the observation that P2X7-transfected cells have a thicker mitochondrial network (105), focused attention on the mitochondria, a crucial organelle for intracellular ion homeostasis and energy metabolism.
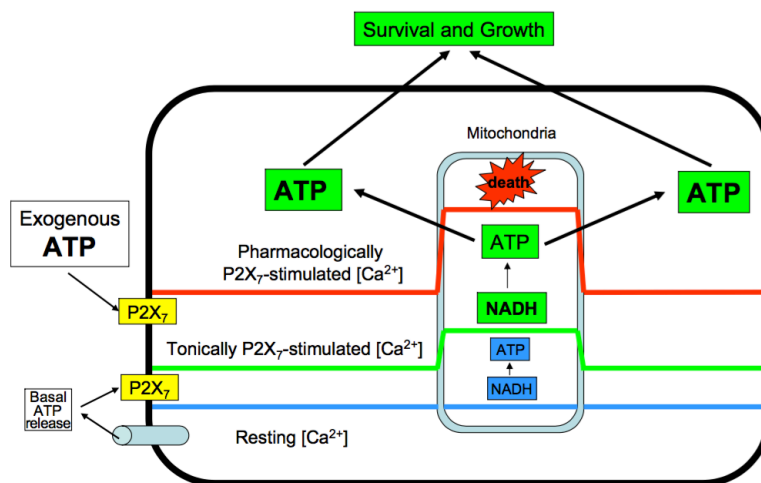
Fig. 5 Schematic rendition of the differential effects of P2X7- stimulated intracellular Ca^{2+} increases. ATP is continuously released into the extracellular environment via as yet poorly characterized pathways. This causes tonic stimulation of the P2X7 receptor leading to moderately increased cytoplasmic Ca^{2+}, which translates into an elevation of intramitochondrial Ca^{2+} from 0.1–0.2 μM (blue line) to about 1.5–2.0 μM (green line). Such a Ca^{2+} increase stimulates NADH synthesis and ATP production via oxidative phosphorylation. Increased cellular ATP content then facilitates cell survival and growth. However, in the presence of massive amounts of extracellular ATP, the P2X7 receptor is overstimulated, this leads to uncontrolled Ca^{2+} influx and unchecked increase in the cytoplasm as well as the mitochondria (red line), with catastrophic consequences on the cell. Adapted from Di Virgilio et al; (2009).

P2X7 activation induces reactive oxygen species production

Several studies have indicated a role for P2X7 in reactive oxygen species (ROS) production. Lenertz, in 2009,(108) showed that P2X7 mediates ROS production in primary human monocytes and RAW264.7 macrophages, and that generation of ROS most likely involves activation of ERK1/2 and the NADPH oxidase complex. These findings were consistent with the work published one year later by Noguchi (109) who demonstrated that P2X7-induced ROS production in RAW264.7 macrophages is sensitive to the NADPH oxidase inhibitor apocynin and can be prevented by lowering the expression of the NADPH subunit gp91phox in these cells. Moreover, this study demonstrated that ROS formation plays a role in P2X7-induced apoptosis of RAW264.7 macrophages.

1.3 Pattern recognition receptors (PRRs)

The mammalian immune system defends against internal and external threats using innate immunity and adaptive immunity (110). The innate immune system engages an array of germline-encoded pattern-recognition receptors (PRRs) to detect invariant microbial motifs. PRRs are expressed mainly innate and adaptive immune cells such as monocytes, macrophages, neutrophils, dendritic cells (DCs) (111,112). They present antigens to the adaptive immune system to generate long-lasting protection (113). Microbe- or pathogen-associated molecular patterns (MAMPs, PAMPs) , which are antigens common of pathogens (114,115), are normally recognized by four different classes of PRRs: Toll-like receptors (TLR), C-type lectin receptors (CLR),which scan the extracellular milieu and endosomal compartments, the RNA-sensing RIG- like helicases (RLHs) and NOD-like receptor (NLR) which can also recognize host-derived indicators of cellular damage, danger associated molecular patterns, DAMPs (116,117). The more recent discovery of NLRs as cytosolic PRRs suggested that microbes evading extracellular surveillance encounter a second line of recognition in the host cytosol The signal transduction from these receptors converges on a common set of signaling modules, often including the activation of the NF-kB and AP-1 transcription factors that drive proinflammatory cytokine/chemokine production and members of the IRF transcription factor family that mediate type I interferon (IFN)-dependent antiviral responses. One of the most important pro-inflammatory cytokine, IL-1β is released in mature form after inflammasome activation.

NLR family

The NLR family is one of the best-characterized PRR families composed by 22 and 34 members in humans and mice, respectively (118).The NLR proteins are commonly organized into three domains, a C-terminal leucine-rich repeat (LRR) domain, an intermediate nucleotide binding and oligomerization domain (NOD, also called NACHT domain), and a N- terminal pyrin (PYD), caspase activation and recruitment domain (CARD) or a baculovirus inhibitor of apoptosis repeat domain (BIR). The N-terminal domains, mediate protein–protein interactions. The LRR domains of these proteins are hypothesized to interact with putative ligands and play a role in autoregulation of these proteins. The NACHT domain can bind to ribonucleotides, which regulates the self-oligomerization and inflammasome assembly (119). NLR family can be divided into five subfamilies: NLRA, NLRB, NLRC, NLRP, and NLRX. The NLRA (NLR family acidic domain containing) group contains only CIITA, which present a CARD domain in the amino terminus, and has been reported to regulate genes involved in inflammation (120). The NLRB (NLR family BIR domain containing) subfamily, is characterized by the presence of a BIR at the amino terminus, and the members are named NAIP, NLR family-apoptosis inhibitory protein. These proteins are specialized in detect bacterial flagellin and contributed to NLRP4 function, infact Naip proteins do not seem to be able to assemble in an individual inflammasome complex. The NLRX, consists in one member NLRX1 with a mitochondria-targeting amino terminus. During infection with RNA viruses, the association between NLRX1-MAVS (mitochondrial antiviral signaling protein)are broken and MAVS is then able to stimulate IFN I production (121). The NLRC (NLR family containing a CARD domain) subfamily numbers five members: NLRC1 (NOD1), NLRC2 (NOD2), NLRC3, NLRC4 (ICE protease-activating factor, IPAF), and NLRC5. NOD1 and NOD2 both recognize breakdown products of bacterial cell walls (mesodiaminopimelic acid and muramyl dipeptide [MDP], respectively) and, upon ligand sensing, oligomerize and recruit RIP2 via CARD-CARD interactions. Assembly of NOD1 and NOD2 signalosomes ultimately culminates in the activation of the NF-kB transcription factor, which drives proinflammatory gene regulation (122). Mutations in NOD2 are associated with human inflammatory diseases such as Crohn's disease and Blau syndrome (123). The largest NLR subfamily is the NLRP (NLR family pyrin domain containing) subfamily, which consists of 14 human (NLRP1–14) and 20 mouse members, respectively (124). NLRP1 is the only NLRP protein containing a contains a C-terminal extension that harbours a CARD domain, which can interact directly with procaspase-1 and bypass the requirement for ASC, although ASC inclusion in the complex augmented human NLRP1 inflammasome activity (125). Unlike human NLRP1, murine NLRP1 lack functional PYD domains and are predicted to be unable to interact with ASC. Indeed, ASC is dispensable for caspase-1

activation by NLRP1b in mouse macrophages (126). In addition to caspase-1, NLRP1 also interacts with caspase-5, which may contribute to IL-1β processing in human cells (127). The exact mechanisms of NLRP1 activation remain obscure, but, as for NLRP3, K+ efflux appears to be essential (128). NLRP3 (see below). NLRP4 was known d as an inhibitor of autophagy via its binding to Beclin while NLRP6 seems to be implicated in intestinal bacterial homeostasis. NLRP5 and NLRP7 are involved in embryogenesis, and NLRP7 was located in inflammasome complex assembly in response to microbial acylated lipopeptides, thus causing IL-1β and IL-18 secretion and restricting bacterial replication (129). NLRP9 was recently implicated in the pathogenesis of systemic-onset juvenile idiopathic arthritis (130) whereas NLRP10 in recent data was described modify DC migration from inflammatory sites (131). NLRP12 was responsible for NF-kB inhibition and in mouse seems to be implicated in intestinal homeostasis and preventing
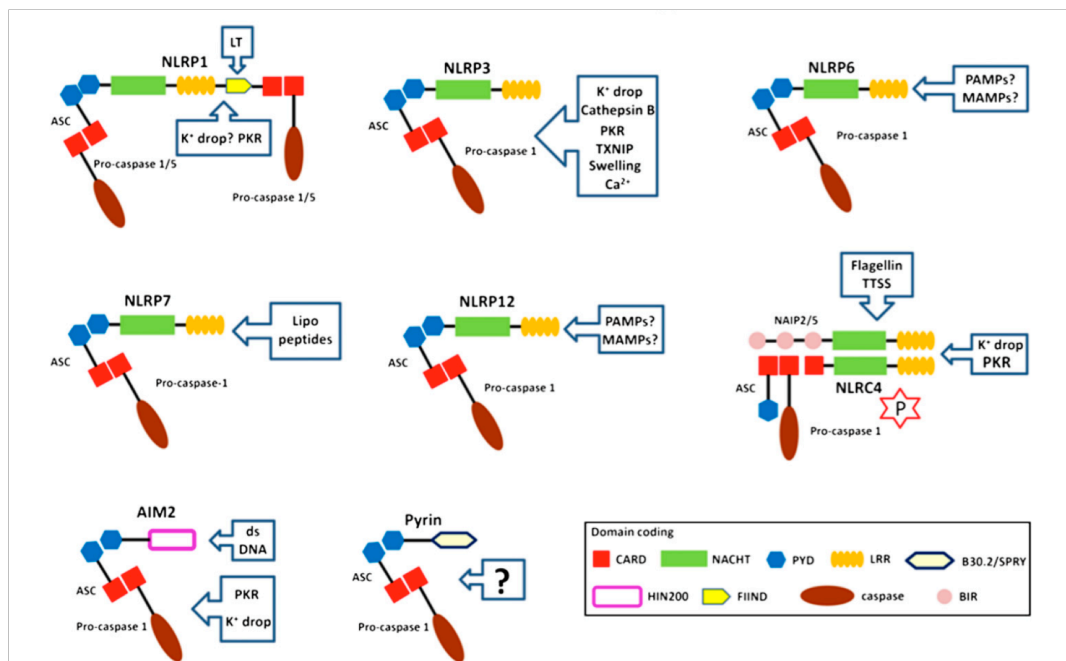
carcinogenesis (132). NLRP14 is expressed in the testis, and involved in spermatogenesis (133). To date the functions of NLRP8, NLRP11, and NLRP13 are not still clear.

Fig. 6. Inflammasome subtypes. Inflammasome subtypes are classified according to their scaffold components. Adapted from Di Virgilio (2013).

1.4 NLRP3

The NLRP3 inflammasome is the most important molecular machine responsible of maturation and release of IL-1β and for this the most fully characterized inflammasome. NLRP3 consists in different domain: a central NACHT, a series of C-terminal LRRs, and a N-terminal PYD. The

NACHT domain allows ATP-dependent oligomerization, and the LRR domain is responsible for PAMP/MAMP /DAMP sensing and autoinhibition. PYD mediates protein-protein interaction. It is thought that LRRs maintain NACHT domains in inhibited state thus preventing oligomerization and activation with out signal. Keeping Nlrp3 in an inactive state may be helped by interaction with the chaperone proteins SGT1 and HSP90 (134). NLRP3 is activated upon exposure to whole pathogens, as well as a number of structurally diverse PAMPs, DAMPs, and environmental irritants. Whole pathogens demonstrated to activate the NLRP3 inflammasome include the fungi *Candida albicans* and *Saccharomyces cerevisiae* (135), bacteria that produce pore-forming toxins, including *Listeria monocytogenes* and *Staphylococcus aureus* (136), and viruses such as Sendai virus, adenovirus, and influenza virus (137,138).

Matzinger's 'Danger Model' (140) proposes that germline-encoded PRRs have evolved not only to respond to foreign antigens but also to mediate immune responses to endogenous danger signals, this idea is increasingly supported by evidences that NLRP3 inflammasome can be activated by host-derived molecules, indicators of cellular danger or stress (141). A number of host-derived molecules indicative of injury activate the NLRP3 inflammasome, including extracellular ATP (142) and hyaluronan (143) that are released by injured cells. Fibrillar amyloid-b peptide, the major component of Alzheimer's disease brain plaques, also activates the NLRP3 inflammasome (144). The NLRP3 inflammasome also detects signs of metabolic stress, including elevated extracellular glucose (145) such as that occurring in metabolic syndrome, and monosodium urate (MSU) crystals that form as a consequence of hyperuricemia in the autoinflammatory disease gout (146). The extraordinary number of NLRP3 activators suggests that it may be a general detector of cellular stresses resulting from sterile trauma, intrinsic metabolic disturbances or pathogen infection.

Models for NLRP3 Activation

The NLRP3 inflammasome is assembled when the amino-terminal PYD of NLRP3 engages in homotypic interactions with the PYD of ASC to recruit caspase-1. However, the mechanisms associated with activation of the NLRP3 inflammasome continue to be debated. This inflammasome is activated by bacterial, viral, and fungal pathogens, pore-forming toxins, crystals, aggregates such as β-amyloid, and DAMPs such as ATP and hyaluronan (147). It is generally agreed that detection of such a diversity of agents cannot be direct. Instead, NLRP3 is thought to monitor some host-derived factor that is altered by these agents. Several hypotheses for NLRP3 activation have been formulated. They can be summarized as follows: NLRP3 is activated by: (1) K^+ efflux (148), (2) the production of mitochondrial reactive oxygen species (149), (3) the cytosolic release of lysosomal

cathepsins (Fig.7) (150). A single unifying event has not emerged because some of these events do not occur with all NLRP3 activating agents, or they are associated with multiple inflammasomes, or their occurrence is contested (151,152,153).

First model "P2X7-K⁺ efflux": P2X7 cation channels activation by ATP induces the rapid dissipation of normal trans-plasma membrane K+, Na+, and Ca2+ gradients (154). This event is understood to cause local changes in the cytoplasmic ionic strength sufficient to trigger the conformational changes in NLRP3 that, by relieving LRR-mediated inhibition of PYD and by unmasking NACHT, drive inflammasome assembly. Extracellular ATP has been shown to be required for NLRP3 inflammasome activation by several bacteria or bacterial toxins that can cause ATP release (155,156,157). ATP/P2X7-dependent caspase-1 activation and IL-1β secretion is abrogated in either ASC-null (158) or NLRP3-null (159) macrophages primed with LPS. Activation of the NLRP3 inflammasome by P2X7R is likely mediated by altered cytoplasmic [K+]/[Na+] homeostasis, as well as by the increased intracellular [Ca2+]. Changes in mitochondrial function and generation of mitochondria-dependent reactive oxygen species (ROS) might also have a role. Recent studies have demonstrated that P2X7 stimulation triggers rapid release of oxidized mitochondrial DNA (mitoDNA) into the cytosol whereby the mitoDNA facilitates (possibly by direct binding to NLRP3) assembly of active NLRP3/ASC/caspase-1 complexes (160,161). Moreover, P2X7 activation additionally stimulates the rapid co-release of active caspase-1, a 60 kDa tetrameric complex, (162) as well as the ASC inflammasome scaffolding protein.
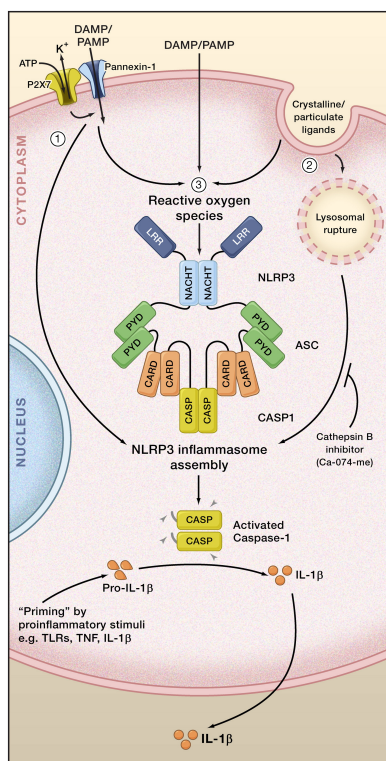
Fig. 7 NLRP3 Inflammasome Activation Three major models for NLRP3 inflammasome activation: (1) The NLRP3 agonist, ATP, triggers P2X7-dependent pore formation, an efflux of K⁺, which was sense from NLRP3. (2) Crystalline or particulate NLRP3 agonists are engulfed, and their physical characteristics lead to lysosomal rupture. The NLRP3 inflammasome senses lysosomal content in the cytoplasm, for example, via cathepsin- B-dependent processing of a direct NLRP3 ligand. (3) All danger-associated molecular patterns (DAMPs) and pathogen-associated molecular patterns (PAMPs), including ATP and particulate/crystalline activators, trigger the generation of reactive oxygen species (ROS). A ROS-dependent pathway triggers NLRP3 inflammasome complex formation. Caspase-1 clustering induces autoactivation and caspase-1-dependent maturation and secretion of proinflammatory cytokines, such as interleukin-1b (IL-1β) and IL-18. Adapted from Tschopp et al; (2010)

*Second model "lysosomal damage:*A second model was proposed for activators that form crystal-line or particulate structures, such as MSU, silica, asbestos, amyloid-b, and alum, wherein engulfment of these agonists by phagocytes leads to lysosomal damage, resulting in cytosolic release of lysosomal contents that are somehow sensed by the NLRP3 inflammasome. A role for the lysosomal protease, cathepsin B, in activation of a direct NLRP3 ligand was suggested in this model (163,164). However, cathepsin B-deficient macrophages exhibit normal caspase-1 activation and IL-1β maturation in response to particulate NLRP3 agonists (165), implicating off-target effects of the cathepsin B inhibitor, as was recently suggested for NLRP1 (166).

Third model "ROS generation": All NLRP3 agonists trigger the generation of ROS, and this common pathway engages the NLRP3 inflammasome. The production of ROS represents one of the most evolutionarily conserved pathways of response to infection or injury. In support of this model, all NLRP3 agonists tested, including ATP and particulate activators, induce ROS and ROS blockade by chemical scavengers suppresses inflammasome activation (167,168,169,170). Mechanisms directing ROS-dependent NLRP3 inflammasome activation remain to be characterized in detail; however, a recent report implicates a ROS-sensitive NLRP3 ligand, thioredoxin-interacting protein (TXNIP/VDUP1), in NLRP3 activation. Thioredoxin (TXN) belongs to a family of small redox-sensitive ubiquitous proteins found in many organisms, from bacteria to animal cells. TXN participates in the formation of a network of redox signaling pathways crucial to the regulation of cell metabolism, proliferation, differentiation, and apoptosis (171). ROS generation causes dissociation of TXN from TXNIP, which is thus free to interact with NLRP3 and trigger inflammasome assembly (172). It is possible that ROS act at multiple levels in NLRP3 inflammasome activation, i.e., at the level of NLRP3 gene expression and as final triggers of inflammasome activation (173).

Regulation of Inflammasome and IL-1β

IL-1β is a primary proinflammatory cytokine whose local and circulating levels are tightly regulated to prevent aberrant activation of pathways that can lead to chronic inflammatory diseases (174). In response to various pathogen-associated molecular pattern (PAMP) molecules that target toll-like receptors (TLR), IL-1β accumulates as a biologically inactive 33 kDa procytokine (proIL-1β) in the cytoplasm of monocytes and macrophages. Conversion to the biologically active 17 kDa form requires proteolytic maturation by caspase-1 which itself is regulated by the assembly of inflammasomes. Although PAMPs, such as LPS, stimulate rapid toll-like receptor (TLR)-dependent transcription and translation of proIL-1β, they elicit only modest production of mature IL-1β due to inefficient assembly of active caspase-1 inflammasomes. However, when PAMP-primed

macrophages are additionally stimulated with extracellular ATP, they rapidly release large amounts of mature IL-1β at rates up to 100 times faster than with PAMP exposure alone (175,176). Moreover macrophages isolated from mice depleted of ASC or NALP3 are unable to mature and secrete IL-1β in response to ATP. Changes in intracellular ionic concentration seem to induce conformational modification at inflammasome and that enables NLRP3 activation. There is evidence that changes in ionic strength might trigger the processing and activation of isolated pro-casp-1 (177).

1.5 Mitochondrial structure

Mitochondria are organelles with extremely complex structures and functions. They are derived from an a-proteobacterium-like ancestor, due to an ancient "invasion" that occurred more than a billion years ago (178). The acquisition of mitochondria (and plastids) was a key event in the evolution of the eukaryotic cell, supplying it with bioenergetic and biosynthetic factors.

Mitochondria are made of an outer membrane (OMM), mostly permeable to ions and metabolites up to 10 kDa, a highly selective inner mitochondrial membrane (IMM), characterized by invaginations called cristae, and the mitochondrial matrix. The space between OMM and IMM referred to as the intermembrane space (IMS). The IMM is further subdivided into two distinct compartments: the peripheral inner boundary membrane and the cristae (179). Cristae are not simply random folds, but rather internal compartments formed by profound invaginations originating from very tiny "point-like structures" in the inner membrane. These narrow tubular structures, called cristae junctions, can limit the diffusion of molecules from the intra-cristae space towards the IMS, thus creating a microenvironment where mitochondrial electron transport chain (ETC) complexes (as well as other proteins) are hosted and protected from random diffusion. The inner boundary membrane is enriched with structural proteins and components of the import machinery of mitochondria (180).

Mitochondrial morphology in living cells is heterogeneous and can range from small spheres to interconnected tubules (181). This heterogeneity results from the balance between fusion and fission, and represents a process termed mitochondrial dynamics (182). Growing evidence indicates that mitochondrial morphology is critical for the physiology of the cell and changes in mitochondrial shape have been related to many different processes such as development, neurodegeneration, calcium (Ca^{2+}) signalling, ROS production, cell division, and apoptotic cell death (183). Mitochondrial shape is controlled by the recently identified "mitochondria-shaping proteins", which regulate the fusion-fission equilibrium of the organelle. In mammals, key components of the fusion machinery include the homologues MFN1 and MFN2 (184). The only dynamin-like GTPase currently identified in the IMM is OPA1, a fusion protein which is mutated in dominant optic atrophy (DOA), the most common cause of inherited optic neuropathy. Post-transcriptional mechanisms, including proteolytic processing, tightly regulate OPA1 activity. In mammalian cells, mitochondrial division is regulated by DRP1 and FIS1 (185,186). The large GTPase DRP1 is a cytosolic dynamin-related protein whose inhibition or downregulation results in a highly interconnected mitochondrial network (187). The same phenotype is caused by downregulation of FIS1 (188), a protein of the OMM, proposed to act as a mitochondrial receptor for DRP1 (189). For example, mitochondrial dynamics seem to influence production of ROS and cellular longevity. DRP1-dependent fragmentation of the mitochondrial reticulum is a crucial component for accumulation of ROS in pathological conditions (190). How mitochondrial fission is required for ROS production and lifespan remains unclear, although a link between the two

processes seems plausible. Hence, factors other than mitochondrial metabolism *per se* could have a role in the pathogenesis of ROS-related diseases (191). Interestingly, many ROS (as well as Reactive Nitrogen Species, RNS) sources and targets are localized in the mitochondria or ER and are relevant for different pathways (192).

Mitochondria are the site for major energy production

Within cells, energy is provided by oxidation of "metabolic fuels" such as carbohydrates, lipids and proteins. It is then used to sustain energy-dependent processes, such as the synthesis of macromolecules, muscle contraction, active ion transport or thermogenesis. The oxidation process results in free energy production that can be stored in phosphoanhydrine "high-energy bonds" within molecules such as nucleoside diphosphate and nucleoside triphosphate (*i.e*., adenosine 5' diphosphate and adenosine 5' trisphosphate, ADP and ATP, respectively), phosphoenolpyruvate, carbamoyl phosphate, 2,3-bisphosphoglycerate, and other phosphates like phosphoarginine or phosphocreatine. Among them, ATP is the effective central link—the exchange coin—between energy producing and the energy demanding processes that effectively involve formation, hydrolysis or transfer of the terminal phosphate group.

In general, the main energy source for cellular metabolism is glucose, which is catabolized in the three subsequent processes: glycolysis, tricarboxylic acid cycle (TCA or Krebs cycle), and finally oxidative phosphorylation to produce ATP. In the first process, when glucose is converted into pyruvate the amount of ATP produced is low. Subsequently, pyruvate is converted to acetyl coenzyme A (acetyl-CoA) which enters the TCA cycle, enabling the production of NADH. Finally, NADH is used by the respiratory chain complexes to generate a proton gradient across the inner mitochondrial membrane, necessary for the production of large amounts of ATP by mitochondrial ATP synthase. In addition, it should be mentioned that acetyl-CoA could be generated also by lipid and protein catabolism.

Citric Acid Cycle

The TCA, also known as the citric acid cycle, was elucidated by Sir Hans Krebs in 1940 when he concluded, "*the oxidation of a triose equivalent involves one complete citric acid cycle*" (184). The "*triose*" deriving from glycolysis is completely oxidized into three molecules of CO_2 during a sequence of reactions that allow the reduction of cofactors NAD and flavin adenine nucleotide (FAD), providing energy for the respiratory chain in the form of electrons. In 1949 it was demonstrated by Kennedy and Lehningher that the entire cycle occurs inside mitochondria (185). The starting material for the citric acid cycle is directly provided by the pyruvate coming from

glycolysis through the activity of the pyruvate dehydrogenase complex. This enzymatic complex, composed of multiple copies of the three enzymes pyruvate dehydrogenase (E1), dihydrolipoyl transacetylase, (E2) and dihydrolipoyl dehydrogenase (E3), oxidizes pyruvate to acetyl-CoA and CO_2 in an irreversible reaction in which the carboxyl group is removed from pyruvate as a molecule of CO_2. This reaction is strictly related to the cycle, even if is not comprised in it. The acetyl group introduces two carbons in each turn of the cycle; these carbons will then leave the cycle as CO_2. The first reaction of the citric acid cycle is the condensation of one Acetyl-CoA and a molecule of citrate to generate oxaloacetate and is catalysed by citrate synthase. Citrate is then transformed into isocitrate by aconitase through the formation of cis-aconitate. This step is reversible and could lead to the formation of both citrate and isocitrate. Only the fast consumption of isocitrate by its dehydrogenase can force the reaction to the proper direction. Isocitrate dehydrogenase catalyses the first irreversible oxidation leading to the decarboxylation of isocitrate, generating CO_2 and á-ketoglutarate. The second carbon leaves the cycle in the following step, when the newly generated á-ketoglutarate is immediately decarboxylated by the á-ketoglutarate dehydrogenase complex in a reaction similar to the pyruvate decarboxylation. In fact, both these complexes share high similarities in enzyme amino acid composition and in the organization of the different subunits. Energy released from both oxidations is used to generate NADH from NAD that directly feeds into the respiratory chain.
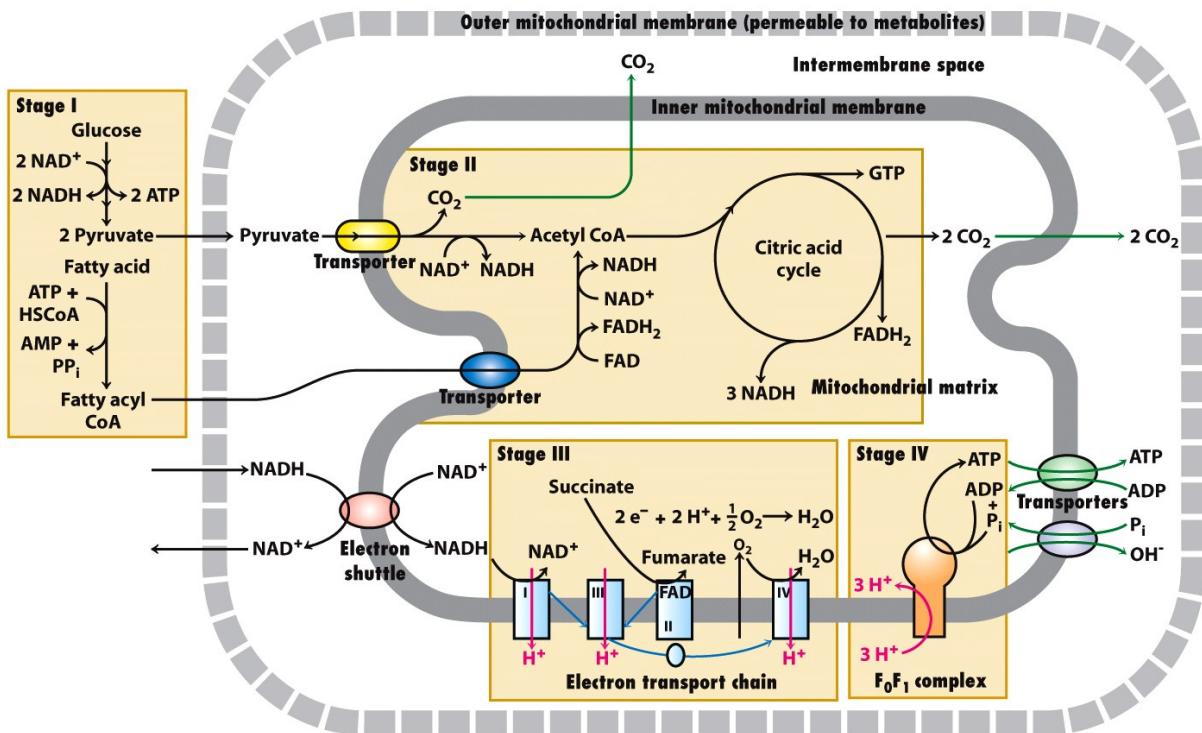
Figure 12-8
Molecular Cell Biology, Sixth Edition
© 2008 W. H. Freeman and Company

Fig 8. A schematic representation of principal metabolic reactions occurring within mitochondria Glycolysis, TCA cycle and oxidative phosphorylation are rapresented. Adapted from Molecular Cell Biology, Sixth Edition (2008).

The following step is catalysed by succinyl-Coa synthetase and utilizes the energy derived from the CoA removal to phosphorylate GDP (or ADP) to GTP (or ATP). Selectivity for the nucleotide is determined by the isozyme involved. It has been well established that at least two isozymes of succinyl-CoA synthetase are expressed in animal tissues (186) and the proportion between them seems to be tissue specific.

The succinate generated in the previous step is the 4 carbon compound that is then converted, by three sequential reactions, to oxaloacetate to conclude the cycle. The first of these steps is the oxidation of succinate to fumarate by succinate dehydrogenase. This enzyme, tightly bound to the inner mitochondrial membrane (IMM), catalyses FAD reduction to $FADH_2$ that provides electrons for the respiratory chain. Fumarate is then hydrated by fumarate hydratase to L-malate. It is particularly interesting that both succinate dehydrogenase and fumarate hydratase are oncosuppressor genes. It has been demonstrated that inactivation of these oncosuppressors leads to the accumulation of succinate and fumarate that spread in the cytosol and promote hypoxia-inducible factor 1α(HIF1á) accumulation by inactivating prolyl hydroxilase enzymes (promoter of HIF1á degradation); HIF1á in turn promotes a pseudo-hypoxic condition that favours tumour

26

development (187). The last event that completes the citric acid cycle is the oxidation of L-malate to oxaloacetate. This reaction is performed by L-malate dehydrogenase, which induces the reduction of another molecule of NAD to NADH. The resulting molecule of oxaloacetate is suitable for starting another cycle through condensation with an acetyl group.

During all these processes, only one molecule of ATP (or GTP) is produced, but three molecules of NADH and one of FADH2 (plus one molecule of NADH from pyruvate dehydrogenase), which provide electrons for respiratory chain, are also generated and subsequently result in the production of large amounts of ATP (discussed later).

Respiratory chain and Oxidative Phosphorylation

Respiratory chain comprises a series of components (complexes) conducting electron transfer across the membrane and involved in oxidative phosphorylation (OXPHOS), a process that occurs in aerobic conditions. In eukaryotic cells, electron transport occurs in mitochondria and chloroplasts, whereas in bacteria it is carried out across the plasma membrane. As mentioned, the electron transfer is considered a part OXPHOS, the process through which ADP is phosphorylated into ATP by dint of energy derived from the oxidation of nutrients. Four protein complexes and ATP synthase, all bound to the IMM, as well as two shuttles are the known players of one of the trickiest mechanisms resolved in biochemistry. The first of these complexes is the NADH:ubiquinone oxidoreductase (complex I) which removes electrons from NADH (produced in the citric acid cycle) and passes them on to the first shuttle, ubiquinone, a liposoluble cofactor located within the phospholipid bilayer of the IMM. Succinate dehydrogenase (or complex II) is another entrance site for electrons into the respiratory chain. In this case, electrons derived from the oxidation of succinate are passed through FAD to ubiquinone. Once ubiquinone is reduced to ubiquinol, it is able to pass electrons to the third complex, ubiquinone:cytochrome c oxidoreductase. Here, electrons are moved through several heme groups from the liposoluble shuttle ubiquinone to the water soluble shuttle cytochrome c. Cytochrome c is a small protein (about 12.5 kDa), located in the intermembrane space (IMS), which can accommodate one electron in its heme group. Despite its water solubility, cytochrome c is usually bound to the external surface of the IMM due to the interaction with the cardiolipin (188). This interaction (crucial in the determination of the cell fate) helps the shuttle to reach its electron acceptor, complex IV. Cytochrome c oxidase is the last complex of the electron transport. Electrons from cytochrome c are accumulated in copper centres and passed to oxygen through heme groups. Oxygen is then reduced to water. This constitutes the bulk of oxygen consumption in all aerobic life.
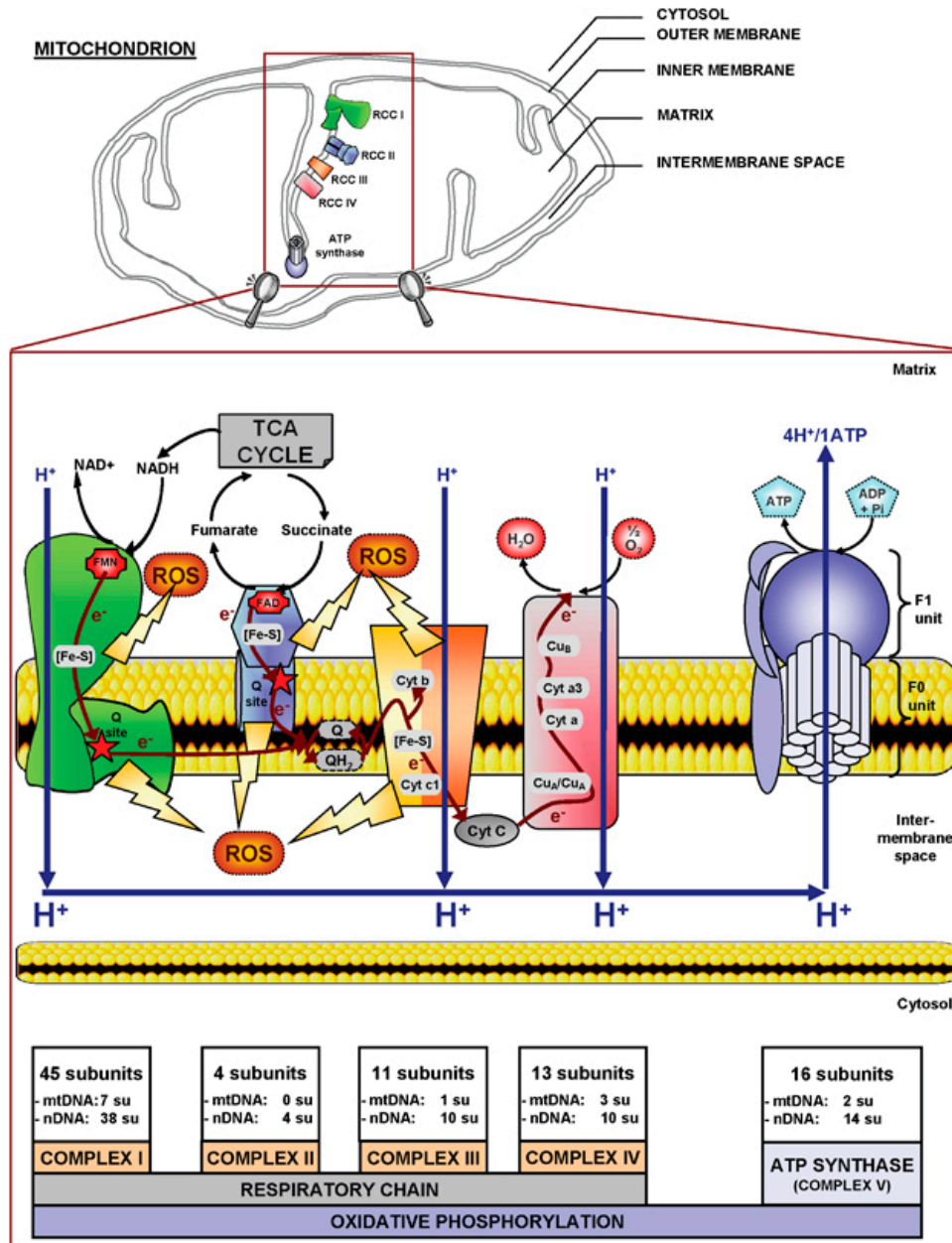
MITOCHONDRION

CYTOSOL
OUTER MEMBRANE
INNER MEMBRANE
MATRIX
INTERMEMBRANE SPACE

RCC I
RCC II
RCC III
RCC IV
ATP synthase

Matrix

TCA CYCLE

$4H^+/1ATP$

H^+ NAD+   NADH

Fumarate   Succinate

FMN
ROS
ROS
ROS
e-
[Fe-S]
FAD
[Fe-S]
Q site
Q A site
e-
e-
e-
e-
Q
QH2
Cyt b
Q site
[Fe-S]
Cyt c1
Cyt C
e-
e-
H_2O
$\frac{1}{2} O_2$
e-
CuB
Cyt a3
Cyt a
CuA/CuA
e-
H^+
H^+
H^+
ATP
ADP + Pi
F1 unit
F0 unit
Inter-membrane space

H^+
H^+
H^+
H^+

Cytosol

45 subunits	4 subunits	11 subunits	13 subunits	16 subunits
- mtDNA: 7 su	- mtDNA: 0 su	- mtDNA: 1 su	- mtDNA: 3 su	- mtDNA: 2 su
- nDNA: 38 su	- nDNA: 4 su	- nDNA: 10 su	- nDNA: 10 su	- nDNA: 14 su
COMPLEX I	COMPLEX II	COMPLEX III	COMPLEX IV	ATP SYNTHASE (COMPLEX V)

RESPIRATORY CHAIN

OXIDATIVE PHOSPHORYLATION

Fig. 9 Representation of the mitochondrial respiratory chain complexes and the oxidative phosphorylation system. Oxidative phosphorylation begins with the entry of electrons into the electron-transport chain on the inner mitochondrial membrane (IMM), which is impermeable to low-molecular-weight solutes. There are four membrane-bound protein complexes (complex I–IV) in the electron-transport chain, and the electrons pass through them (black arrows) with the aid of the electron carriers, namely ubiquinone (Q), cytochromes and iron-sulphur proteins. The transfer of the electrons yields a highly exergonic reaction that is used to pump protons out of the mitochondrial matrix. This generates the membrane potential ($\Delta\psi_m$) across the IMM and electrochemical energy, in the form of a proton-motive force, in the IMM. The proton-motive force then drives the synthesis of ATP as protons flow passively back into the mitochondrial matrix through a proton pore that is associated with ATP synthase. Adapted from Lemaire et al; (2011).

Electron transport through complexes I, III and IV induces the pumping of protons from the matrix to the IMS. Specifically, for every two electrons coming from one molecule of NADH, four H^+ are moved by complex I, four by complex III, and two by complex IV. The second respiratory complex does not generate any proton movement (189). The respiratory chain in active mitochondria generates a large difference in $[H^+]$ across the IMM, resulting in the generation of an electrical potential (about -180 to -200 mV) and variation in the pH of about 0.75. A constant proton motive force drives the ATP synthesis trough the last step of OXPHOS, the ATP synthase. Understanding the activity and organization of this enzyme won researchers more than one Nobel Prize. First, Peter Mitchell in 1978 received his prize for the formulation of the chemiosmotic theory. Initially he hypothesized how an enzymatic activity could at the same time involve ion transport (proton transport through the IMM) and a chemical reaction (ATP phosphorylation). Almost two decades later, in 1997, the Nobel Prize was awarded to Paul Boyer and John Walker who elucidated the mechanism of action of ATP synthase, here briefly reviewed. ATP synthase could be divided in two main components: F_0 that allows the channelling of protons, and F_1 that catalyses ATP phosphorylation. The F_0 is embedded in the IMM, while the F_1 resides in the mitochondrial matrix and is bound to the F_0 through a ã subunit (which drives conformational changes) and a b2ä dimer (that holds F_0 and F_1 together). The protons flow from the intermembrane space to the matrix through the F_0 inducing its rotation; the movement is transmitted from the ã subunit to the F_1 causing conformational rearrangements. The F_1 has a trimeric structure consisting of áâ dimers. The sequential changes are linked to the binding of substrates, phosphorylation and release of ATP. The three available dimers are never in the same conformational state and, what is more, the conformational changes in one dimer drive rearrangements in the other (for a more detailed explanation refer to (190)). It has been calculated that for the synthesis of one ATP molecule, 4 protons are required (3 for the ATP synthase rearrangements and 1 for ATP, ADP and Pi transport, (191)). Once synthetized, ATP can locate inside mitochondrial matrix or be transported into the IMS by the nucleotide exchanger adenine nucleotide translocase (ANT) that passively exchanges ATP with ADP. Once in the IMS, ATP can freely pass the OMM through the voltage dependent anion channel (VDAC).

Mitochondria: versatile players between cell proliferation and death

At the same time, mitochondria are also important checkpoints of the apoptotic process, as they may release caspase cofactors (192). Indeed, the apoptotic intrinsic pathway is activated by the release of several mitochondrial proteins into the cytosol. The main player in the finely tuned

apoptotic activation process is undoubtedly cytochrome c. The majority of cytochrome c is tightly bound to mitochondrial inner membrane, thanks to its electrostatic interactions with acidic phospholipids, but a small fraction probably exists loosely attached to inner mitochondrial membrane and available for mobilization.

This protein is an irreplaceable component of the mitochondrial electron transport chain, shuttling electrons from complexes III to IV, and is thus essential to life: the disruption of its only gene is embryonic lethal (195). Once released in the cytoplasm, this protein drives the assembly of a caspases activating complex together with Apaf-1 (apoptosis–protease activating factor 1) and caspase 9, the so-called 'apoptosome'. Cytochrome c, once in the cytosol, induces the rearrangement and heptaoligomerization of Apaf-1: each of these complexes can recruit up to seven caspase molecules, leading to their proteolytic self-processing and consequent activation (194). Mitochondria contain several other proapoptotic, intermembrane space-resident proteins, such as Smac/ DIABLO, HtrA2/Omi, AIF and EndoG. DIABLO (direct inhibitor of apoptosis-binding protein with a low isoelectric point) and HtrA2 (high temperature requirement protein A2) both have an N-terminal domain that can interact and inhibit IAPs (inhibitor of apoptosis proteins). IAPs, such as XIAP, cIAP-1 and cIAP-2, are cytosolic soluble peptides that normally associate and stabilize procaspases, thus preventing their activation. Conversely, apoptosis-inducing factor and EndoG (endonuclease G) translocate from intermembrane space to the nucleus upon treatment with several apoptotic stimuli where they seem to mediate chromatin condensation and DNA fragmentation (195). In HeLa cells upon ceramide treatment, we observed Ca^{2+} elease from the ER and loading into mitochondria. As a consequence, organelle swelling and fragmentation were detected that were paralleled by the release of cytochrome c. These changes were prevented by Bcl-2 expression as well as experimental conditions that lowered $[Ca^{2+}]_{er}$ (202).

Mitochondria also undergo a more 'macroscopic' remodelling of their shape during the programed cell death. Indeed, after apoptosis induction, mitochondria become largely fragmented, resulting in small, rounded and numerous organelles. This process occurs quite early in apoptotic cell death, soon after Bax/Bak oligomerization, but before caspase activation. Interestingly, the perturbation of the equilibrium between fusion and fission rates seems to correlate with cell death sensitivity. In particular, conditions in which mitochondrial fission is inhibited, such as DRP1 (dynamin-like protein 1) downregulation or mitofusins overexpression, strongly delay caspase activation and cell death induced by numerous stimuli. Similarly, stimulation of organelle fission (by DRP1 overexpression or Mfn1/2 and OPA1 inhibition) promotes apoptosis by facilitating cytochrome c release and apoptosome assembly (203). However, the relationship between mitochondrial

fusion/fission and apoptosis is complex and mitochondrial fragmentation is not necessarily related to apoptosis. Indeed, mitochondrial fission per se does not increase cell death and DRP1 overexpression has been reported to protect cells from some apoptotic challenges, such those dependent on mitochondrial Ca^{2+} overload (204).

Another hallmark of apoptosis is the loss of mitochondrial membrane potential, secondary to the opening of mPTP triggered by different pathological conditions (e.g., Ca^{2+} overload, ATP depletion, oxidative stress, high inorganic phosphate or fatty acid). The molecular structure of this pore is currently highly debated (205). The availability of chemical mPTP inhibitors such as cyclosporine A and related compounds lacking the cytosolic inhibitory effect on calcineurin, as well as the development of cyclophilin D knockout mouse will help to clarify the role of mPTP in physiological and pathological condition and identify areas of pharmacological intervention in common disorders such as ischemia-reperfusion injury, liver diseases, neurodegenerative and muscle disorders (206- 208).

P2X7 expression modulates NLRP3 levels

2. AIMS

In the past years the ability of the P2X7 receptor to cause IL-1β release from immune cells was thought to be a side effect of P2X7 receptor-dependent cytotoxicity, effectively all the factors that cause apoptosis are potent stimuli for IL-1β release (231). However, it has subsequently become evident that P2X7 receptor-driven IL-1β secretion is the end result of a complex chain of intracellular events specifically triggered by this receptor that induced NLRP3 inflammasome assembly. The P2X7 is not an integral constituent of the NLRP3 inflammasome; nonetheless, NLRP3 is required to drive P2X7-dependent pro-IL-1β processing (213), and in addition, many NLRP3 stimulants act via P2X7 (214).

This project proposes to investigate the relationship and contribution of P2X7 in modulate NLRP3 levels and, vice versa, NLRP3 expression and activity might modulate P2X7 levels. Therefore we analysed the mRNA levels of P2X7 and NLRP3 in microglia N13 cells after activations of P2X7 with ATP or its pharmacologic analog BzATP and stimulations of NLRP3 with LPS. To verify whether NLRP3 modulation by P2X7 expression is a general finding, we extended the investigation to additional mouse cell models that natively express both P2X7 and NLRP3 at a high level: primary peritoneal macrophages and primary microglial cells from C57Bl/6 WT and P2X7$^{-/-}$ mice and P2X7-silenced B16 mouse melanoma cells.

Present data suggest that, although the P2X7 is not an integral inflammasome component, it associates to the inflammasome at discrete foci in the subplasmalemmal region, in both resting and activated conditions. Close interaction between P2X7 and NLRP3 has important implications for the mechanism of inflammasome activation because it localizes NLRP3 exactly where the K$^+$ drop occurs, maximizing NLRP3 stimulation and minimizing possible untoward effects caused by an unrestricted loss of cytoplasmic K. Therefore we analysed the P2X7 receptor and NLRP3 localization and possible direct interaction trough different method such as immunofluorescence and co-immunoprecipiation.

These data have appeared in the following publication co-authored by the Candidate:
Franceschini A, Capece M, Chiozzi P, Falzoni S, Sanz JM, Sarti AC, Bonora M, Pinton P, and Di Virgilio F (2015) The P2X7 receptor directly interacts with the NLRP3 inflammasome scaffold protein The FASEB Journal 14-268714

3. RESULTS

3.1 P2X7 expression modulates NLRP3 levels

In the past years the ability of the P2X7 receptor to cause IL-1β release from immune cells was thought to be a side effect of P2X7 receptor-dependent cytotoxicity, effectively all the factors that cause apoptosis are potent stimuli for IL-1β release (209). However, it has subsequently become evident that P2X7 receptor-driven IL-1β secretion is the end result of a complex chain of intracellular events specifically triggered by this receptor that induced NLRP3 inflammasome assembly. The P2X7 is not an integral constituent of the NLRP3 inflammasome; nonetheless, NLRP3 is required to drive P2X7-dependent pro-IL-1β processing (210), and in addition, many NLRP3 stimulants act via P2X7 (211). To verify whether P2X7 expression and activity might modulate NLRP3 levels and, vice versa, NLRP3 expression and activity might modulate P2X7 levels, we selectively activated the P2X7 with ATP or its pharmacologic analog BzATP or stimulated NLRP3 with LPS. We initially used N13 mouse microglial cells as a model, which is a cell line widely used to investigate purinergic signaling and IL-1β maturation and release. N13 cells are available as the N13wt, characterized by high P2X7 expression, and the ATP-resistant (N13ATPR) variant, characterized by reduced P2X7 expression, and are therefore useful to investigate P2X7-ependent responses. As shown in Fig. 1A, B, ATP stimulation enhanced P2X7 and NLRP3 mRNA accumulation. A statistically significant ATP-stimulated increase in P2X7 mRNA occurred as early as 15 minutes, whereas a statistically significant increase in NLRP3 levels only occurred 60 min after P2X7 stimulation. BzATP had a similar effect, except that the NLRP3 mRNA increase was already detected at 30 min (Fig. 1C, D). Microglia challenge with LPS had no effect on P2X7 mRNA accumulation (Fig. 1C) but caused a large increase in NLRP3 mRNA levels (Fig. 1D). ASC mRNA accumulation did not change in response to either BzATP or LPS (Fig. 1E). Expression of the P2X7 protein was not affected by either LPS or BzATP treatment (Fig. 1F), whereas NLRP3 expression was up-modulated by LPS (Fig. 1G). ASC expression was in- creased by LPS or BzATP but not in a statistically signifi- cant fashion (Fig. 1H). A representative Western blot from control (CTR), LPS, or BzATP-stimulated N13 cells is shown in Fig. 1I. Fig. 1 shows that P2X7 stimulation, by ATP or BzATP, increases NLRP3 expression and suggests that NLRP3 levels might be up-modulated by P2X7 expression. To test this hypothesis, we took advantage of the N13ATPR cells selected for low P2X7 expression (212).
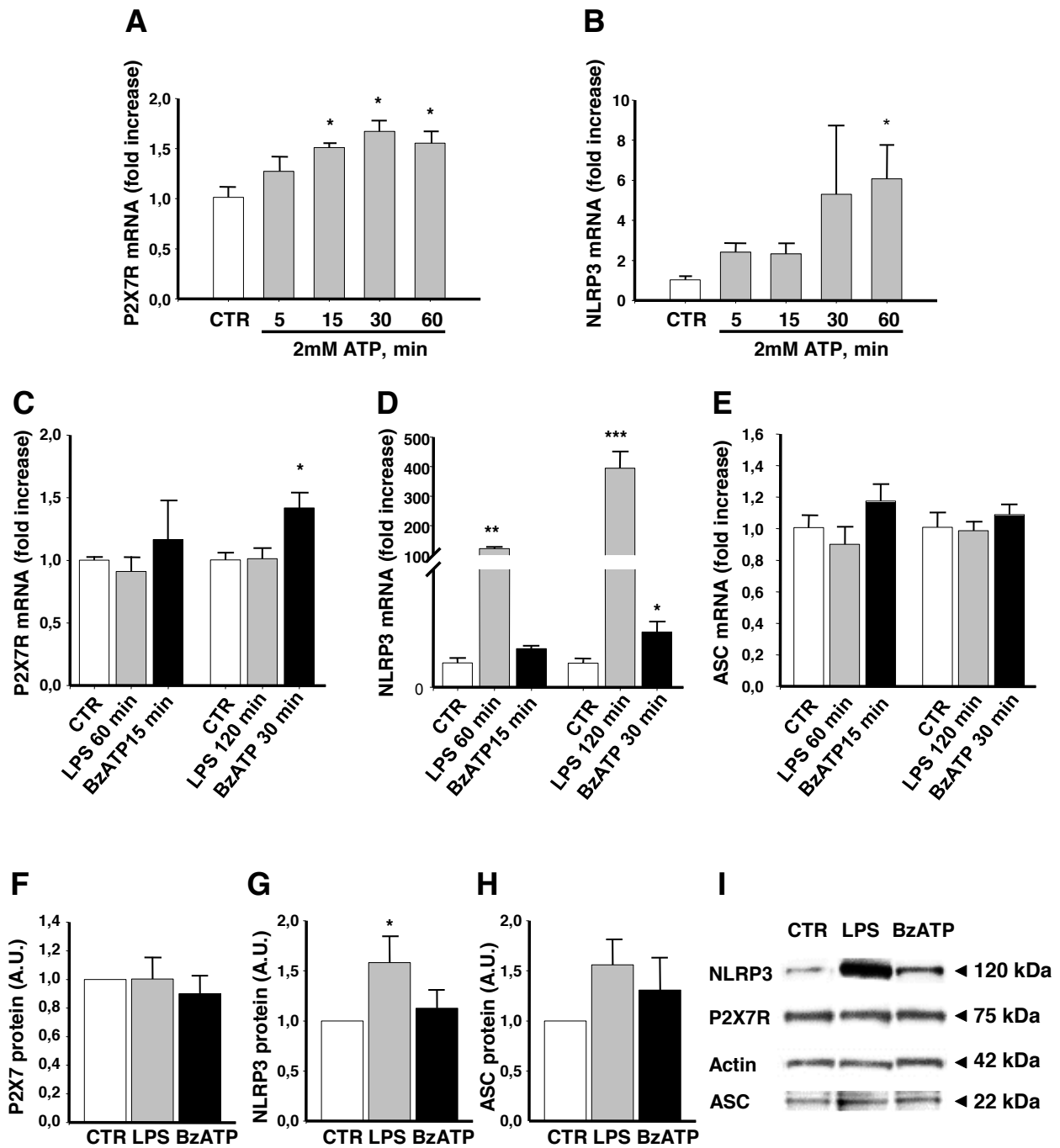
Figure 1. Purinergic and TLR4 agonists modulate P2X7 and NLRP3 expression. A, B) Time course of ATP-stimulated P2X7 and NLRP3 mRNA accumulation in N13 microglia, normalized (CTR, n = 3). C–E) LPS- or BzATP-stimulated accumulation of P2X7 (C), NLRP3 (D), and ASC (E) mRNA (n = 3). F–H) Densitometric analysis of P2X 7(F), NLRP3 (G), and ASC (H) protein in response to LPS or BzATP expressed as a fold increase over controls (n = 3). P2X7, NLRP3, and ASC bands were normalized over the actin band. (I) Exemplificative Western blot showing P2X7, NLRP3, and ASC accumulation in nonstimulated (CTR) and LPS- or BzATP-stimulated cells. Data are represented as mean 6 SEM. *P , 0.05; **P , 0.01; ***P , 0.001.

The N13ATPR cells express P2X7 mRNA and protein to a level of ;50% and 25% that of the N13wt population, respectively (Fig. 2A, B). NLRP3 mRNA content of N13ATPR was almost 8-

fold higher than that of N13wt, but this striking increase in mRNA content did not translate into an increased protein level. In fact, NLRP3 protein in N13ATPR was ;30% that of WT cells (Fig. 2C, D). ASC mRNA showed little change, whereas ASC protein in N13ATPR was ;30% that of N13wt cells (Fig. 2E, F). A representative blot of NLRP3, P2X7, and ASC protein expression in N13wt and N13ATPR cells is shown in Fig. 2G. Western blot data were confirmed by immunofluorescence, which showed a striking reduction of both P2X7 and NLRP3 labeling in N13ATPR cells (Fig. 1H). These findings suggested P2X7 expression modulates NLRP3 expression levels.
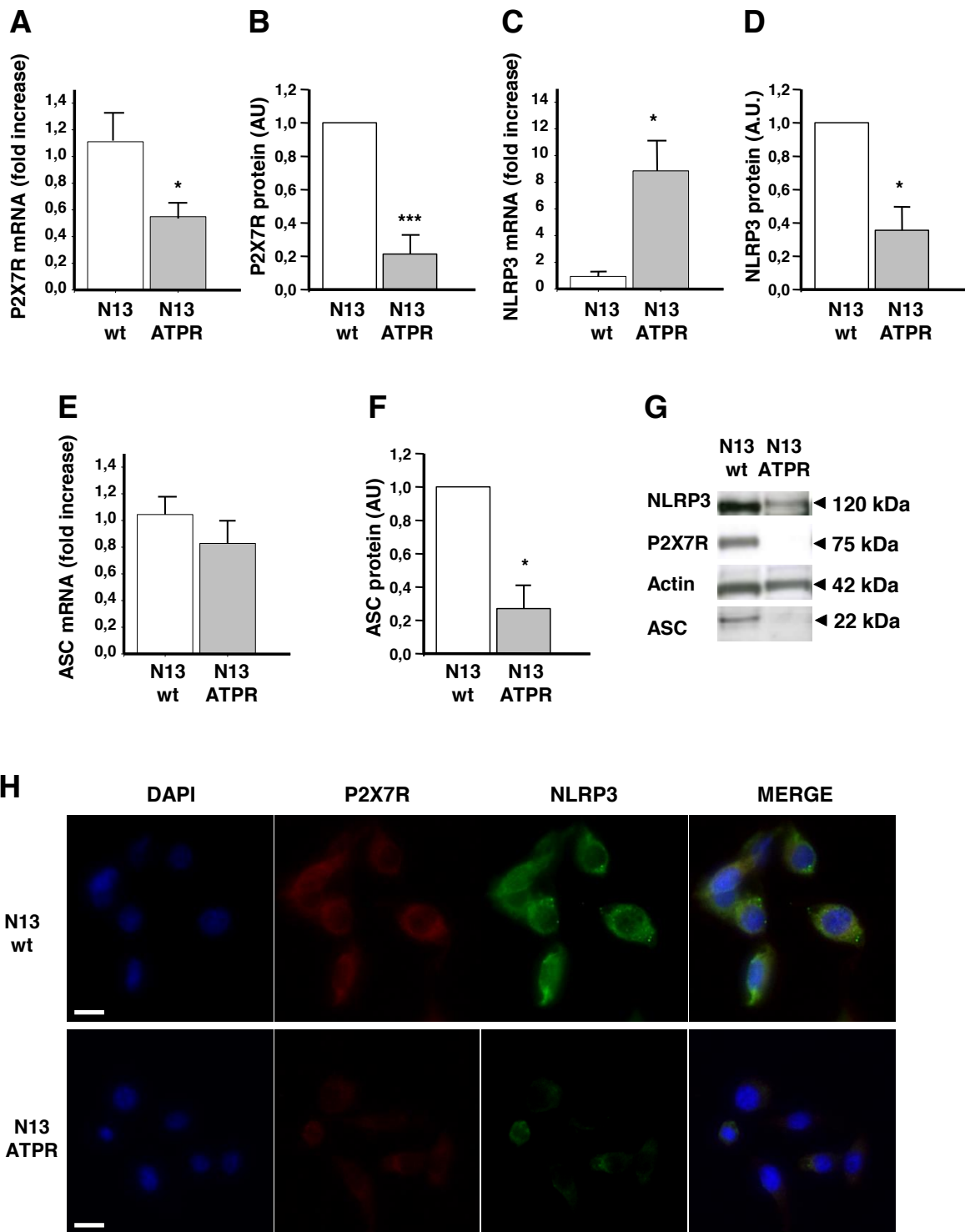
Figure 2. ATPR N13 cells express high NLRP3 mRNA and low NLRP3 protein levels. A–D) P2X7 and NLRP3 mRNA (n = 5) and protein (n = 3) levels in wild-type (N13wt) and ATP-resistant (N13ATPR) N13 microglia. E, F) ASC mRNA and protein levels in N13wt and N13ATPR microglia (n = 3). P2X7, NLRP3, and ASC mRNA levels of N13ATPR cells . G) Representative blot of P2X7, NLRP3, and ASC expression in N13wt and N13ATPR microglia. H) Immunofluorescence labeling of P2X7 and NLRP3 proteins in N13wt and N13ATPR cells. Cells were stained with DAPI (blue) and immunolabeled with anti-P2X7 (red) and anti-NLRP3Abs (green). Merge, fourth column. Bar = 10 mm. Data are represented as mean 6 SEM. *P , 0.05; ***P , 0.001.

To verify whether NLRP3 modulation by P2X7 expression is a general finding, we extended the investigation to additional mouse cell models that natively express both P2X7 and NLRP3 at a high level: primary peritoneal macrophages and primary microglial cells from C57Bl/6 WT and P2X7$^{-/-}$ mice and P2X7-silenced B16 mouse melanoma cells. Fig. 3A, B shows that, as expected, P2X7 mRNA and protein were fully absent in peritoneal mac- rophages from P2X7$^{-/-}$ mice. NLRP3 mRNA was increased (Fig. 3C), but contrary to N13ATPR, NLRP3 protein was ;2-fold higher than in WT mice, albeit the increase was not statistically significant (P = 0.6; Fig. 3D). ASC mRNA and protein showed no changes (Fig. 3E, F). Western blot of macrophage proteins and immunofluo- rescence pictures are shown in Fig. 3G, H). A marked in- crease in NLRP3 mRNA and protein was also observed in P2X7$^{-/-}$ microglia (Fig. 3I–K). In P2X7$^{-/-}$ microglia, the increase in NLRP3 levels was clear cut and statistically significant compared with WT microglia, thus supporting the finding in P2X7$^{-/-}$ macrophages shown in Fig. 3D. These experiments show that in genetically deleted animals, the absence of P2X7 increased NLRP3 mRNA and NLRP3 protein. We also investigated the B16 melanoma cell model. In B16 cells, both P2X7 mRNA and protein were reduced by shRNA transfection to ;50% of control levels, causing in parallel a marked increase of NLRP3 and ASC mRNA and a decrease of NLRP3 protein, whereas ASC protein was unchanged (data not shown). Although P2X7 down-modulation was achieved in N13ATPR microglia and B16 melanoma cells by different means, the end result was the same, i.e., a decrease in P2X7 expression caused a large increase in NLRP3 mRNA. However, at variance with macrophage and microglia from the P2X7$^{-/-}$ mouse, the increase in NLRP3 mRNA did not translate into an increase in NLRP3 protein.
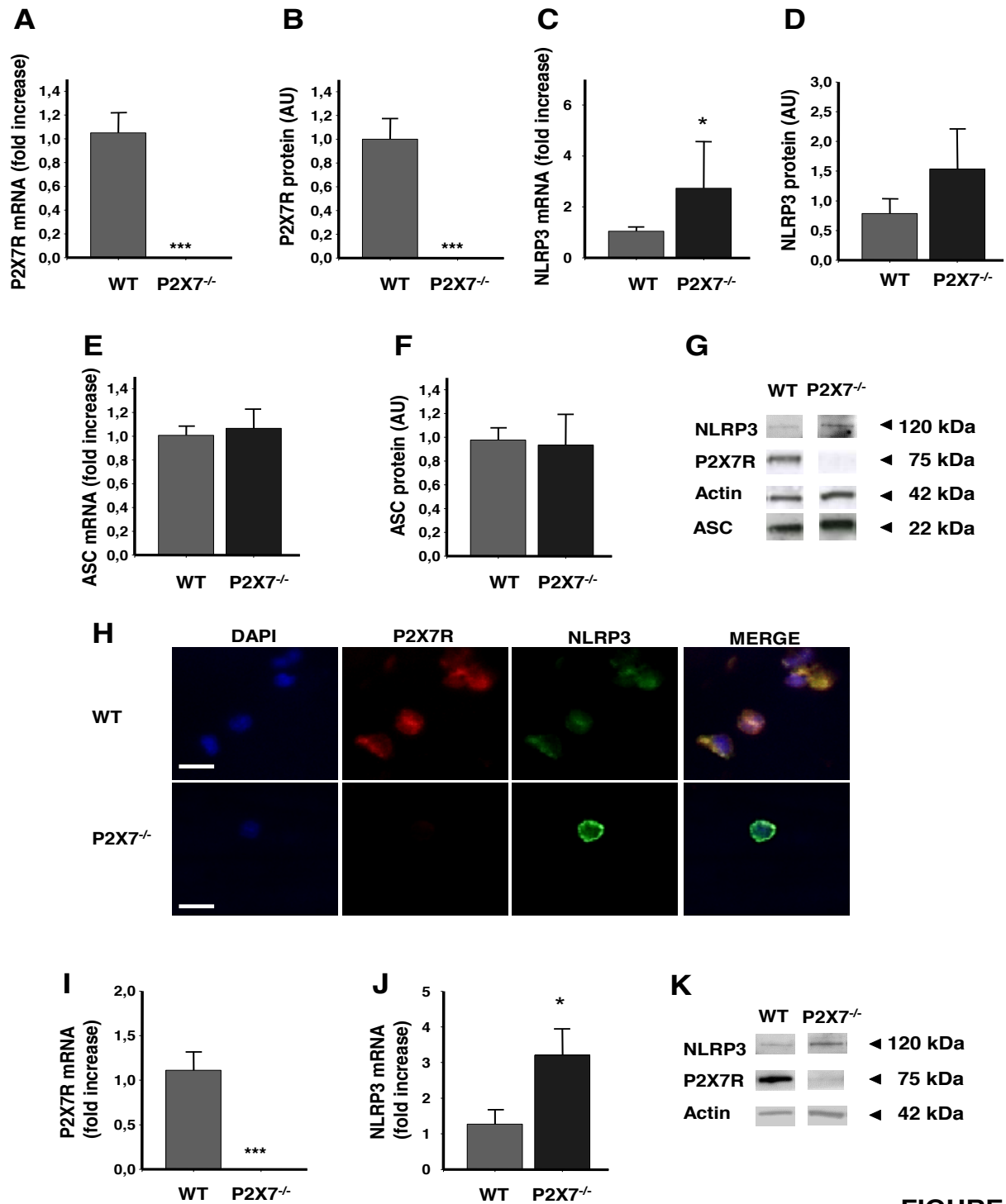
Figure 3. NLRP3 is up-regulated in macrophages and microglia from P2X7$^{-/-}$ mice. A, B,C,D,E,F) P2X7, NLRP3 and ASC expression in peritoneal macrophages from WT and P2X$_7$$^{-/-}$ mice (n = 4). G) Representative Western blot of NLRP3, P2X7, and ASC proteins from peritoneal macrophages from WT and P2X7$^{-/-}$ mice. H) Immunofluorescence labeling with anti-P2X7 (red) and anti-NLRP3 (green) of peritoneal macrophages from WT and P2X7$^{-/-}$ mice. Nuclei were stained with DAPI (blue). I, J) P2X7 and NLRP3 mRNA expression in microglia from WT and P2X7$^{-/-}$ mice (n = 3). K) Representative Western blot showing P2X7 and NLRP3 expression in microglia from WT and P2X7$^{-/-}$ mice. Protein levels were quantified by densitometry and normalized over actin protein content. Data are represented as mean 6 SEM. *P , 0.05; ***P , 0.001. Bar = 10 mm.

3.2 P2X7 and NLRP3 colocalize

Data shown in Figs. 1–3 suggested that P2X7 and NLRP3 might colocalize and interact. A more detailed confocal microscopy analysis indeed showed that P2X7 and NLRP3 did colocalize in N13wt cells (Fig. 4A–D). $P2X_7$ and NLRP3 fluorescence distribution was analyzed at the single cell level by acquiring the fluorescence intensity profile across a single focal plan, as shown in Fig. 4A, B. In addition, an orthogonal re- construction of a Z-stack (7 planes; width pass, 0.8 mm) was performed to highlight sites of enhanced P2X7 and NLRP3 colocalization (Fig. 4C, D). P2X7 showed a strong cytoplasmic and subplasmalemmal localization, whereas the plasma membrane signal was rather weak (Fig. 4A, B). NLRP3 was also localized within the cytoplasmic and the subplasmalemmal regions (Fig. 4B). The nucleus was largely negative for both $P2X_7$ and NLRP3. The 3D orthogonal reconstruction shown in Fig. 4C revealed "hot spots," 1 or 2 per cell, close to the plasma membrane, where P2X7 and NLRP3 colocalized.

$P2X_7$/NLRP3 interaction was further investigated by immunoprecipitation. Fig. 4E, F shows that NLRP3 was immunoprecipitated together with P2X7, and reciprocally, P2X7 was immunoprecipitated together with NLRP3. ASC was also found in the immunoprecipitated complexes.
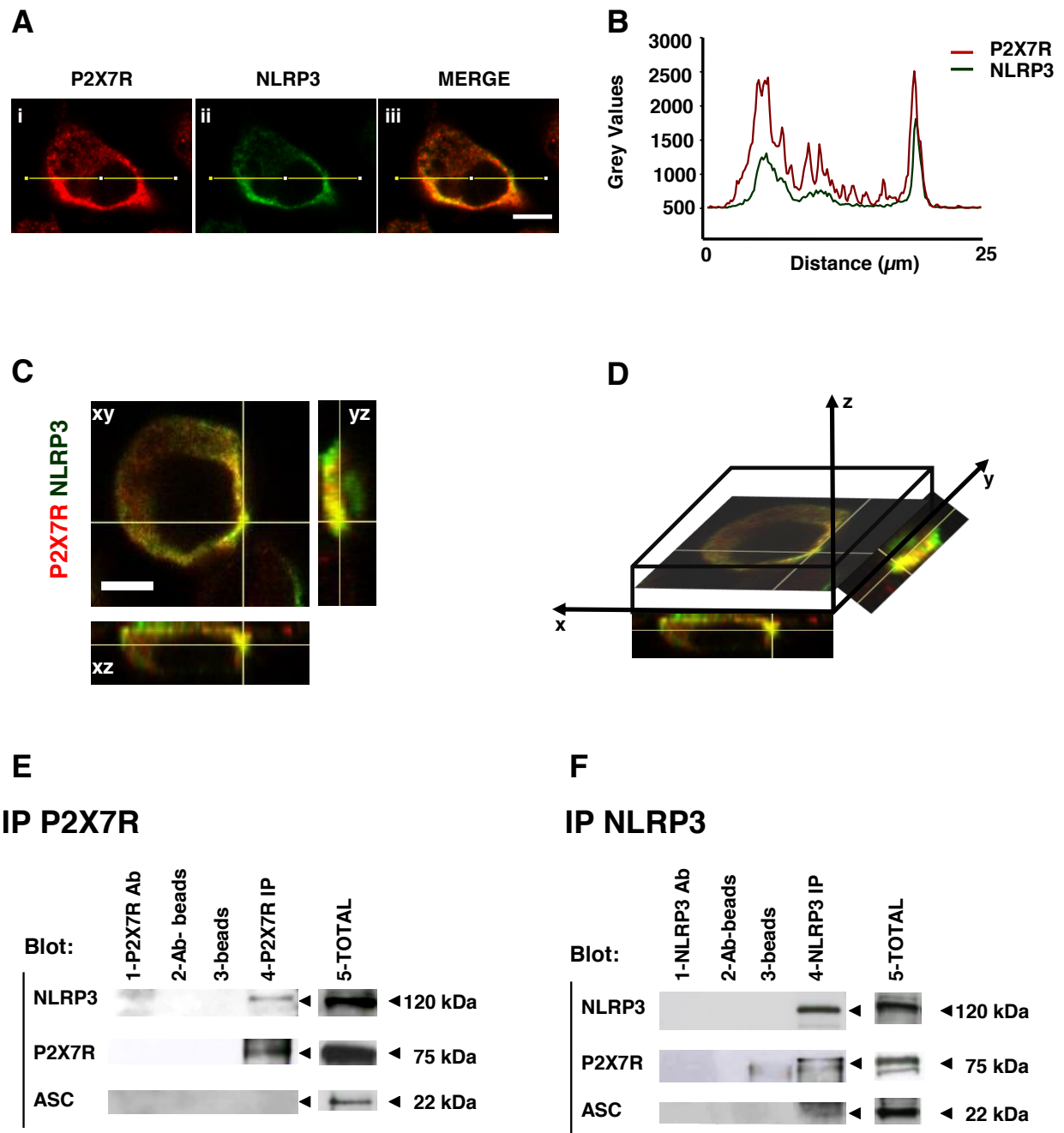
Figure 4. P2X7 and NLRP3 colocalize and closely interact. A, B) Immunoflorescence labeling of microglial cells as described in Materials and Methods, the fluorescence profile was run across the x-y axes of the cell body (yellow line) at a focal plan set at 3 mm and shown as intensity profile. C, D) 3D reconstruction of merged images obtained with confocal Z-stack E) P2X7 immunoprecipitation (n = 3). Lane 1, anti-P2X7 Ab in the absence of cell lysate; lane 2, eluate from Ab-coated beads in the absence of cell lysate; lane 3, eluate from Ab-uncoated beads incubated together with the cell lysate; lane 4, immunoprecipitate; lane 5, whole cell lysate. F) NLRP3 immunoprecipitation (n = 3). Lane 1, anti-NLRP3 Ab in the absence of cell lysate; lane 2, eluate from Ab-coated beads in the absence of cell lysate; lane 3, eluate from Ab-uncoated beads incubated together with the cell lysate; lane 4, immunoprecipitate; lane 5, whole cell lysate.

41

Next, we analyzed the single cell fluorescence profile and the Z-stack of individual LPS- or BzATP-treated cells. Fig. 5A–D shows that LPS or BzATP stimulation caused a slight increase in the expression of both P2X7 and NLRP3 and a shift of fluorescence from the cell body to the periphery. Z-stack analysis showed a single hot spot of increased P2X7/NLRP3 interaction near the plasma membrane (Fig. 5E, F). Effect of BzATP or LPS stimulation on the P2X7/NLRP3 interaction was also analyzed by coimmunoprecipitation experiments (Fig. 5G, H). Stimulation with BzATP significantly increased the amount of P2X7 or NLRP3 protein found in the complex, irrespective of whether anti-P2X7 or anti-NLRP3 antibodies were used for immunoprecipitation (Fig. 5I, J). On the contrary, BzATP or LPS treatment did not increase the content of ASC protein in the anti-NLRP3 antibody-immunoprecipitated samples (Fig. 5H, K), whereas in BzATP-treated cells, ASC protein was mostly detectable in P2X7 immunoprecipitated samples (Fig. 5G).
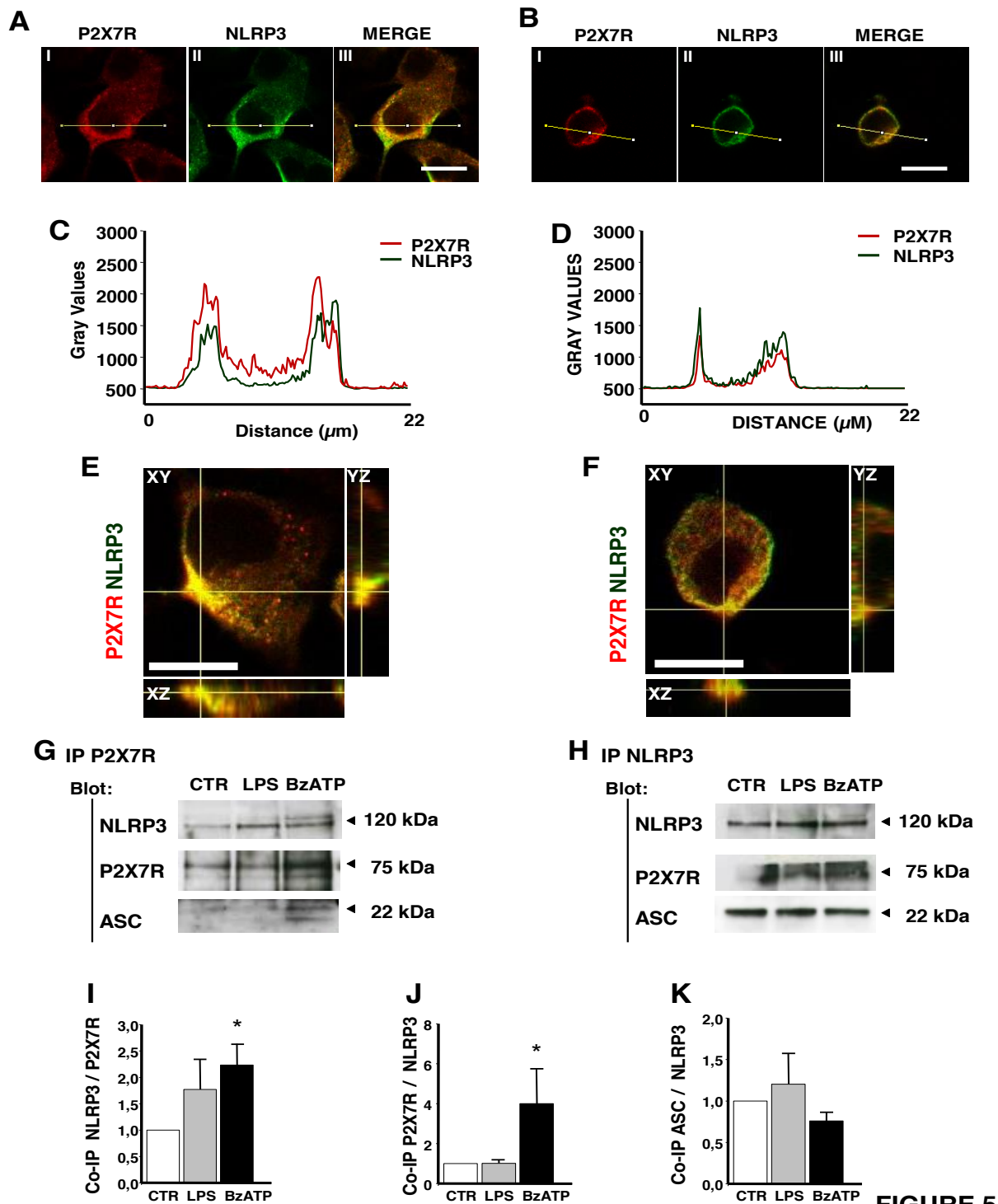
Figure 5. Stimulation with BzATP or LPS increases P2X₇/NLRP3 colocalization. A–F) Microglial cells were stimulated with either LPS (1 mg/ml, 2 h, A, C, E), or BzATP (300 mM, 30 min, B, D, F), fixed, and stained as described in Materials and Methods, fluorescence profile was run across the x-y axes (yellow line) of the cell body at a focal plan set at 3 mm. 3D reconstruction of LPS- (E) or BzATP-treated (F) cells obtained with confocal Z-stack G, H) Coimmunoprecipitation of P2X₇ and NLRP3 proteins in the absence or presence of LPS or BzATP, using an anti-P2X7 (G) or and anti-NLRP3 (H) immunoprecipitating antibody. I–K) Densitometry of immunoprecipitated NLRP3 normalized over P2X7signal (I) (n = 4), and P2X7 (J) (n = 4) and ASC (K) (n = 4) over NLRP3 signal. Data are represented as mean 6 SEM. *P , 0.05. Scale bar, 5 mm.

43

The P2X7 has a major role in the activation of NLRP3 in immune cells because this receptor is the main effector of the drop in cytosolic K^+ that is generally thought to be the main trigger of NLRP3 inflammasome activation. However, it is reasonable to assume that changes in the K^+ cytoplasmic concentration are spatially restricted to avoid a generalized, potentially deadly, depletion of intracellular K^+. Thus, we hypothesized that the colocalization of P2X7 and NLRP3 might be functional to restrict P2X7-dependent ion changes at discrete sites of the subplasmalemmal cytoplasm, where inflammasome activation could be maximized. As a model to test this hypothesis, we used HEK293 cells stably transfected with a GFP-tagged P2X7 (HEK293-P2X7-GFP), and, because of the lack of suitable indicators of intracellular K^+, the cytoplasmic Ca^{2+} indicator Fura-2 as a sensor of local changes in the ion concentration. As shown in Fig. 6, a BzATP puff applied with a patch pipette caused a rapid increase in the cytoplasmic Ca^{2+} concentration in the region under the pipette tip (Fig. 6C) but not in the distal cytoplasm (Fig. 6D). This fast Ca^{2+} rise was followed within several seconds by recruitment of additional P2X7 recetors to the site of stimulation (Fig. 6). P2X7 was not recruited at sites distal to the point of application of BzATP, where no Ca^{2+} increase occurred (Fig. 6D). The Ca^{2+} increase and the associated P2X7 recruitment were specifically dependent on P2X7 activation, as shown by lack of a Ca^{2+} increase and of P2X7 recruitment in the presence of the highly selective P2X7 blocker AZ10606120 (Fig. 6).
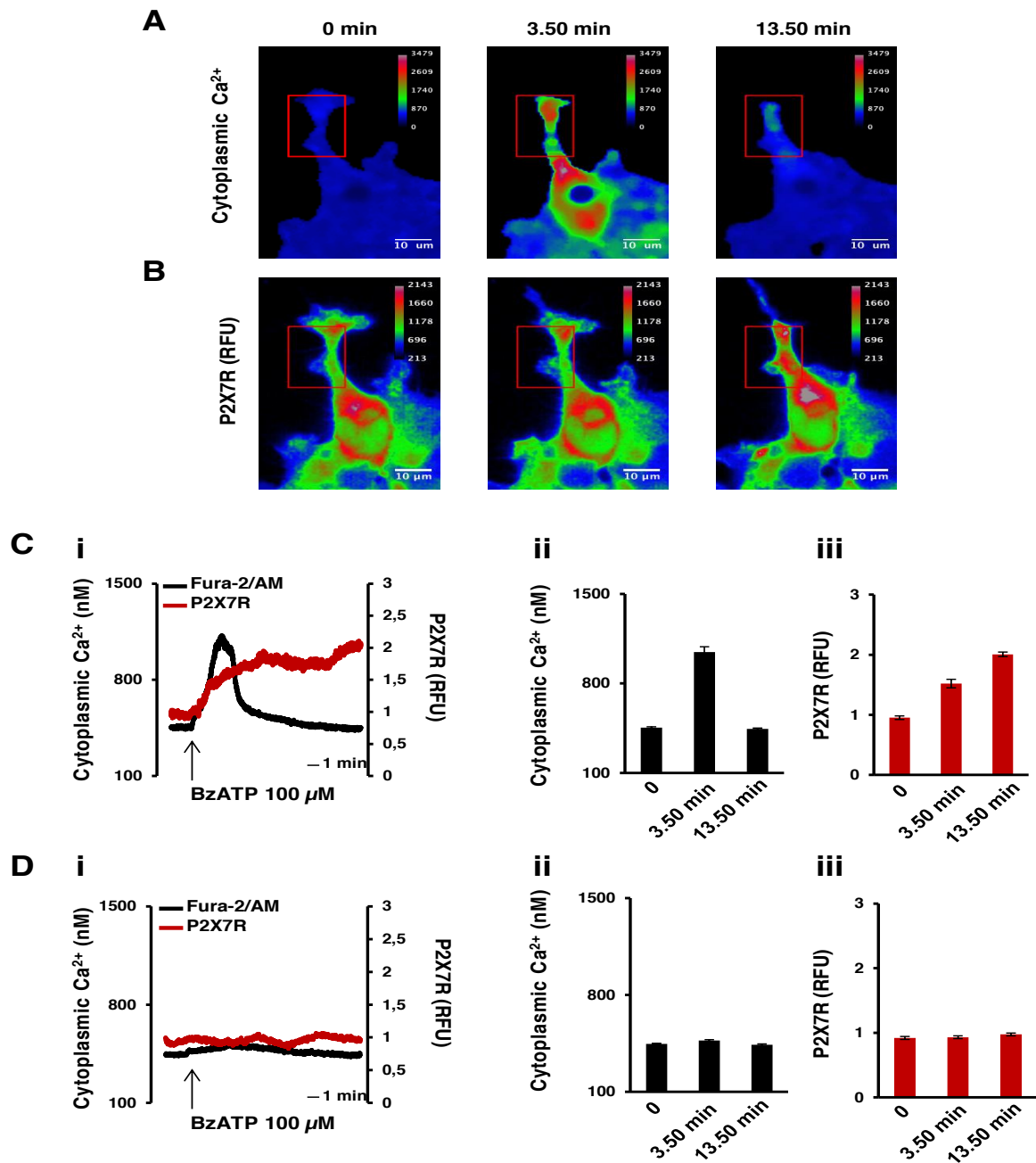
Figure 6. P2X7 activation drives P27X recruitment at discrete subplasmalemmal foci. HEK293 cells were t ransfected with rat P2X7 -GFP, as described in Materials and Methods, loaded with Fura-2/AM, placed in an open, thermostatted Leyden chamber at 37°C, and challenged with a BzATP puff (100 mM) delivered with an Eppendorf femtotip connected to an Eppendorf microinjector system (Materials and Methods). Images were acquired at the indicated time points as described in Materials and Methods. A) BzATP-triggered cytoplasmic Ca^{2+} changes. B) BzATP-triggered P2X7 -GFP recruitment. Ci–Ciii) Kinetics and statistic analysis of BzATP-triggered cytoplasmic Ca^{2+} changes and P2X7 -GFP recruitment measured in area within the red square shown in A and B (n = 10). Di–Diii) Kinetics and statistical analysis of BzATP-triggered cytoplasmic Ca^{2+} changes and P2X7-GFP recruitment measured at a cytoplasmic site distal to the site of stimulation (n = 10). Data are represented as mean 6 SEM. Bar = 10 mm.

DISCUSSION

The inflammasome consists of a multiprotein complexes responsible of the conversion of inflammatory pro-caspase-1 into caspase- 1 and subsequentially this enzyme induces the conversion of pro-IL-1β and pro-IL- 18 into the respective mature forms. (213,214). A thorough understanding of the molecular mechanism of activation is of fundamental importance in the context of inflammation and cancer where IL-1β is one of the major molecules involved in both conditions. Different inflammasome subtypes have been identified in the years based on scaffold molecule and NLRP3 are the best characterized most probably for its involvement in human disease (215). The NLRP3 inflammasome has been implicated in the pathogenesis of a wide variety of diseases, including genetically inherited autoinflammatory conditions as well as chronic diseases in which IL-1β play a causative role (216). Several triggers for the NLRP3 inflammasome have been identified: cytoplasmic release of cathepsin B, the PKR kinase, thioredoxin inhibitory protein, cell swelling, an increase in the intracellular Ca^{2+} concentration, and efflux of cytosolic K^+. One of the most potent stimuli for NLRP3 inflammasome activation is extracellular ATP which it acts as an inflammatory mediator (217,218).

Extracellular ATP is a ubiquitous DAMP that operate through a complex purinergic signaling network (219). The purinergic P2 receptor family is comprised of the P2Y and P2X subfamilies, numbering 8 and 7 members each (12). The P2X7 is the only P2 member associated with NLRP3 inflammasome activation (220). The P2X7 receptor is a trimeric ATP-gated cation channel that, on sustained stimulation, triggers the opening of a large conductance pore that mediates massive K^+ efflux and Na^+ and Ca^{2+} influx, as well as uptake of hydrophylic solutes of MW up to 900 Da (221). P2X7 and NLRP3 are obviously functionally linked given the prominent role of extracellular ATP as a DAMP and a stimulus for IL-1β maturation and release. In addition, present findings show that these 2 molecules are intimately linked, as P2X7, besides inducing NLRP3 activation, also modulated NLRP3 expression levels. P2X7 down-modulation, whether induced by prolonged exposure to high extra-cellular ATP concentrations (N13ATPR cells), by shRNA (B16 melanoma cells) transfection, or by genetic deletion (P2X7 $^{-/-}$ macrophage and microglia cells), was always associated to a large increase in NLRP3 mRNA accumulation. However, at the protein level, induced vs. genetic P2X7 down-modulation had opposite effects: induced P2X7 down-modulation was paralleled by a decrease in NLRP3 protein expression, whereas on the contrary, genetic P2X7 deletion was associated to a striking increase in NLRP3 expression. ASC expression did not show a clear-cut pattern of changes in response to P2X7 down-modulation, because in N13ATPR cells,

ASC protein was significantly reduced compared with N13wt, whereas in shRNA-treated B16 cells, despite a large increase in mRNA accumulation, it was unchanged. In cells from P2X7 $^{-/-}$ mice, neither ASC mRNA nor protein expression differed compared with WT. It needs to be stressed that the procedures used to acutely down- modulate P2X7 inevitably cause cell activation (because of sustained stimulation with extracellular ATP or to shRNA transfection), which despite increased mRNA accumulation, might accelerate NLRP3 protein degradation; thus, they are not directly comparable to genetic deletion.

A typical feature of the P2X7 is its ability to drive large transmembrane cation fluxes via a poorly characterized nonselective large conductance pore (222,223). The physiologic significance of the large P2X7 pore is currently unknown. It has been hypothesized that it is involved in cytotoxicity (224), but although it is undisputed that under certain in vitro conditions P2X7 mediates necrotic or apoptotic cell death, it is also pretty clear that P2X7 functions are not restricted to cell death (225,226). This is even more cogent as the role of P2X7 in inflammation and immunity increasingly appears to be important (227). The proinflammatory function of the P2X7 large pore might be easier to understand if its activation was restricted to localized cytoplasmic sites where the associated Ca^{2+} increase and K^+ drop were sensed by an appropriate transduction system. The NLRP3 inflammasome is likely to be the chief transduction apparatus that converts the drop in cytosolic K^+ caused by P2X7 receptor activation into a proinflammatory signal. Although P2X7 is not necessary for NLRP3 activation by certain stimuli that gain direct access to the cytoplasm (228,229), it is now clear that K^+ efflux is the common final pathway that drives NLRP3 inflammasome activation (230). Few, if any, plasma membrane receptors are able to trigger fast and massive K^+ fluxes like P2X7, and in turn, P2X7 -mediated inflammasome activation is entirely dependent on NLRP3 expression (210). Present data suggest that, although the P2X7 is not an integral inflammasome component, it associates to the inflammasome at discrete foci in the subplasmalemmal region, in both resting and activated conditions. Close in- teraction between P2X7 and NLRP3 has important implications for the mechanism of inflammasome activation because it localizes NLRP3 exactly where the K^+ drop occurs, maximizing NLRP3 stimulation and minimizing possible untoward effects caused by an unrestricted loss of cytoplasmic K. Furthermore, increased P2X7 /NLRP3 recruitment triggered by P2X7 stimulation provides a molecular mechanism for the amplification of the initial proinflammatory stimulus. Recruitment of P2X7 at discrete plasma membrane sites might be beneficial in additional ways, e.g., to concentrate P2X7 where it is needed for inflammasome activation and to remove P2X7 from areas where its activation might cause an unnecessary and even detrimental perturbation of cytoplasmic ion

homeostasis. Interestingly, P2X7 stimulation promoted P2X7 and NLRP3 colocalization but had a small effect on total cellular P2X7 or NLRP3 levels. On the contrary, LPS was an efficient stimulus for both colocalization and enhanced P2X7 and NLRP3 expression, both at the mRNA and protein level. In response to ATP, BzATP, or LPS, the adaptor molecule ASC showed little changes, whether at the mRNA or protein level.

In conclusion, we show that P2X7 and NLRP3 closely interact and colocalize at discrete sites in the subplasmalemmal cytoplasm where P2X-7dependent changes in the ion concentration occur. This allows inflammasome activation and prevents possible cell damage caused by a generalized and uncontrolled increase in cytoplasmic Ca^{2+} and depletion of cytosolic K^{+}.

P2X7R is expressed in Mitochondria

4. AIMS

P2X7 receptor is a trimeric ATP-gated cation channel principally known for induce cell death after longer activation by ATP, which leads to membrane permeabilization and cell death. On the contrary, its brief activation produces rapid inward cationic currents and intracellular signalling pathways associated with numerous physiological processes such as the induction of the inflammatory cascade, cell proliferation and survival. The role of P2X7 receptor in cell proliferation would seem a nonsense, but there is clear evidence from different cell types. The molecular mechanism of this process is not well clarified, but mitochondria seems play a pivotal role. HEK-293 cells transfected with P2X7 receptor resulted in higher concentration of mitochondrial Ca^{2+} and ATP store due to a more efficient oxidative phosphorylation. Moreover measurement of mitochondrial membrane potential in P2X7-trasfected cells displayed a P2X7-dependent hyperpolarization.

This project aims at investigating P2X7 localization to the mitochondria and the P2X7 role in mitochondrial physiology. P2X7 receptor is known as plasma membrane ATP-gated cation channel but we hypothesizes a possible intracellular distribution. Therefore we investigated P2X7 localization in the mitochondrial compartment.

P2X7-trasfected cells have been demonstrated to display a more efficient oxidative phosphorylation and higher intracellular ATP content that confers growth advantage. Therefore we analysed a range of parameters linking P2X7 receptor to mitochondria metabolism and function, such as energy profile in primary cell cultures from P2X7-WT or KO mice, and in several cell lines with variable P2X7 expression. Metabolic parameters were correlated with ROS production and cell migration.

5. RESULTS

5.1 The P2X7 is expressed in Mitochondria

P2X7R fluorescence intensity increases after different stressor stimuli.

To investigate the relationship between P2X7 receptor and mitochondria when cells are exposed to cellular stress stimuli, we first analyzed P2X7 fluorescence expression and followed modulation in time. We used the widely used P2X7 agonist BzATP and mitochondrial-stress stimuli, such as rotenone which induced inhibition of mitochondrial respiratory chain at complex I, and hydrogen peroxide (H_2O_2) which can be reduced to hydroxyl radical (OH). We used a stable clone of human embryonic kidney 293 human P2X7 receptor cell line (HEK293-hP2X7R). Treatment with BzATP and Rotenone induced an increase of P2X7 fluorescence intensity, significant after 1 and 6 hours whereas H_2O_2 had an effect in the early phase of treatment with an important fluorescence gain after only 20 minutes, maintained in the course of time.
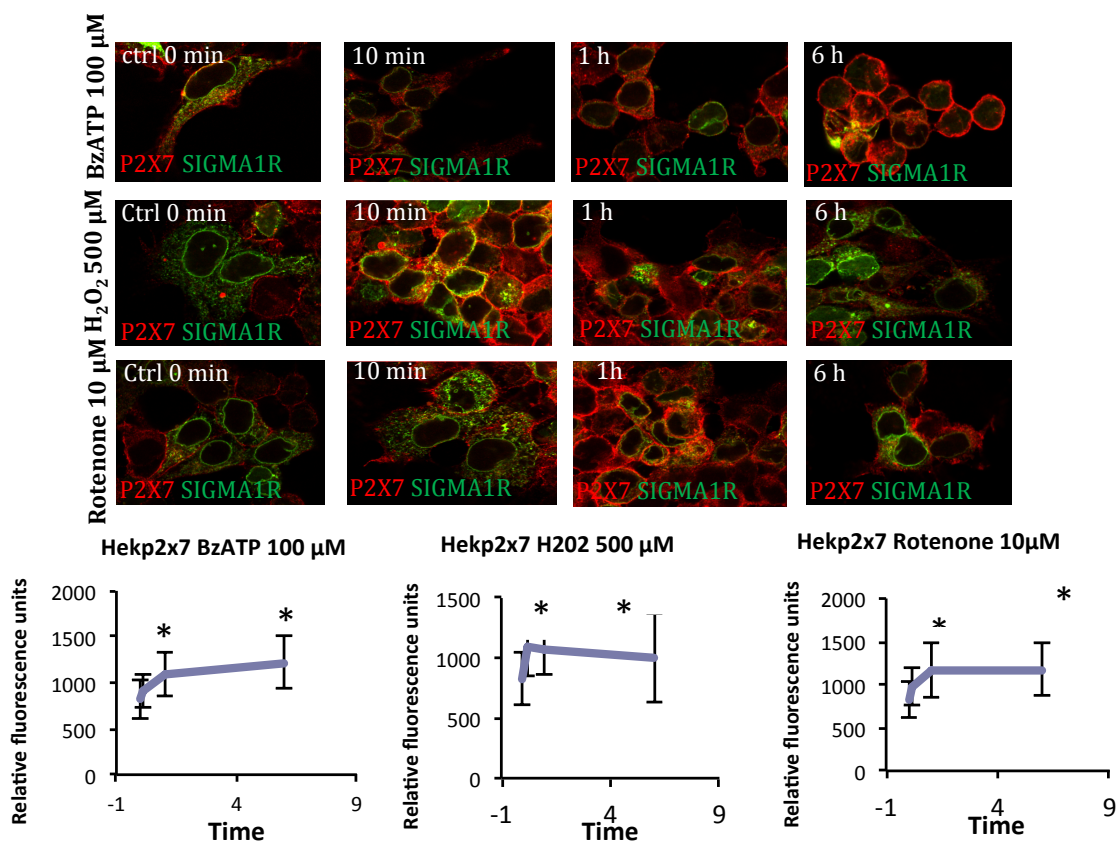
Figure 8. Increase of P2X7 fluorescence intensity over time. Confocal microscopy images of P2X7 (red) and Sigma1R (green) co-stained in fix HekP2X7h cells, in basal condition and after 3 different stimuli, BzATP (100 uM), H_2O_2(500 uM) and Rotenone (10uM). The graph shows the trend of P2X7R fluorescence over the time, with BzATP and Rotenone there is an significant increase after 1 and 6 h and with H202 after 20 minutes and 1 h (*p <0,05; bars S.D.).

P2X7R is localized to mitochondria.

To analyze the mitochondrial localization of P2X7, we performed detailed subcellular fractionation in mouse embryonic fibroblasts cells from wild-type mice, Mefs wild-type cells. We isolated crude mitochondria, nuclei and a cytosolic fraction containing lysosomes and microsomes. Subsequent ultracentrifugation of the cytosolic fraction results in the separation of ER and cytosol, whereas the crude mitochondria preparation was further fractionated on a Percoll gradient to obtain purified mitochondria. We evaluated total homogenate, crude mitochondria, pure mitochondria and cytosol fractions by immunoblot analyses (Figure 9 A) using IP_3R_3 as a marker of MAMs, β-tubulin as marker of cytosol, VDAC as marker for mitochondria and Sigma 1RE as a marker of endoplasmicreticulum.

We verified the intracellular distributions of P2X7 in HEK293-hP2X7R cells stained with anti-P2X7 Abs and anti-Tom 20 as a specific marker for the mitochondria. Immunofluorescence analyses confirmed the presence of P2X7 at the mitochondria. Loalization of P2X7 to the mitochondria increases treatment cellular stress stimuli such as BzATP (100 uM), H_2O_2 (500 uM) and Rotenone (10 uM) (Figure 9B).
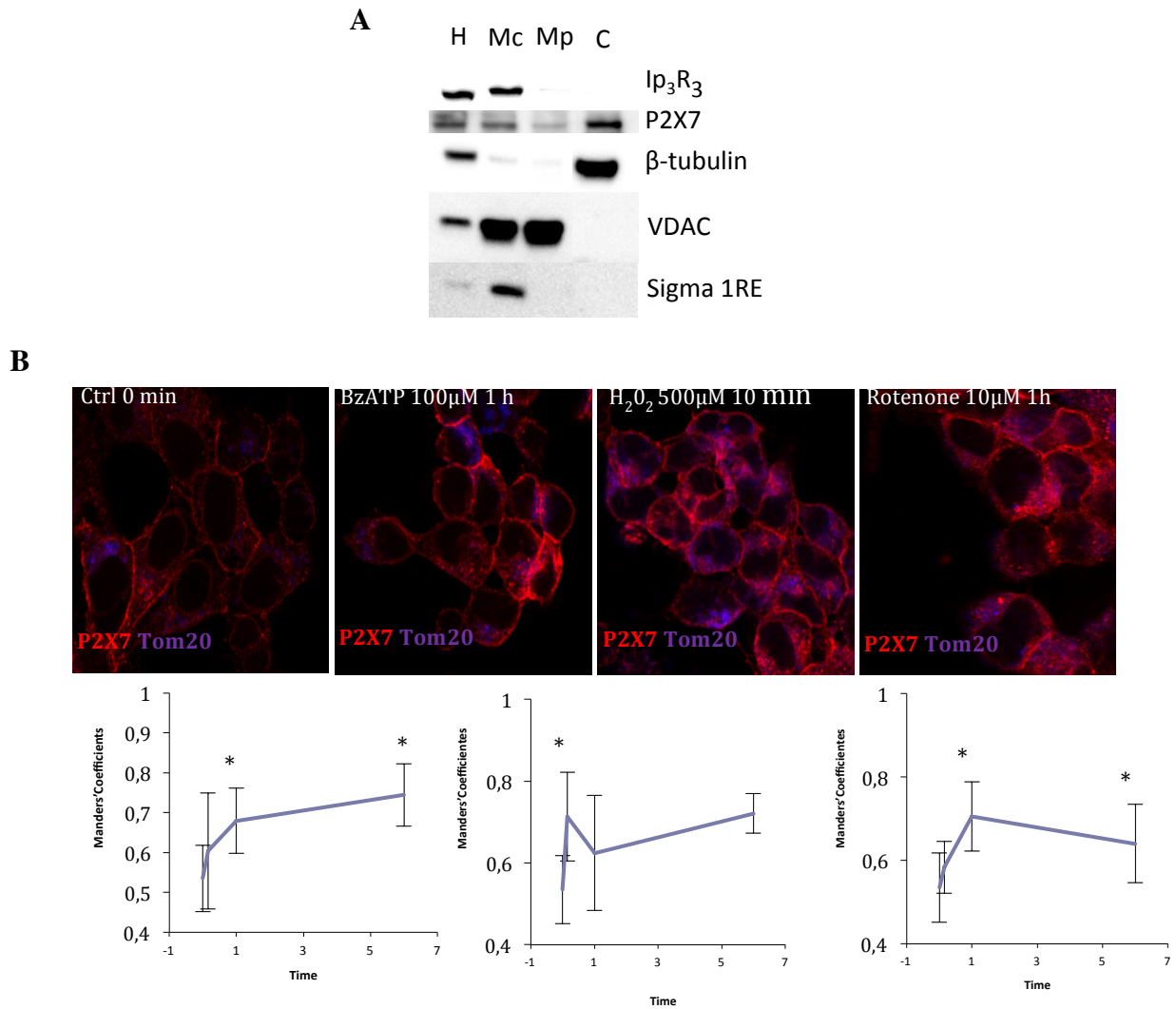
Figure 9. P2X7 intracellular localization. A Subcellular fraction of mouse embryonic fibroblasts (Mefs); H, homogenate; Mc, crude mitochondrial fraction; Mp, pure mitochondrial fraction C, cytosol. Ip3R3 was used as subcellular marker for MAMs, VDAC for mitochondria and Sigma1R for Endoplasmic reticulum. P2X7 is present in different district, cytosol, Mc fraction and in Mp fraction. **B** The below panel shows confocal microscopy images of P2X7 (red) and TOM 20 (violet) co-stained in HekP2X7h cells, at different time point after treatment with BzATP, H_2O_2 or Rotenone. Graphs under the microscopy images show the colocalization of P2X7 VS mitochondria (TOM 20) measured by Mandre's Coefficient.*p <0,05; bars S.D.

5.2-P2X7 modulates mitochondrial metabolism

P2X7 receptor modulates mitochondrial metabolism

We measured oxygen consumption rate (OCR), maximal respiratory capacity, spare respiratory capacity, ATP coupled respiration, and proton leak of the electron transport chain (ETC) in the microglial cell line (N13) and in primary cell cultures (microglia, Mef) from WT or P2X7-KO mice using the Seahorse XFe96 Analyzer (Seahorse Bioscience, Massachusetts, USA QUESTO LO METTI NEI MATERIALI E METODI). Mitochondrial OCR and ECAR allowed to measure the effect of P2X7 expression/activation on oxidative phosphorylation (OXPHOS) and glycolysis, respectively. The difference in mitochondrial function of N13-WT Vs N13-R, microglia-WT VS microglia P2X7-KO, Mef-WT VS Mef-P2X7-KO was analyzed by sequentially adding specific mitochondrial inhibitors, which allowed investigation of individual coupling sites of the respiratory chain. The addition of oligomycin, a natural antibiotic that inhibits F0/F1 ATPase (complex V), differentiates the ATP-linked respiration from the proton leak. Following oligomycin addition, the maximal respiratory rate was determined by subsequent addition of FCCP, an uncoupler that maximally stimulates OCR. Finally, antimycin A addition inhibited the electron flux at complex III and allowed to measure residual OCR from non-mitochondrial respiration. As shown in Figure 10 all the mitochondrial respiratory parameters were severly inhibited in P2X7 null cells or in xells with reduced P2X7 expression. Changes in mitochondrial metabolism in $P2X7_{-KO}$ versus WT cells might be due to a reduced mitochondrial content. To exclude this possibility, we quantitated the amount of TOM 20 (a protein present in the outer mitochondrial membrane), Tim 23 (localize in inner membrane) and Hsp60 (present in the matrix) in the different mitochondrial preparations. A s shown in Fig.11, there was no significant change in mitochondrial content in the different cell types.
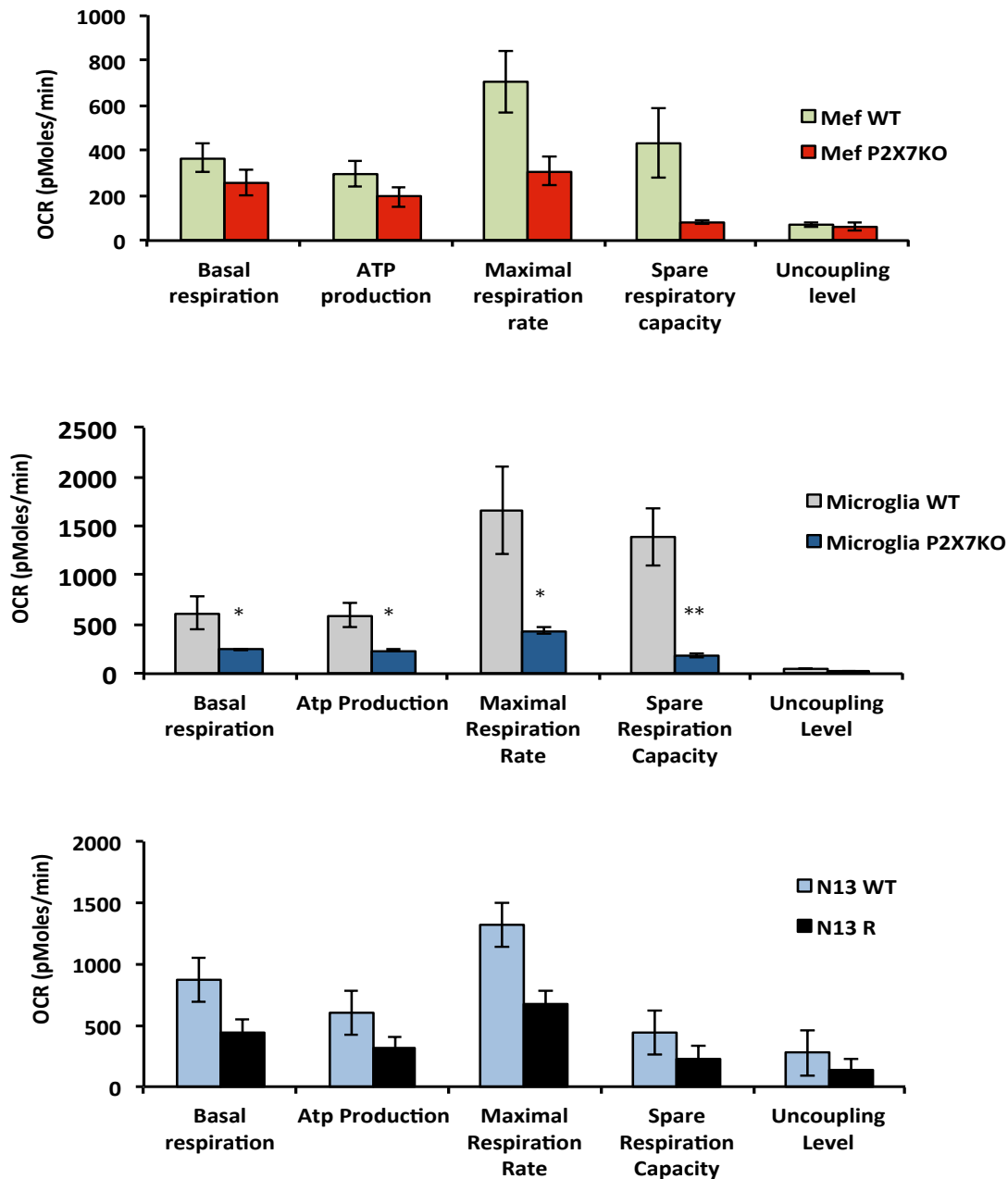
Figure 10. P2X7 modulate mitochondrial metabolism. Oxygen Consumption Rates (OCR) and respiration parameters in 2 different primary culture of cells P2X7 wt or ko (Mefs and Microglia) and one cell line P2X7 wt or P2X7 poor (N13). Oxygen Consumption Rate (OCR) trace was determined using a Seahorse XF24 Analyzer. Basal respiration, Atp production, Maximal Respiratory Capacity, Spare Respiratory Capacity and Proton leak where all decreased in cells without or with a lower expression of P2X7. * p<0.05 **p <0.02 bars S.D.
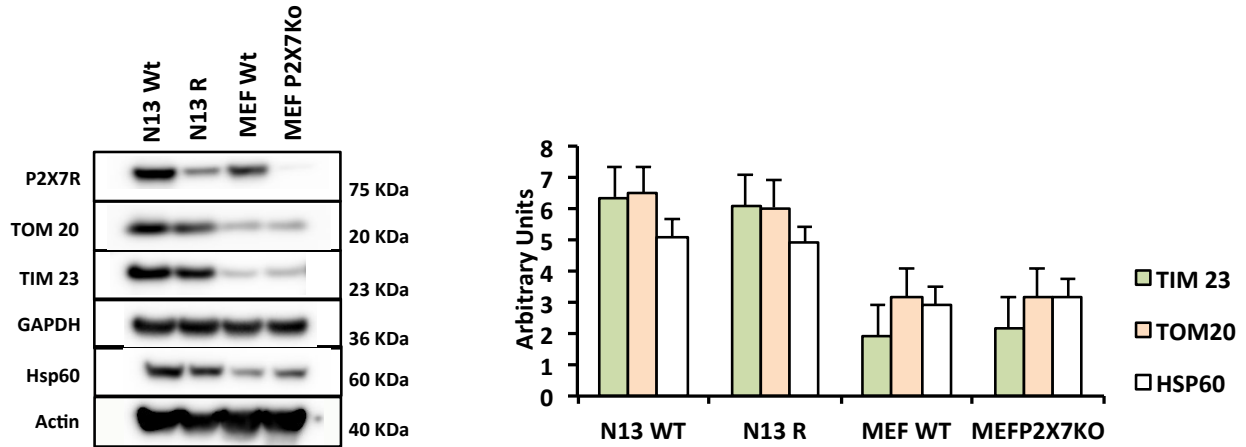
P2X7R-dependent changes in mitochondrial metabolism are not due to changes in mitochondrial protein content

Figure 11. Western blot analysis of different mitochondrial protein in P2X7Rwt or R N13 cells and in P2X7RWT or KO Mefs cells. Tom 20 was used as a marker of outer mitochondria membrane, Tim 23 as a marker of inner mitochondria membrane and Hsp60 as a matrix marker. The right graph shows no difference in the content of the same protein in N13 wt VS N13 R and in MefWT VS MefP2X7KO. bars S.D.

P2X7R down-regulation reduce mitochondrial membrane potential

The respiratory chain and mitochondrial ATP production are coupled through the mitochondrial membrane potential (Ψm), providing the proton motive force needed for ATP synthesis at mitochondrial complex V. Tetramethyrhodamine methyl ester (TMRM) is a lipophilic potentiometric dye used as a fluorescent probe to monitor the membrane potential of mitochondria. We used TMRM for analyzed the cellular impacts of P2X7 receptor deficiency, using P2X7-knockout cells line and primary culture, on mitochondrial membrane potential. Ψm appeared to be decreased in N13R, microglia P2X7KO and Mef P2X7KO cells.
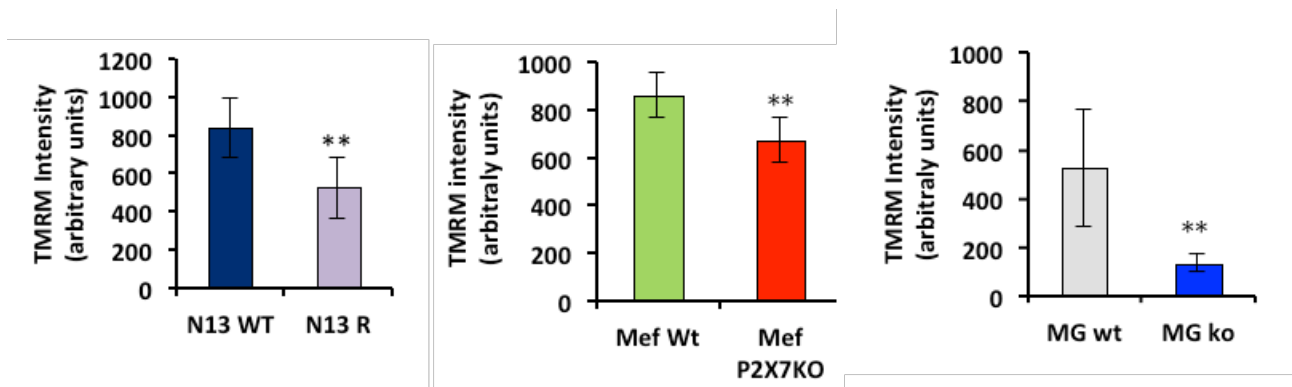
Figure 12. Mitochondrial membrane potential in P2X$_7$wt or KO cells .N13 , Microglia and Mefs cells are staining with TMRM (50 nM, red) and treated with FCCP (10 μM). The intensity of TMRM reflects the level of $\Delta\Psi_m$. The TMRM signal is reduced in P2X7RKO or P2X$_7$-less cells relative to wild-type cells.

Lack of P2X7 receptor does not impair electron flux in isolated mitochondria.

To better understand P2X7 receptor role in the modulation of mitochondrial metabolism we analysed isolated mitochondria from liver of P2X7-WT or P2X7-KO mice. This experiment is designed to investigate each single complex of the electron transport chain by the addition to uncoupled mitochondria of specific inhibitors of the different coupling sites (Fig.13). No differences in electron flow throughout all the different conditions tested were observed. These data suggest that P2X7 effects on mitochondrial metabolism depend on a signalling pathway requiring and intact intracellular environment.

Figure 13. P2X7 receptor doesn't influence complex of respiratory chain in isolated mitochondria. Electron flow bioenergetics experiment. A: General oxygen consumption rate (OCR) profile after the consecutive addition of rotenone, succinate, antimycin A, and ascorbate/TMPD. Initial maximal respiration is under FCCP. Each assayed in six replicates. Bar S.D

5.3 P2X7 receptor stimulates cell migration and stimulates ROS production.
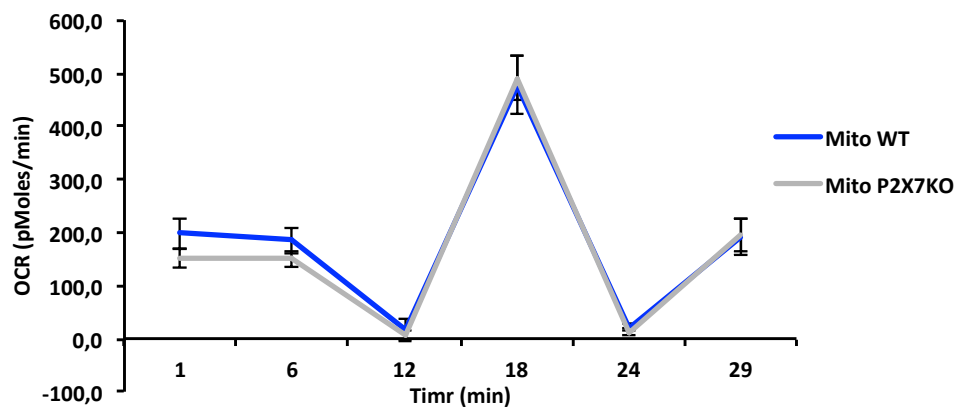
P2X7 receptor raises cell migartion trought Ros production

P2X7 activation has been reported to induce ROS formation in a number of cell types, including primary microglia (Parvathenani et al; 2003). Thus, ROS formation in the N13 cell line was investigated using the ROS sensitive probe DCF. Cells loaded with H2DCFDA (which is converted to DCF inside cells) were incubated in the absence or presence of mitochondrial substrate methyl succinate (electron donor at complex II of respiratory chain). Incubation with 2.5 mM methyl succinate induced significant ROS formation in both N13 wt and N13 R cells compared to control cells. N13R cells became after treatment able to produce an amount of Ros similar to wild type cells (Fig.14 D). Moreover to address the role of P2X7-mitochondria-Ros on cell migration, we employed the wound-healing test. Cells were induced to migrate into a wound created by scratching confluent cultures with a pipette tip to examine the migration of N13 R cell lines respect N13 WT. N13 were selected for this experiment because of their characterized high migratory potential. Closure of wounded area was monitored for 24 h. As shown in 14 A, the open area was rapidly partial covered by the N13 wt cells in comparison with N13 R cells after 24 h. Furthermore, methyl succinate accelerated wound closure in N13 R cells at 24 h than the untrated cells (Fig.14). Quantification of wound closure is represented in bar diagram in Fig. 14 B. The quantified open area in vector control cells were reduced from 100% to 42%, N13WT cells and only 57 % in N13 R cells where shrunk from 100 to 35%, after methyl succinate tratment. These data suggest that induction of Ros production via mitochondria respiratory chain significantly accelerates motility of the N13 R cells.
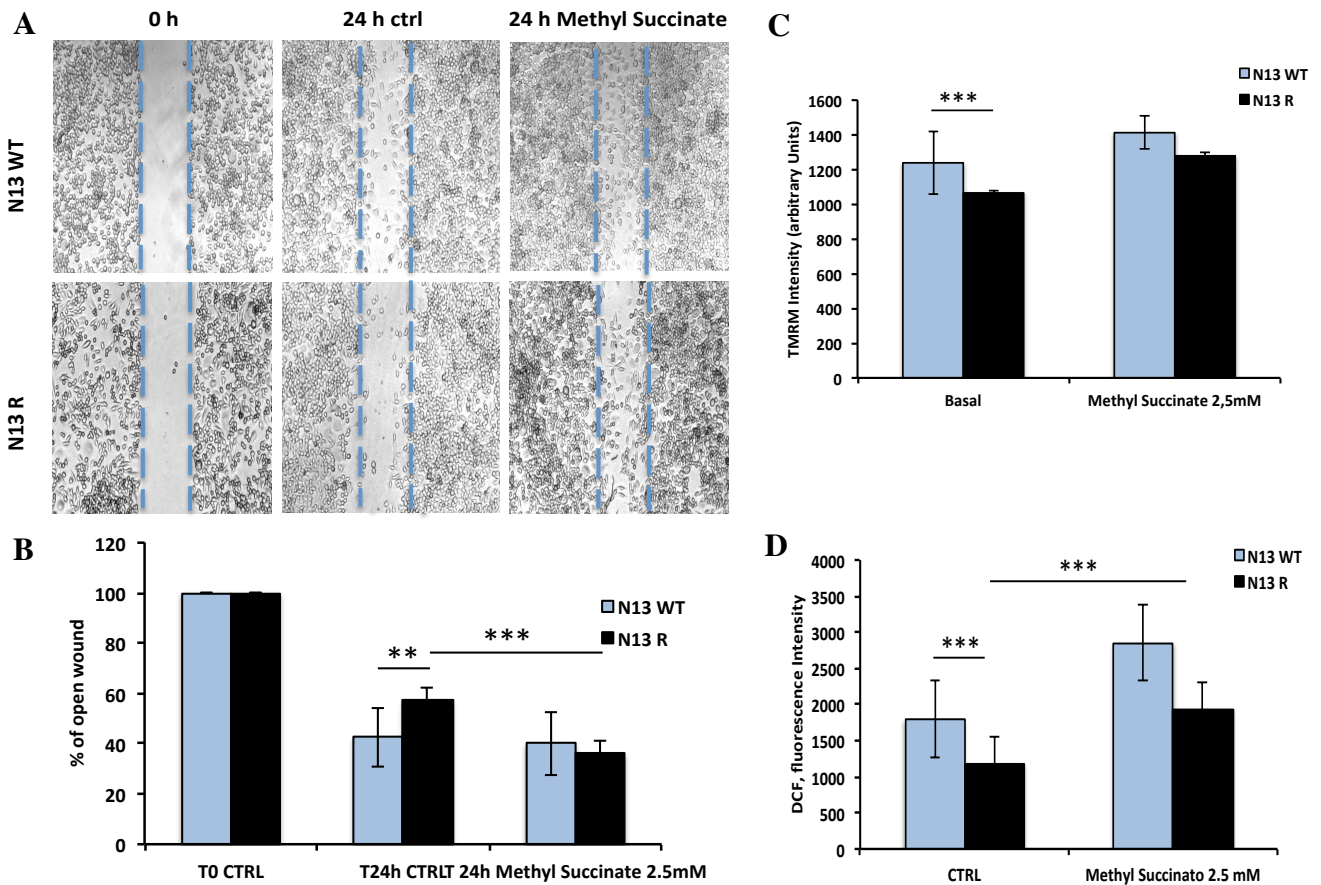
Fig.14. P2X7 receptor raises cell migartion trought Ros production. Phase contrast photographs of the cultures taken at 0 h (immediately after scratching) and at the indicated time intervals show the wound closure by cells showing N13 WT (up panels) and N13 R (below panel) **(B)** Quantification of the wounded area invaded at different time points by treated/untreated N13 WT or N13 R. Results represent the mean of five measures of each wounded area, obtained on triplicate biological samples. Error bars indicate s.d. **(C)** Effects of Methyl Succinate on mitochondria membrane potential. The mitochondrial membrane potential ($\Delta\Psi$) was monitored using TMRM staining. N13 cells were preloaded with TMRM (50 nM) 30 min before Methyl Succinate (2.5 mM) treatment. The intensity of TMRM fluorescence was detected using a fluorescent microscope and followed in time course. Methyl Succinate induced an increse of the mitochondria membrane potential within 30 min. **(D)** N13 WT and N13 R were stained with H_2DCF-DA to measure intracellular ROS, in control or treated conditions with Methyl Succinate for 30 minutes analyzed by image-based cytometer. Histograms are then generated to display cell size and GFP fluorescence intensity. Graphs represent the mean ± SD from three replicates. P***<0.005.

DISCUSSION

P2X7 receptor is a trimeric ATP-gated cation channel found predominantly on immune cells. It is principally known to induce cell death through apoptosis after longer activation by ATP, which leads to membrane permeabilization and cell death. On the contrary, its brief activation produces rapid inward cationic currents and intracellular signalling pathways associated with numerous physiological processes such as the induction of the inflammatory cascade, cell proliferation and survival. (233). The role of P2X7 receptor in cell proliferation would seem a nonsense, but there are clear evidences provided from different cell types, P2X7-transfected leukemic cells, normal T- and B-lymphocytes, microglia, fibroblasts (100;1001;102; 103;104).

The molecular mechanism of this process is not well clarified. In an attempt to understand the role of P2X7 receptor in cell proliferation, our laboratory did a series of experiments in which (105) there were shown how HEK-293 cells transfected with the P2X7 receptor resulted in higher resting concentrations of mitochondrial Ca^{2+} and the subsequent release of large amounts of this cation from intracellular stores. In turn, this increase of Ca^{2+} stimulated NADH synthesis and ATP production via oxidative phosphorylation. This elevated intracellular ATP content facilitated cell survival and growth. Moreover, starting from this result, a second study has shown how P2X7 expression in transfected HEK-293 cells increased intracellular Ca^{2+} by disrupting endoplasmic reticulum function leading to the activation of the nuclear factor of activated T-cells (NFATc1) and consequently to the improvement of cell survival and cell protection from apoptosis (106). These evidences suggest an important role-played by mitochondria in P2X7-mediated cell proliferation or cell death and Ca^{2+} was hypothesized to be a linker between P2X7 and mitochondria. Furthermore cytotoxicity due to a strong P2X7 stimulation is preceded by mitochondrial swelling or even disruption of the mitochondrial network.

For better understand the relationship between P2X7 and mitochondria we investigated in major detail the intracellular distribution of P2X7 receptor using different technique, such as cellular fractionation or immunofluorescence. Our results showed that P2X7 receptor is present not only in the plasma membrane but also in mitochondria and this data reinforce our idea of the pivotal role of this receptor in the mitochondrial energy state modulation or influence. The immunofluorescence had shown an initial colocalization between P2X7 receptor and mitochondria, which increases after cellular stress stimuli. These observations can suppose an enrichment of P2X7 at this compartment.

To outline the functional relevance of P2X7 localization in mitochondria we analysed the energy

profile in different cell type, such as primary culture (Mefs, Microglia) and cell lines (N13). Cells knocked-out for P2X7 receptor have shown a decrease of all the mitochondrial key parameters compared to wild-type cells, with a minor basal respiration, ATP production and respiratory capacity. The lower levels of respiration could arise from a decrease of the mitochondria's number, but this explanation is unlikely since the amount of mitochondrial proteins were similar both in the wild-type and in knock-out cells. To support this finding, the resting mitochondrial membrane potential was higher in wild-type cells and is coupled with respiratory chain for providing the proton motive force needed for ATP production at mitochondrial complex V. It is well established that an increased mitochondrial membrane potential contributes to higher rates of mitochondrial ROS production (*234*), and its already reported the link between P2X7 receptor activation and ROS production (87). Our results confirm the correlation between P2X7 receptor, mitochondrial membrane potential and ROS production. Indeed the P2X7 KO cells exhibit a lower mitochondrial potential and a reduction of capacity to generate Ros. These data linked perfectly with the impaired mitochondrial metabolism. Moreover ROS (235) and N13R presents in fact a reduced ability to close the wound compared to wild-type cell (Wound hilling assay). We demonstrated the possibility to restore the migratory ability of cells trough the administration of an electron donor for complex II of respiratory chain, Methyl Succinate, which increased mitochondrial membrane potential leading to a major ROS production. All these observations support the important role of P2X7 in favourite cell functions which reclaim the contribute of functional mitochondria to produce ATP and to provide a wider framework of P2X7-vantage, in physiological and in pathological conditions. In different cancer P2X7 receptor is overexpress leading to benefits, such as more efficient mitochondrial metabolism and ATP synthesis. The efficient mitochondrial metabolism implicates a sustain mitochondrial potential and this is correlated with resistance to hypoxia, anchorage-independent growth, and invasion of the basement membrane (236). The biochemical mechanism by which an increased mitochondrial potential allows better survival and growth is unknown, but our finding suggest that cells with hyperpolarized mitochondria accumulate higher cellular ATP stores providing a reasonable physiological explanation as adequate energy stores are a pre-requisite for any cell function.

6. MATERIALS AND METHODS

Reagents

Benzoyl ATP (BzATP) was purchased from Sigma-Aldrich (St. Louis, MO). TMRM (Molecular Probes, Leiden, The Netherlands) was dissolved in DMSO to obtain a 10 mM stock solution and then diluted in the appropriate buffer. Carbonyl cyanide *a*-[3-(2-benzothiazolyl)6-[2-[2-[bis(carboxymethyl)amino]-5-methylphenoxy]-2-oxo-2*H*-1-benzopyran-7yl]-   *b*-(carboxymethyl)-tetrapotassium salt (FCCP) (Sigma-Aldrich) was solubilized in ethanol to a final stock concentration of 10 mM.

Cells culture

HEK293 cell was cultured in DMEM-F12 (Sigma- Aldrich). Media was complemented with 10% heat-inactivated fetal bovine serum (FBS), 100 U/ml penicillin, and 100 mg/ml streptomycin (all from Invitrogen, San Giuliano Milanese, Italy). Stable P2X$_7$R clones were kept in the continuous presence of 0.2 mg/ml G418 sulfate (Geneticin) (Cal- biochem, La Jolla, CA). Experiments, unless otherwise indicated, were performed in the following saline solution, also referred to as "standard saline" in the text: 125 mM NaCl, 5 mM KCl, 1 mM MgSO4, 1 mM NaH$_2$PO4, 20 mM HEPES, 5.5 mM glucose, 5 mM NaHCO$_3$, and 1 mM CaCl$_2$, pH 7.4. Microglial wild-type (WT; N13wt) and ATP-resistant (N13ATPR) N13 cells were obtained and cultured in RPMI 1640 medium (Sigma-Aldrich, St. Louis, MO, USA), supplemented with 10% heat-inactivated fetal bovine serum, 100 U/ml penicillin, and 100 mg/ml streptomycin (Euroclone, Milano, Italy) . Primary mouse microglia cells were isolated from 2- to 4-day-old postnatal mice as described previously (13). Primary MEFs Wt and P2X7Ko were prepared from embryos at day 13.5 of development (E13.5). Embryos were harvested and the individual MEFs were cultured in DMEM medium supplemented with 10% FBS, penicillin/streptomycin, and 2 mM L-glutamine. B16 cells were grown in RPMI medium supplemented with 10% fetal bovine serum, 100 U/mL penicillin, 100 mg/mL streptomycin, and nonessential amino acids (Sigma-Aldrich). B16 transfection was performed with TransIT-2020 transfection reagent (Tema Ricerca, Bologna, Italy) following the manufacturer's instructions. The P2X7 short hairpin RNA (shRNA) in pSuper.neo.green fluorescent protein (GFP) vector was a kind gift of Dr Diaz-Hernandez (Universidad Complutense, Madrid, Spain). Stably transfected cell lines were obtained by se- lection with G418 sulfate (0.2–0.8 mg/ml; Calbiochem, La Jolla, CA, USA). Single cell-derived clones (B16 shRNA) were ob- tained by limiting dilution. HEK293 ratP2X7-GFP cells (HEK293- P2X7R-GFP) were obtained and cultured as previously descri- bed by Lemaire et al. (12).

Immunoprecipitation

For coimmunoprecipitation experiments, cells were incubated on ice for 45 minutes in the following lysis buffer: 150 mM NaCl, 5 mM EDTA, 20 mM Tris, pH 7.5, 1% Triton X-100, 1 mM ben- zamidine, 1 mM phenylmethylsulfonyl fluoride, and protease inhibitor cocktail (all from Sigma-Aldrich). Lysates were clarified by centrifugation for 5 minutes at 20,000 g before use. Total protein content of cell lysates was measured with the Bradford assay. Immunoprecipitation was performed using Dynabeads Protein A (Life Technologies, Carlsbad, CA, USA) according to the manufacturer's instructions. Dynabeads were preincubated with polyclonal rabbit anti-NLRP3 (cat no. ab91525; Abcam) and polyclonal rabbit anti-P2X7 (cat no. P8232; Sigma-Aldrich) antibodies before addition of lysates. As negative controls, eluates from antibody-coated beads in the absence of cell lysate and eluates from antibody-uncoated beads incubated together with the cell lysate were loaded

Quantitative RT-PCR

Total mRNA was extracted with TRIzol Reagent and the PureLink RNA Mini Kit (Life Technologies). RNA quality and concentra- tion were checked by electrophoresis on 1.5% agarose gel and spectrophotometric analysis, respectively. Quantitative RT-PCR was performed with the High-Capacity cDNA Reverse Tran- scription Kits (Applied Biosystems/Life Technologies, Foster City, CA, USA). Samples were run in triplicate in an AB StepOne. Real Time PCR (Applied Biosystems) with TaqMan Gene Ex- pression Master Mix (Applied Biosystems) using the following primers: Mm00440578m1 (P2X7), Mm00840904m1 (NLRP3), Mm00445747g1 (ASC), and 4352339E (mouse glyceraldehyde 3-phosphate dehydrogenase, mGAPDH) (Applied Biosystems Life Technologies). Quantitative RT-PCR was performed in duplicate following Minimum Information for Pub-lication of Quantitative Real-Time PCR Experiments guidelines (15).

Subcellular Fractionation

Cells were harvested, washed by centrifugation at 500 g for 5 min with PBS, resuspended in homogenization buffer (225 mM mannitol, 75 mM sucrose, 30 mM Tris-HCl pH 7.4, 0.1 mM EGTA, and PMSF) and gently disrupted by dounce homogenisation. The homogenate was centrifuged twice at 600 g for 5min to remove nuclei and unbroken cells, and then the supernatant was centrifuged at 10,300 g for 10 min to pellet crude mitochondria. The resultant supernatant was centrifuged at 100,000 g for 90 min (70-Ti rotor, Beckman) at 4 °C to pellet the ER fraction. The crude mitochondrial fraction, resuspended in isolation buffer (250 mM mannitol, 5 mM HEPES pH

7.4 and 0.5 mM EGTA), was subjected to Percoll gradient centrifugation (Percoll medium: 225 mM mannitol, 25 mM HEPES pH 7.4, 1 mM EGTA and 30% vol/vol Percoll) in a 10- ml polycarbonate ultracentrifuge tube. After centrifugation at 95,000 g for 30 min a dense band containing purified mitochondria was recovered approximately at the bottom of the gradient (and further processed as described in (rif. 232)). The quality of the preparation has been checked by western blot analysis using different markers for the fractions obtained.

Immunoblot

The P2X7 receptor directly interacts with the NLRP3 inflammasome scaffold protein:

Proteins were analyzed on Bolt Mini Gels 4–12% SDS-PAGE (Life Technologies) and transferred onto nitrocellulose paper (GE Healthcare Life Sciences, Milano, Italy). Membranes were blocked with 2% nonfat milk (Bio-Rad, Hercules, CA, USA) and 5% bovine serum albumin (Sigma-Aldrich) in TBS-T buffer (10 mM Tris-HCl, 150 mM NaCl, pH 8.0, and 1% Tween-20) and probed overnight at 4°C with rabbit anti-P2X7R (1:200 dilution; Sigma-Aldrich), rat anti-NLRP3 (1:250 dilution; R&D Systems), monoclonal mouse anti-ASC (1:2000 dilution, cat. no. 04147; Millipore, Billerica, MA, USA), or rabbit anti-actin (1:1000 di- lution, cat. no. A2668; Sigma-Aldrich) antibodies. Membranes were washed 3 times for 5 min with TBS-T buffer and incubated in the same buffer for 2 hours at room temperature with horseradish peroxidase-conjugated secondary polyclonal antibody goat anti- mouse (1:500 dilution, cat no. ab97240; Abcam), goat anti-rabbit (1:500 dilution, cat no. ab7090; Abcam), or goat anti-rat (1:500 dilution, cat no. ab97057; Abcam) antibodies. After washing with TBS-T buffer, proteins were detected using ECL reagent (GE Healthcare Life Sciences). Gray values were quantified with ImageJ software.

P2X7R is expressed in Mitochondria:

Total cell lysates were prepared in RIPA buffer (50 mM Tris-HCl pH 7.8, 150 mM NaCl, 1% IGEPAL CA-630, 0.5% sodium deoxycholate, 0.1% SDS, 1 mM DTT) supplemented with proteases and phosphatases inhibitors (Inhibitor Cocktail). Proteins (15 μg) were quantified using the Bradford assay (Bio-Rad Laboratories), separated by SDS-PAGE and transferred to nitrocellulose membranes for standard western blotting. Antibodies were purchased from the following sources and used at the indicated dilutions: P2X7 (1: (1:500) FROM Alomone Labs, TOM 20 (1:1000) and TIM 23 (1:2000) GAPDH (1:3000) actin (1:5000), from Cell Signaling; Densitometric analysis of protein levels were performed with ImageJ software .

Immunofluorescence

The P2X7 receptor directly interacts with the NLRP3 inflammasome scaffold protein:

For microscopy, cells were fixed with 4% paraformaldehyde/PBS for 10 minutes at room temperature, followed by a 45-minute incubation with blocking solution (5% bovine serum albumin, 5% fetal bovine serum, and 0.1% Triton-X 100). The following antibodies were used: polyclonal rabbit anti-mouse P2X7 (1:100 dilution; cat no. P8232; Sigma-Aldrich) and monoclonal rat anti- mouse NLRP3 (1:25 dilution, cat no. MAB 7578; R&D Systems, Minneapolis, MN, USA). The following secondary antibodies were used: donkey anti-rabbit AlexaFuor 594-conjugated (cat no. ab150064) and goat anti-rat AlexaFuor 488-conjugated (cat. no. ab150157; 1:500 dilution; Abcam, Cambridge, United Kingdom). Cells were counterstained with DAPI (Fluoroshield Mounting Medium; Abcam).

P2X7R is expressed in Mitochondria:

HEK293-hP2X7R cells were fixed in 4% paraformaldehyde in PBS for 15 min, washed three times with PBS, permeabilized for 10 min with 0.1% Triton X-100 in PBS and blocked in PBS containing 2% BSA for 20 min. Cells were then incubated O/N at 4°C in a wet chamber with the following antibodies: anti-P2X7 (Sigma- Aldrich) for P2X7 receptor, anti-Tom 20 (Cell Signaling) , dilute 1:100 with 2% BSA in PBS. Staining was then carried out with Alexa 543 anti-rabbit for P2X7 receptor, with Alexa 633 anti-mouse for TOM 20, secondary antibodies. After each antibody incubation, cells were washed three times with 0.1% Triton X-100 in PBS. Samples were mounted in ProLong Gold antifade (Invitrogen) and images were obtained by confocal fluorescence microscopy (LSM 510; Carl Zeiss MicroImaging, Inc.)

P2X7-GFP and Fura-2/AM imaging

The cytosolic Ca^{2+} concentration was measured using the fluo- rescent Ca^{2+} indicator Fura-2/AM (Life Technologies). HEK293- P2X7-GFP cells were grown on 24-mm coverslips and incubated at 37°C for 30 minutes in 1 mM Ca^{2+}-containing Krebs Ringer phosphate buffer supplemented with 2.5 mM Fura-2/AM, 0.02% Pluronic F-68 (Sigma-Aldrich) and 0.1 mM sulfinpyrazone (Sigma-Aldrich). Cells were then rinsed and resuspended in 1 mM Ca^{2+}-containing Krebs Ringer phosphate. For Ca^{2+} measure- ments, cells were placed in an open Leyden chamber on a 37°C thermostatted microscopy stage and imaged with and Olympus Xcellence microscopy system (Olympus, Shinjuku, Tokyo, Japan). Excitation filters 340/26 and 380/11 nm were used for Fura-2/AM and 485/20 nm for GFP (Chroma, Bellows Falls, VT, USA). Emission filter was 500/10 for both fura-2 and GFP imaging. Images were acquired with a Hamamatsu Orca R2 camera (Hamamatsu Photonics, Hamamatsu, Japan) using an exposure time of 20 ms, with a 500 ms delay per cycle. Micro- injections were performed using an Eppendorf transjector 5246 microinjector

system (Eppendorf, Hamburg, Germany). Stimuli were loaded into Eppendorf femtotips (Eppendorf) placed closer than 1 mm to the cell edge. Single puffs (150 mM saline solution or 100 mM BzATP dissolved in the same solution) were generated by applying a 200 hPa pressure pulse for 0.5 s. Control experiments were performed with the selective P2X7R antagonist AZ10606120 (300 nM; Tocris Bioscience, Bristol, UK). Fura-2/AM and P2X7R- GFP fluorescence emission (expressed as relative fluorescence units) was measured in the proximity of the site of stimulation and in an area distal to the stimulation site.

Isolation of liver mitochondria

Mitochondria from C57bl/6 (male) mice aged 6 weeks were isolated by one methods, based upon Schnaitman and Greenawalt protocol (Schnaitman C 1968). Specifically, the liver was extracted and minced in ~10 volumes of MSHE+BSA (4°C), and all subsequent steps of the preparation were performed on ice. The material was rinsed several times to remove blood. The tissue was disrupted using a drill-driven Teflon glass homogenizer with 2–3 strokes. Homogenate was centrifuged at 800 g for 10 min at 4°C. Following centrifugation, fat/lipid was carefully aspirated, and the remaining supernatant was centrifuged at 8000 g for 10 min at 4°C. After removal of the light mitochondrial layer, the pellet was resuspended in MSHE+BSA, and the centrifugation was repeated. The final pellet was resuspended in a minimal volume of MSHE+BSA. Total protein (mg/ml) was determined using Bradford Assay reagent (Bio-Rad). Typically, ~7.5 mg of mitochondria (100 μl volume) was obtained from a single mouse liver.

Seahorse mitochondrial flux analyses.

Oxygen consumption and extracellular acidification in Cell line (N13) and Primary cell culture (Microglia, Mef) were measured using the Seahorse XF96 Extracellular Flux Analyzer instrument. The first day cells were seeded in triplicate in 80 ul DMEM complete medium at a adequate density in XF96 96-well cell culture plate (Seahorse Bioscience). The XF96 sensor cartridge was hydrated with 200 μl/well of XF Calibrant buffer and placed in incubator without CO_2 for all the night. The second day, before running the assay, we replaced complete media, of the cells, with Seahorse assay medium supplemented with Glucose (10mM) and Sodium Piruvate (2mM), pH to 7.4 and equilibrated for 1 h at 37 °C without CO_2. Through different port in the cartridge we injected Oligomycin, inhibits ATP synthesis by blocking the proton channel of the F_o portion ATP synthase (Complex V); Carbonyl cyanide 4-(trifluoromethoxy) phenylhydrazone (FCCP), an uncoupling agent because it disrupts ATP synthesis by transporting hydrogen ions across the mitochondrial membrane instead of the proton channel of ATP synthase (Complex V) and a mix of

Rotenone/Antimycin A, a Complex I/III inhibitor. After the calibration the cell plate was placed in analyzer and extracellular acidification rate (ECAR) and oxygen consumption rates (OCR) were simultaneously measured before and after the injection of the different compounds. We normalized ECAR and OCR measurements to cells content in each well determined via crystal violet.

Respiration in isolated mitochondria

Electron flow experiments were conducted in isolated mitochondria using an XF96 extracellular flux analyzer (Seahorse Bioscience, North Billerica, MA). Immediately following mitochondrial isolation, protein was quantified using the Bradford assay (Bio-Rad Laboratories) and mitochondria were plated on Seahorse cell culture plates at a concentration of 10 μg/ well in the presence of 10 mM pyruvate (P5280; Sigma-Aldrich, St. Louis, MO) and 5 mM malate (P5280; Sigma-Aldrich, St. Louis, MO) which stimulated mitochondrial electron transport; with succinate (10 mM, in the presence of the Complex I inhibitor rotenone, 2μM, in order to direct the electron flow exclusively through complexes II, III and IV) or with the artificial substrates ascorbate/TMPD (10 mM/100μM,respectively, in the presence of the Complex III inhibitor antimycin at 4μM, in order to selectively activateComplex IV) (Rogers et al; 2011).

Mitochondrial membrane potential measurements

Mitochondrial membrane potential ($\Delta\Psi$m) was measured using 10 nM tetramethyl rhodamine methyl ester (TMRM) on a confocal microscope (model LSM 510; Carl Zeiss MicroImaging, Inc.). FCCP (carbonyl cyanide p-trifluoromethoxyphenylhydrazone), to collapses mitochondrial $\Delta\Psi$. The signal was collected as total emission >570 nm.

Diclorofluoresceina (DCF) fluorescence measurement of reactive oxygen species.

The fluorogenic substrate 2′,7′-dichlorofluorescein diacetate (DCFDA) is a cell-permeable dye that is oxidized to highly fluorescent 2′,7′-dichlorofluorescein (DCF) by H2O2. Levels of ROS were assessed by DCFDA fluorescence in N13 WT and R untreated or treated with 2.5 mM Methyl Succinate for 30 minutes prior to measurement.Intensity fluorescence was measured using a image-based cytometer (Tali™ Image-based Cytometer, Invitrogen).The cells were pipetted into a Tali Cellular Analysis Slide and loaded into the cytometer. Bright field, green fluorescence images are captured and analyzed using assay specific algorithms. Histograms are then generated to display cell size and GFP fluorescence intensity. Graphs represent the mean ± SD from three replicates. P***<0.005.

Wound healing assay.

N13 WT and N13 R cells were grown to confluence in 24-well and the wounds were made simultaneously in all the wells with sterilized one-milliliter pipette tip. Phase contrast pictures were taken at 0 and 24 hours. Cell migration was observed in control condition and after the treatment with 2.5 mM Methyl Succinate.

The open wound area at 0 hours was regarded as 100%. Images were then analyzed using open source ImageJ Fiji software. Values represent mean ± SD from three replicates. P***<0.005.

Statistical analyses

Statistical analyses were performed using Student's t-test. A p-value ≤ 0.05 was considered significant. All data are reported as mean ± s.e.m., or means ± SD where indicated.

REFERENCES

1. Burnstock, G. (1976) Purinergic receptors. J. Theor. Biol. 62, 491-503.
2. Burnstock, G. (1978). A basis for distinguishing two types of purinergic receptor.Cell Membrane Receptors for Drugs and Hormones: A Multidisciplinry Approach 107– 118.
3. Apasov S, Koshiba M, Redegelt F, Sitkovsky M. (1995) Role of Extracellular ATP and P1 and P2 classes of Purinergic receptors in T-cells development and cytotoxic T lymphocyte functions. Immunol Rev 146: 5.
4. Ralevic V and Burnstock G. (1998) Receptors for purines and pyrimidines. Pharmacol Rev 50: 413–492.
5. Chambers JK, Macdonald LE, Sarau HM, Ames RS, Freeman K, Foley JJ, Zhu Y, McLaughlin MM, Murdock P, McMillan L, Trill J, Swift A, Aiyar N, Taylor P, Vawter L, Naheed S, Szekeres P, Hervieu G, Scott C, Watson JM, Murphy AJ, Duzic E, Klein C, Bergsma DJ, Wilson S, and Livi GP. (2000) A G protein-coupled receptor for UDP-glucose. J Biol Chem 275: 10767–10771.
6. Communi D, Gonzalez NS, Detheux M, Brezillon S, Lannoy V, Parmentier M, and Boeynaems JM. (2001)Identification of a novel human ADP receptor coupled to Gi. J Biol Chem 276: 41479–41485.
7. Harden TK. (1998) The G-protein-coupled P2Y receptors. In: Cardiovascular Biology of Purines, edited by Burnstock G, Dobson JGJ, Liang BT, and Linden J. London: Kluwer Academic,p. 181–205.
8. Chambers JK, Macdonald LE, Sarau HM, Ames RS, Freeman K, Foley JJ, Zhu Y, McLaughlin MM, Murdock P, McMillan L, Trill J, Swift A, Aiyar N, Taylor P, Vawter L, Naheed S, Szekeres P, Hervieu G, Scott C, Watson JM, Murphy AJ, Duzic E, Klein C, Bergsma DJ, Wilson S, and Livi GP.(2000) A G protein-coupled receptor for UDP-glucose. J Biol Chem 275: 10767–10771.
9. Abbracchio MP, (2006) International Union of Pharmacology LVIII: update on the P2Y G protein-coupled nucleotide receptors: from molecular mechanisms and pathophysiology to therapy. Pharmacol Rev.58:281–341.
10. North RA (2002) Molecular physiology of P2X receptors. Physiol Rev.82(4):1013-67.
11. T.M. Egan, B.S. Khakh,(2004) Contribution of Calcium Ions to P2X Channel Responses J. Neurosci. 3413–3420.
12. Surprenant A, North RA. (2009) Signaling at purinergic P2X receptors. Annu Rev Physiol. 71:333-59.
13. Kahlenberg JM, Dubyak GR (2004) Mechanisms of caspase-1 activation by P2X7 receptor-mediated K+ release Am J Physiol Cell Physiol.286(5):C1100-8.
14. Qureshi OS1, Paramasivam A, Yu JC, Murrell-Lagnado RD. (2007) Regulation of P2X4 receptors by lysosomal targeting, glycan protection and exocytosis. J Cell Sci.120(Pt 21):3838-49
15. Huang P, Zou Y, Zhong XZ, Cao Q, Zhao K, Zhu MX, Murrell-Lagnado R, Dong XP (2014) P2X4 forms functional ATP-activated cation channels on lysosomal membranes regulated by luminal pH. J Biol Chem. 289(25):17658-67.
16. North RA (2002) Molecular physiology of P2X receptors. Physiol Rev.82(4):1013-67.
17. Zhou et al., 2009
18. Feng YH, Li X, Wang L, Zhou L, and Gorodeski GI (2006) A truncated P2X7 receptor variant (P2X7-j) endogenously expressed in cervical cancer cells antagonizes the full-length P2X7 receptor through hetero-oligomerization. J Biol Chem 281:17228–17237.
19. Lingyin Zhou,1 Liping Luo,1 Xiaoping Qi,1 Xin Li,1 and George I. Gorodeski (2009) Regulation of P2X7 gene transcription Purinergic Signal. 5(3): 409–426.
20. Di Virgilio F. (1998) ATP as a death factor. Biofactors. 8(3-4):301-3.
21. Costa-Junior HM, Vieira FS, and Robson Coutinho-Silva (2011) C terminus of the P2X7 receptor: treasure hunting Purinergic Signal.7(1): 7–19.
22. Kim M, Jiang LH, Wilson HL, North RA, Suprenant A. (2001) Proteomic and functional evidence for a P2X7 receptor signaling complex. EMBO J.20:6347–6358.
23. Surprenant A, Rassendren F, Kawashima E, North RA, Buell G. (1996) The cytolytic P2z receptor for extracellular ATP identified as a P2X receptor (P2X7) Science.272:735–738.
24. Surprenant A, Rassendren F, Kawashima E, North RA, Buell G. (1996) The cytolytic P2z receptor for extracellular ATP identified as a P2X receptor (P2X7) Science.272:735–738.
25. Sluyter R, Shemon AN, Hughes WE, Stevenson RO, Georgiou JG, Eslick GD, Taylor RM, and Wiley JS (2007) Canine erythrocytes express the P2X7 receptor: greatly increased function compared with human erythrocytes. Am J Physiol Regul Integr Comp Physiol 293:R2090–R2098.
26. Adinolfi E, Melchiorri L, Falzoni S, Chiozzi P, Morelli A, Tieghi A, Cuneo A, Castoldi G, Di Virgilio F, Baricordi OR. (2002) P2X7 receptor expression in evolutive and indolent forms of chronic B lymphocytic leukemia. Blood.99(2):706-8.
27. Suh, B.C, Kim, J.S, Namgung, U, Ha, H, Kim, K.T, (2001) P2X7 nucleotide receptor mediation of membrane pore formation and superoxide generation in human promyelocytes and neutrophils , J Immunol, Vol. 166, Pg. 6754 6763.

28. Gudipaty L1, Humphreys BD, Buell G, Dubyak G (2001) Regulation of P2X(7) nucleotide receptor function in human monocytes by extracellular ions and receptor density. Am J Physiol Cell Physiol.280(4):C943-53.

29. Wareham K, Vial C, Wykes RC, Bradding P, Seward EP. (2009) Functional evidence for the expression of P2X1, P2X4 and P2X7 receptors in human lung mast cells. Br J Pharmacol.157(7):1215-24.

30. Ferrari D, Chiozzi P, Falzoni S, Dal Susino M, Melchiorri L, Baricordi OR, Di Virgilio F (1997) Extracellular ATP triggers IL-1b release by activating the purinergic P2Z receptor of human macrophages. J Immunol 159:1451–1458

31. Di Virgilio F (2007) Purinergic signalling in the immune system. A brief update Purinergic Signal.3(1-2): 1–3.

32. Bianco F, Ceruti S, Colombo A, Fumagalli M, Ferrari D, Pizzirani C, Matteoli M, Di Virgilio F, Abbracchio MP, and Verderio C (2006) A role for P2X7 in microglial proliferation. J Neurochem 99:745–758.

33. Sugiyama T, Lee SY, Horie T, Oku H, Takai S, Tanioka H, Kuriki Y, Kojima S, and Ikeda T P2X7 receptor activation may be involved in neuronal loss in the retinal ganglion cell layer after acute elevation of intraocular pressure in rats. Mol Vis 19:2080–2091.

34. Li M, Chang TH, Silberberg SD, and Swartz KJ (2008) Gating the pore of P2X receptor channels. Nat Neurosci 11:883–887.

35. Penolazzi, L, Bianchini, E, Lambertini, E, Baraldi, P.G, Romagnoli, R, Piva, R, Gambari, R, (2005) N-Arylpiperazine modified analogues of the P2X7 receptor KN-62 antagonist are potent inducers of apoptosis of human primary osteoclasts , J Biomed Sci. 1013-20.

36. Li, Q, Luo, X, Zeng, W, Muallem, S, (2003), Cell-specific behavior of P2X7 receptors in mouse parotid acinar and duct cells , J Biol Chem, 47554 47561.

37. Miras-Portugal M. T., Diaz-Hernandez M., Giraldez L., Hervas C., Gomez-Villafuertes R., Sen R. P., Gualix J. and Pintor J. (2003) P2X7 receptors in rat brain: presence in synaptic terminals and granule cells. Neurochem. Res. 28, 1597–1605.

38. Leon D., Sanchez-Nogueiro J., Maron-Garcõa P. and Miras-Portugal M. T. (2008) Glutamate release and synapsin-I phosphorylation induced by P2X7 receptors activation in cerebellar granule neurons. Neurochem. Int. 52, 1148–1159.

39. P. Marín-García,J. Sánchez-Nogueiro, R. Gómez-Villafuertes, D. León And M. T. Miras-Portugalsynaptic(2008) Terminals From Mice Midbrain Exhibit Functionalp2x7 Receptor Neuroscience 151 361–373

40. Hillman KA, Harada H, Chan CM, Townsend-Nicholson A, Moss SE, Miyamoto K, et al. Chicken DT40 cells stably transfected with the rat P2X7 receptor ion channel: a system suitable for the study of purine receptor-mediated cell death. Biochem Pharmacol. 2003;66:415–424.

41. Koshi, R., Coutinho-Silva, R., Cascabulho, C.M., Henrique-Pons, A., Knight, G.E., Loesch, A., Burnstock, G., (2005) Presence of the P2X purinergic receptor on immune cells that invade the rat endometrium during oestrus , J Reprod Immunol, 127 140.

42. Emmett, D.S., Feranchak, A., Kilic, G., Puljak, L., Miller, B., Dolovcak, S., McWilliams, R., Doctor, R.B., Fitz, J.G., (2008) Characterization of ionotrophic purinergic receptors in hepatocytes , Hepatology, 698 705.

43. White, N. and Burnstock, G, (2006) P2 receptors and cancer , Trends Pharmacol. Sci, 211 217.

44. Cheewatrakoolpong B, Gilchrest H, Anthes J.C, Greenfeder S, (2005) Identification and characterization of splice variants of the human P2X7 ATP channel , Biochem. Biophys.l Res. Comm,17 27.

45. Feng Y.H, Li X, Wang L,(2006) A truncated P2X7 receptor variant (P2X7-j) endogenously expressed in cervical cancer cells antagonizes the full-length P2X7 receptor through hetero-oligomerization , J Biol Chem, 17228-17237.

46. Nicke A, Kuan Y-H, Masin M, Rettinger J, Marquez-Klaka, B, Bender O, Gorecki D.C, Murrell-Lagnado R.D, Soto F, (2009) A functional P2X7 splice variant with an alternative transmembrane domain 1 escapes gene inactivation in P2X7 KO mice, J. Biol.Chem., 25813-22.

47. Masin M, Young C, Lim K, Barnes SJ, Xu XJ, Marschall V, Brutkowski W, Mooney ER, Gorecki DC, Murrell-Lagnado R. (2012) Expression, assembly and function of novel C-terminal truncated variants of the mouse P2X7 receptor: re-evaluation of P2X7 knockouts. Br J Pharmacol. 978-93.

48. Caseley EA, Muench SP, Roger S, Ju Mao H, Baldwin SA Lin-Hua Jiang (2014) Non-Synonymous Single Nucleotide Polymorphisms in the P2X Receptor Genes: Association with Diseases, Impact on Receptor Functions and Potential Use as Diagnosis Biomarkers nt. J. Mol. Sci.13344-13371;

49. Dubyak GR. (2007) Go it alone no more-P2X7 joins the society of heteromeric ATP-gated receptor channels. Mol Pharmacol. 1402-5.

50. Khakh SB & North AR(2006) P2X receptors as cell-surface ATP sensors in health and disease Nature 442, 527-532

51. North RA (2002) Molecular physiology of P2X receptors. Physiol Rev.1013-67.

52. Lambrecht G, Friebe T, Grimm U, Windscheif U, Bungardt E, Hildebrandt C, Bäumert HG, Spatz-Kümbel G, and Mutschler E (1992) PPADS, a novel functionally selective antagonist of P2 purinoceptor-mediated responses. Eur J Pharmacol 217:217–219.

53. Murgia M, Hanau S, Pizzo P, Rippa M, Di Virgilio F. (1993) Oxidized ATP. An irreversible inhibitor of the macrophage purinergic P2Z receptor. J Biol Chem. 8199-203.

54. Gargett CE, Wiley JS.(1997) The isoquinoline derivative KN-62 a potent antagonist of the P2Z-receptor of human lymphocytes. Br J Pharmacol. 1483-90.

55. Murgia M, Hanau S, Pizzo P, Rippa M, Di Virgilio F. (1993) Oxidized ATP. An irreversible inhibitor of the macrophage purinergic P2Z receptor. J Biol Chem.8199-203.

56. Beigi RD, Kertesy SB, Aquilina G, Dubyak GR. (2003) Oxidized ATP (oATP) attenuates proinflammatory signaling via P2 receptor-independent mechanisms. Br J Pharmacol. 507-19.

57. Di Virgilio F. (2004) New pathways for reactive oxygen species generation in inflammation and potential novel pharmacological targets. Curr Pharm Des. 1647-52. Review.

58. Gargett CE, Wiley JS. (1997) The isoquinoline derivative KN-62 a potent antagonist of the P2Z-receptor of human lymphocytes. Br J Pharmacol. 1483-90.

59. Chessell IP, Michel AD, Humphrey PP.(1998) Effects of antagonists at the human recombinant P2X7 receptor. Br J Pharmacol. 1314-20.

60. Jiang LH, Mackenzie AB, North RA, (2000) Surprenant A.Brilliant blue G selectively blocks ATP-gated rat P2X(7) receptors. Mol Pharmacol. 82-8

61. Baraldi PG1, del Carmen Nuñez M, Morelli A, Falzoni S, Di Virgilio F, Romagnoli R. (2003) Synthesis and biological activity of N-arylpiperazine-modified analogues of KN-62, a potent antagonist of the purinergic P2X7 receptor. J Med Chem.1318-29.

62. Friedle SA, Brautigam VM, Nikodemova M, Wright ML, Watters JJ. (2011) The P2X7-Egr pathway regulates nucleotide-dependent inflammatory gene expression in microglia. Glia.1-13.

63. Jiang L. H. (2012). P2X receptor-mediated ATP purinergic signalling in health and disease. Cell Health Cytoskelet. 4, 83–10110.2147

64. Nelson,D.W., Gregg, R.J., Kort, M.E., Perez-Medrano, A., Voight, E.A., Wang, Y., Grayson G., Namovic M.T., Donnelly-Roberts D.L., Niforato W., Honore P, Jarvis M.F, Faltynek C.R, Carroll W.A, (2006) Structure-activity relationship studies on a series of novel, substituted 1-benzyl-5-phenyltetrazole P2X7 antagonists , J.Med.Chem, 3659.

65. D L Donnelly-Roberts, M F Jarvis (2007) Discovery of P2X7 receptor-selective antagonists offers new insights into P2X7 receptor function and indicates a role in chronic pain states Br J Pharmacol. 571–579.

66. McGaraughty S1, Chu KL, Namovic MT, Donnelly-Roberts DL, Harris RR, Zhang XF, Shieh CC, Wismer CT, Zhu CZ, Gauvin DM, Fabiyi AC, Honore P, Gregg RJ, Kort ME, Nelson DW, Carroll WA, Marsh K, Faltynek CR, Jarvis MF. (2007) P2X7-related modulation of pathological nociception in rats. Neuroscience. 1817-28.

67. Zhang X, Gao F, Yu LL, Peng Y, Liu HH, Liu JY, Yin M, Ni J. (2008) Dual functions of a monoclonal antibody against cell surface F1F0 ATP synthase on both HUVEC and tumor cells. Acta Pharmacol Sin. 29:942–950.

68. Stagg J, Divisekera U, McLaughlin N, Sharkey J, Pommey S, Denoyer D, Dwyer KM, Smyth MJ. (2010) Anti-CD73 antibody therapy inhibits breast tumor growth and metastasis. Proc Natl Acad Sci U S A. 107:1547–1552.

69. Virginio C, Church D, North RA, Surprenant A.(1997) Effects of divalent cations, protons and calmidazolium at the rat P2X7 receptor.Neuropharmacology. 1285-94.

70. Michel AD, Chessell IP, Humphrey PP. (1999) Ionic effects on human recombinant P2X7 receptor function. Naunyn Schmiedebergs Arch Pharmacol. 102-9.

71. North RA(2002) Molecular physiology of P2X receptors. Physiol Rev.1013-67.

72. Michel AD, Chessell IP, Humphrey PP. (1999) Ionic effects on human recombinant P2X7 receptor function. Naunyn Schmiedebergs Arch Pharmacol. 102-9.

73. Wiley JS, Chen R, Jamieson GP (1993) The ATP4-receptor-operated channel (P2Z class) of human lymphocytes allows Ba2 and ethidium uptake: inhibition of fluxes by suramin. Arch Biochem Biophys 305:54–60.

74. Stevenson RO, Taylor RM, Wiley JS, Sluyter R. (2009)The P2X(7) receptor mediates the uptake of organic cations in canine erythrocytes and mononuclear leukocytes: comparison to equivalent human cell types. Purinergic Signal. 385-94.

75. Chen Y, Yao Y, Sumi Y, Li A, To UK, Elkhal A, (2010) Purinergic signaling: a fundamental mechanism in neutrophil activation. Sci Signal. 3

76. Abberley L, Bebius A, Beswick PJ, Billinton A, Collis KL, Dean DK, Fonfria E, Gleave RJ, Medhurst SJ, Michel AD, Moses AP, Patel S, Roman SA, Scoccitti T, Smith B, Steadman JG, Walter DS. (2010) Identification of 2-oxo-N-(phenylmethyl)-4-imidazolidinecarboxamide antagonists of the P2X(7) receptor. Bioorg Med Chem Lett. 6370-4.

77. Donnelly-Roberts DL, Namovic MT, Han P, Jarvis MF. (2009) Mammalian P2X7 receptor pharmacology: comparison of recombinant mouse, rat and human P2X7 receptors. Br J Pharmacol. 157:1203–1214.

78. Honore P, Donnelly-Roberts D, Namovic M, Zhong C, Wade C, Chandran P, (2009) The antihyperalgesic activity of a selective P2X7 receptor antagonist, A-839977, is lost in IL-1alphabeta knockout mice. Behav Brain Res. 204:77–81.

79. Burnstock G (2007) Purine and pyrimidine receptors. Cell Mol Life Sci.1471-83.

80. Virginio C, MacKenzie A, North RA, Surprenant A. (1999) Kinetics of cell lysis, dye uptake and permeability changes in cells expressing the rat P2X7 receptor. J Physiol.2:335-46.

81. Surprenant A, Rassendren F, Kawashima E, North RA, Buell G. (1996) The cytolytic P2Z receptor for extracellular ATP identified as a P2X receptor (P2X7).Science. 735-8.

82. Smart ML, Gu B, Panchal RG, Wiley J, Cromer B, Williams DA, Petrou S.(2003) P2X7 receptor cell surface expression and cytolytic pore formation are regulated by a distal C-terminal region. J Biol Chem. 8853-60.

83. Adinolfi E, Cirillo M, Woltersdorf R, Falzoni S, Chiozzi P, Pellegatti P, Callegari MG, Sandonà D, Markwardt F, Schmalzing G, Di Virgilio F. (2010) Trophic activity of a naturally occurring truncated isoform of the P2X7 receptor. FASEB J. 3393-404.

84. Jiang LH, Mackenzie AB, North RA, (2000) Surprenant A. Brilliant blue G selectively blocks ATP-gated rat P2X(7) receptors. Mol Pharmacol.82-8.

85. Pelegrin, P.; Surprenant, A. (2006) Pannexin-1 mediates large pore formation and interleukin-1beta release by the ATP-gated P2X7 receptor. EMBO J., 5071-5082.

86. Marques-da-Silva, C.; Chaves, M.M.; Castro, N.G.; Coutinho- Silva, R.; Guimaraes, M.Z.P.(2011) Colchicine inhibits cationic dye uptake induced by ATP in P2X2- and P2X7-expressing cells: implication for its therapeutic action. Br. J. Pharmacol., 163, 912-926.

87. Hewinson J, Mackenzie AB (2007) P2X(7) receptor-mediated reactive oxygen and nitrogen species formation: from receptor to generators. Biochem Soc Trans.1168-70.

88. Miller CM, Boulter NR, Fuller SJ, Zakrzewski AM, Lees MP, Saunders BM, Wiley JS, Smith NC. (2011) The role of the P2X$_7$ receptor in infectious diseases. PLoS Pathog. 1002212.

89. Di Virgilio F.(2013) The therapeutic potential of modifying inflammasomes and NOD-like receptors. Pharmacol Rev. 872-905.

90. Rissiek B, Haag F, Boyer O, Koch-Nolte F, Adriouch S. (2015) P2X7 on Mouse T Cells: One Channel, Many Functions.Front Immunol.6:204.

91. Bianco F, Ceruti S, Colombo A, Fumagalli M, Ferrari D, Pizzirani C et al (2006) A role for P2X7 in microglial proliferation. J Neurochem 99:745–758

92. Monif, M.; Reid, C.A.; Powell, K.L.; Smart, M.L.; William, D.A. (2009) The P2X7 receptor drives microglial activation and proliferation: a trophic role for P2X7R pore. J. Neurosci., 3781- 3791.

93. White N. and Burnstock G., (2006) P2 receptors and cancer,Trends Pharmacol. Sci, Vol. 211 217.

94. Di Virgilio F, Ferrari D, Adinolfi E (2009) P2X7: a growth-promoting receptor—implications for cancer Purinergic Signal. 251–256

95. Surprenant A, Schneider DA, Wilson HL, Galligan JJ, North RA. (2000) Functional properties of heteromeric P2X(1/5) receptors expressed in HEK cells and excitatory junction potentials in guinea-pig submucosal arterioles. J Auton Nerv Syst. 249-63.

96. EvansRJ,LewisC,BuellG,ValeraS,NorthRA,SurprenantA (1995) Pharmacological characterization of heterologously expressed ATP-gated cat- ion channels (P2Xpurinoceptors). Mol Pharmacol 48:178 –183.

97. Zanovello, P., Bronte, V., Rosato, A., Pizzo, P., and Di Virgilio, F. (1990). Responses of mouse lymphocytes to extracellular ATP. II. Extracellular ATP causes cell type-dependent lysis and DNA frag- mentation. J. Immunol. 145, 1545–1550.

98. Chow SC, Kass GEN, and Orrenius S (1997) Purines and their roles in apoptosis. Neuropharmacology 36:1149–1156

99. Ferrari D, Los M, Bauer MKA, Vandenabeele P, Wesselborg S, and Schulze-Osthoff K (1999) P2Z purinoreceptor ligation induces activation of caspases with distinct roles in apoptotic and necrotic alterations of cell death. FEBS Lett 447:71–75

100. Adinolfi E, Melchiorri L, Falzoni S, Chiozzi P, Morelli A, Tieghi A, Cuneo A, Castoldi G, Di Virgilio F, Baricordi OR.(2002) P2X7 receptor expression in evolutive and indolent forms of chronic B lymphocytic leukemia. Blood. 706-8.

101. Baricordi OR, Ferrari D, Melchiorri L, Chiozzi P, Hanau S, Chiari E, Rubini M, and Di Virgilio F (1996) An ATP-activated channel is involved in mitogenic stimulation of human T lymphocytes. Blood 87:682–690.

102. Baricordi OR, Melchiorri L, Adinolfi E, Falzoni S, Chiozzi P, Buell G, and Di Virgilio F (1999) Increased proliferation rate of lymphoid cells transfected with the P2X(7) ATP receptor. J Biol Chem 274:33206–33208.

103. Budagian V, Bulanova E, Brovko L, Orinska Z, Fayad R, Paus R., Bulfone-Paus S, (2003), Signalling through P2X7 Receptor in Human T Cells Involves p56 MAP Kinases, and Transcription Factors AP-1 and NF- B , J. Biol. Chem., Vol. 278, Pg. 1549-1560.

104. Yip L, Woehrie T, Corriden R, Hirsh M, Chen Y, Inoue Y, Ferrari V, Insel P.A, Jinger W.G, (2009), Autocrine regulation of T-cell activation by ATP release and P2X7 receptors , FASEB J, 1685-1693.

105. Adinolfi E, Callegari MG, Ferrari D, Bolognesi C, Minelli M, Wieckowski MR, Pinton P, Rizzuto R, and Di Virgilio F (2005) Basal activation of the P2X7 ATP receptor elevates mitochondrial calcium and potential, increases cellular ATP levels, and promotes serum-independent growth. Mol Biol Cell 16:3260–3272.

106. Adinolfi E, Callegari MG, Cirillo M, Pinton P, Giorgi C, Cavagna D, Rizzuto R, Di Virgilio F. (2009) Expression of the P2X7 receptor increases the Ca2+ content of the endoplasmic reticulum, activates NFATc1, and protects from apoptosis. J Biol Chem. 10120-8.

107. Di Virgilio F, Ferrari D, Adinolfi E. (2009) P2X(7): a growth-promoting receptor-implications for cancer. Purinergic Signal. 251-6.

108. Lenertz LY, Gavala ML, Hill LM, Bertics PJ.(2009) Cell signaling via the P2X(7) nucleotide receptor: linkage to ROS production, gene transcription, and receptor trafficking. Purinergic Signal. 175-87.

109. Noguchi T, Ishii K, Fukutomi H, Naguro I, Matsuzawa A, Takeda K, Ichijo H.(2008) Requirement of reactive oxygen species-dependent activation of ASK1-p38 MAPK pathway for extracellular ATP-induced apoptosis in macrophage. J Biol Chem. 7657-65.

110. Neill D. R., Wong S. H., Bellosi A., Flynn R. J., Daly M., Langford T. K., et al. (2010). Nuocytes represent a new innate effector leukocyte that mediates type-2 immunity. Nature 464 1367–1370. 10.1038/nature08900

111. Schroder, K., Zhou, R., and Tschopp, J. (2010). The NLRP3 inflammasome: a sensor for metabolic danger? Science 327, 296–300.

112. Fullard N., O'Reilly S. (2015). Role of innate immune system in systemic sclerosis. Semin. Immunopathol. 37 511–517. 10.1007/s00281-015-0503-7

113. Alexandre Y. O., Cocita C. D., Ghilas S., Dalod M. (2014). Deciphering the role of DC subsets in MCMV infection to better understand immune protection against viral infections. Front. Microbiol. 5:378 10.3389/fmicb.2014.00378

114. Medzhitov R. (2009). Approaching the asymptote: 20 years later. Immunity 30 766–775. 10.1016/j.immuni.2009.06.004

115. Abderrazak A., Syrovets T., Couchie D., El Hadri K., Friguet B., Simmet T., et al. (2015b). NLRP3 inflammasome: from a danger signal sensor to a regulatory node of oxidative stress and inflammatory diseases. Redox Biol. 4 296–307. 10.1016/j.redox.2015.01.008

116. Bourgeois C., Kuchler K. (2012). Fungal pathogens-a sweet and sour treat for toll-like receptors. Front. Cell. Infect. Microbiol. 2:142 10.3389/fcimb.2012.00142

117. Dzopalic T., Rajkovic I., Dragicevic A., Colic M. (2012). The response of human dendritic cells to co-ligation of pattern-recognition receptors. Immunol. Res. 52 20–33. 10.1007/s12026-012-8279-5 NLR FAMILY DA QUI IN POI

118. Lamkanfi M and Dixit VM (2012) Inflammasomes and their roles in health and disease. Annu Rev Cell Dev Biol 28:137–161.

119. Duncan JA, Bergstralh DT, Wang Y, Willingham SB, Ye Z, Zimmermann AG, Ting JP: (2007) Cryopyrin/NALP3 binds ATP/dATP, is an ATPase, and requires ATP binding to mediate inflammatory signaling. Proc Natl Acad Sci U S A 104:8041-8046.

120. Wu X, Kong X, Luchsinger L, Smith BD, and Xu Y (2009) Regulating the activity of class II transactivator by posttranslational modifications: exploring the possibilities. Mol Cell Biol 29:5639–5644.

121. Lei Y, Wen H, Yu Y, Taxman DJ, Zhang L, Widman DG, Swanson KV, Wen KW, Damania B, and Moore CB, et al. (2012) The mitochondrial proteins NLRX1 and TUFM form a complex that regulates type I interferon and autophagy. Immunity 36:933–946.

122. Kufer, T.A., Banks, D.J., and Philpott, D.J. (2006). Innate immune sensing of microbes by Nod proteins. Ann. N Y Acad. Sci. 1072, 19–27.

123. Hugot, J.P., Chamaillard, M., Zouali, H., Lesage, S., Cézard, J.P., Belaiche, J., Almer, S., Tysk, C., O'Morain, C.A., Gassull, M., et al. (2001). Association of NOD2 leucine-rich repeat variants with susceptibility to Crohn's disease. Nature 411, 599–603.

124. Mankan, A. K., Dau, T., Jenne, D. and Hornung, V.,(2012) The NLRP3/ASC/Caspase-1 axis regulates IL-1β processing in neutrophils. Eur. J. Immunol. 42: 710–715.

125. Faustin, B., Chen, Y., Zhai, D., Le Negrate, G., Lartigue, L., Satterthwait, A., and Reed, J.C. (2009). Mechanism of Bcl-2 and Bcl-X(L) inhibition of NLRP1 inflammasome: loop domain-dependent suppression of ATP binding and olig- omerization. Proc. Natl. Acad. Sci. USA 106, 3935–3940.

126. Hsu LC, Ali SR, McGillivray S, Tseng PH, Mariathasan S, Humke EW, Eckmann L, Powell JJ, Nizet V, and Dixit VM, et al. (2008) A NOD2-NALP1 complex mediates caspase-1-dependent IL-1beta secretion in response to Bacillus anthracis infection and muramyl dipeptide. Proc Natl Acad Sci USA 105:7803–7808.

127. Martinon F, Burns K, and Tschopp J (2002) The inflammasome: a molecular platform triggering activation of inflammatory caspases and processing of proIL-beta. Mol Cell 10:417–426.

128. Fink, S.L., Bergsbaken, T., and Cookson, B.T. (2008). Anthrax lethal toxin and Salmonella elicit the common cell death pathway of caspase-1-dependent pyroptosis via distinct mechanisms. Proc. Natl. Acad. Sci. USA 105, 4312– 4317.

129. Khare S, Dorfleutner A, Bryan NB, Yun C, Radian AD, de Almeida L, Rojanasakul Y, and Stehlik C (2012) An NLRP7-containing inflammasome mediates recognition of microbial lipopeptides in human macrophages. Immunity 36:464–476.

130. Tadaki H, Saitsu H, Nishimura-Tadaki A, Imagawa T, Kikuchi M, Hara R, Kaneko U, Kishi T, Miyamae T, and Miyake N, et al. (2011) De novo 19q13.42 duplications involving NLRP gene cluster in a patient with systemic-onset juvenile idiopathic arthritis. J Hum Genet 56:343–347.

131. Eisenbarth SC, Williams A, Colegio OR, Meng H, Strowig T, Rongvaux A, Henao-Mejia J, Thaiss CA, Joly S, and Gonzalez DG, et al. (2012) NLRP10 is a NOD-like receptor essential to initiate adaptive immunity by dendritic cells. Nature 484:510–513.

132. Zaki MH, Vogel P, Malireddi RK, Body-Malapel M, Anand PK, Bertin J, Green DR, Lamkanfi M, and Kanneganti TD (2011) The NOD-like receptor NLRP12 attenu- ates colon inflammation and tumorigenesis. Cancer Cell 20:649–660.

133. Westerveld GH, Korver CM, van Pelt AM, Leschot NJ, van der Veen F, Repping S, and Lombardi MP (2006) Mutations in the testis-specific NALP14 gene in men suffering from spermatogenic failure. Hum Reprod 21:3178–3184.

134. Gross O, Thomas CJ, Guarda G, and Tschopp J (2011) The inflammasome: an in- tegrated view. Immunol Rev 243:136–151.

135. Gross O, Poeck H, Bscheider M, Dostert C, Hannesschläger N, Endres S, Hartmann G, Tardivel A, Schweighoffer E, and Tybulewicz V, et al. (2009) Syk kinase sig- nalling couples to the Nlrp3 inflammasome for anti-fungal host defence. Nature 459:433–436.

136. Mariathasan S, Weiss DS, Newton K, McBride J, O'Rourke K, Roose-Girma M, Lee WP, Weinrauch Y, Monack DM, and Dixit VM (2006) Cryopyrin activates the inflammasome in response to toxins and ATP. Nature 440:228–232.

137. Kanneganti, T.D., Body-Malapel, M., Amer, A., Park, J.H., Whitfield, J., Fran- chi, L., Taraporewala, Z.F., Miller, D., Patton, J.T., Inohara, N., and Nuˊn˜ez, G. (2006). Critical role for Cryopyrin/Nalp3 in activation of caspase-1 in response to viral infection and double-stranded RNA. J. Biol. Chem. 281, 36560–36568.

138. Muruve, D.A., Peˊtrilli, V., Zaiss, A.K., White, L.R., Clark, S.A., Ross, P.J., Parks, R.J., and Tschopp, J. (2008). The inflammasome recognizes cytosolic microbial and host DNA and triggers an innate immune response. Nature 452, 103–107

139. Kawai T, Akira S. TLR signaling. Cell Death Differ 2006;13:816–825.

140. Matzinger, P. (1994). Tolerance, danger, and the extended family. Annu. Rev. Immunol. 12, 991–1045.

141. Mariathasan, S., Weiss, D.S., Newton, K., McBride, J., O'Rourke, K., Roose- Girma, M., Lee, W.P., Weinrauch, Y., Monack, D.M., and Dixit, V.M. (2006). Cryopyrin activates the inflammasome in response to toxins and ATP. Nature 440, 228–232.

142. Yamasaki, K., Muto, J., Taylor, K.R., Cogen, A.L., Audish, D., Bertin, J., Grant, E.P., Coyle, A.J., Misaghi, A., Hoffman, H.M., and Gallo, R.L. (2009). NLRP3/ cryopyrin is necessary for interleukin-1beta (IL-1beta) release in response to hyaluronan, an endogenous trigger of inflammation in response to injury. J. Biol. Chem. 284, 12762–12771.

143. Halle, A., Hornung, V., Petzold, G.C., Stewart, C.R., Monks, B.G., Reinheckel, T., Fitzgerald, K.A., Latz, E., Moore, K.J., and Golenbock, D.T. (2008). The NALP3 inflammasome is involved in the innate immune response to amyloid-beta. Nat. Immunol. 9, 857–865.

144. Zhou R, Tardivel A, Thorens B, Choi I, and Tschopp J (2010) Thioredoxin-interacting protein links oxidative stress to inflammasome activation. Nat Immunol 11: 136–140.

145. Martinon F, Pétrilli V, Mayor A, Tardivel A, and Tschopp J (2006) Gout-associated uric acid crystals activate the NALP3 inflammasome. Nature 440:237–241.

146. Lamkanfi M and Dixit VM (2012) Inflammasomes and their roles in health and disease. Annu Rev Cell Dev Biol 28:137–161.

147. Mun˜ oz-Planillo, R., Kuffa, P., Martinez-Colon, G., Smith, B.L., Rajendiran, T.M., and Nunez, G. (2013). Immunity 38, this issue, 1142– 1153.

148. Zhou R, Yazdi AS, Menu P, and Tschopp J (2011) A role for mitochondria in NLRP3 inflammasome activation. Nature 469:221–225.

149. Hornung V, Bauernfeind F, Halle A, Samstad EO, Kono H, Rock KL, Fitzgerald KA, and Latz E (2008) Silica crystals and aluminum salts activate the NALP3 inflammasome through phagosomal destabilization. Nat Immunol 9:847–856.

150. Bauernfeind F, Bartok E, Rieger A, Franchi L, Núñez G, and Hornung V (2011) Cutting edge: reactive oxygen species inhibitors block priming, but not activation, of the NLRP3 inflammasome. J Immunol 187:613–617.

151. Mun˜ oz-Planillo, R., Kuffa, P., Martinez-Colon, G., Smith, B.L., Rajendiran, T.M., and Nunez, G. (2013). Immunity 38, this issue, 1142– 1153.

152. Pétrilli V, Papin S, Dostert C, Mayor A, Martinon F, and Tschopp J (2007) Activation of the NALP3 inflammasome is triggered by low intracellular potassium concen- tration. Cell Death Differ 14:1583–1589.

153. Bauernfeind, F.G., Horvath, G., Stutz, A., Alnemri, E.S., MacDonald, K., Speert, D., Fernandes-Alnemri, T., Wu, J., Monks, B.G., Fitzgerald, K.A., et al. (2009). Cutting edge: NF-kappaB activating pattern recognition and cyto- kine receptors license NLRP3 inflammasome activation by regulating NLRP3 expression. J. Immunol. 183, 787–791.

154. Solle M, Labasi J, Perregaux DG, Stam E, Petrushova N, Koller BH, Griffiths RJ, Gabel CA.(2001) Altered cytokine production in mice lacking P2X(7) receptors. J Biol Chem;276:125–132.

155. Di Virgilio F, Chiozzi P, Ferrari D, Falzoni S, Sanz JM, Morelli A, Torboli M, Bolognesi G, and Baricordi OR (2001) Nucleotide receptors: an emerging family of regulatory molecules in blood cells. Blood 97:587–600.

156. Ferrari D, Chiozzi P, Falzoni S, Dal Susino M, Melchiorri L, Baricordi OR, and Di Virgilio F (1997) Extracellular ATP triggers IL-1 beta release by activating the purinergic P2Z receptor of human macrophages. J Immunol 159:1451–1458.

157. Gross O, Thomas CJ, Guarda G, and Tschopp J (2011) The inflammasome: an in- tegrated view. Immunol Rev 243:136–151.

158. Mariathasan, S., Newton, K., Monack, D.M., Vucic, D., French, D.M., Lee, W.P., Roose-Girma, M., Erickson, S., and Dixit, V.M. (2004). Differential activa- tion of the inflammasome by caspase-1 adaptors ASC and Ipaf. Nature 430, 213–218.

159. Mariathasan S, Weiss DS, Newton K, McBride J, O'Rourke K, Roose-Girma M, Lee WP, Weinrauch Y, Monack DM, and Dixit VM (2006) Cryopyrin activates the inflammasome in response to toxins and ATP. Nature 440:228–232.

160. Nakahira K, Haspel JA, Rathinam VA, Lee SJ, Dolinay T, Lam HC, Englert JA, Rabinovitch M, Cernadas M, and Kim HP, et al. (2011) Autophagy proteins regu- late innate immune responses by inhibiting the release of mitochondrial DNA mediated by the NALP3 inflammasome. Nat Immunol 12:222–230.

161. Shimada K, Crother TR, Karlin J, Dagvadorj J,Chiba N, Chen S,RamanujanV K,Wolf A J, Vergnes L, Ojcius D M,Rentsendorj A,Vargas M, Guerrero C, Wang Y, Fitzgerald K A, Underhill D M,Town T, Ardit M (2012) Oxidized Mitochondrial DNA Activates the NLRP3 Inflammasome during Apoptosis Immunity 401–414

162. Mariathasan, S., Newton, K., Monack, D.M., Vucic, D., French, D.M., Lee, W.P., Roose-Girma, M., Erickson, S., and Dixit, V.M. (2004). Differential activation of the inflammasome by caspase-1 adaptors ASC and Ipaf. Nature 430, 213–218.

163. Halle A, Hornung V, Petzold GC, Stewart CR, Monks BG, Reinheckel T, Fitzgerald KA, Latz E, Moore KJ, and Golenbock DT (2008) The NALP3 inflammasome is involved in the innate immune response to amyloid-beta. Nat Immunol 9:857–865.

164. Hornung V, Bauernfeind F, Halle A, Samstad EO, Kono H, Rock KL, Fitzgerald KA, and Latz E (2008) Silica crystals and aluminum salts activate the NALP3 inflammasome through phagosomal destabilization. Nat Immunol 9:847–856.

165. Dostert C, Guarda G, Romero JF, Menu P, Gross O, Tardivel A, Suva ML, Stehle JC, Kopf M, and Stamenkovic I, et al. (2009) Malarial hemozoin is a Nalp3 inflam- masome activating danger signal. PLoS ONE 4:e6510.

166. Newman, Z.L., Leppla, S.H., and Moayeri, M. (2009). CA-074Me protection against anthrax lethal toxin. Infect. Immun. 77, 4327–4336.

167. Cassel, S.L., Eisenbarth, S.C., Iyer, S.S., Sadler, J.J., Colegio, O.R., Tephly, L.A., Carter, A.B., Rothman, P.B., Flavell, R.A., and Sutterwala, F.S. (2008). The Nalp3 inflammasome is essential for the development of silicosis. Proc. Natl. Acad. Sci. USA 105, 9035–9040.

168. Cruz, C.M., Rinna, A., Forman, H.J., Ventura, A.L., Persechini, P.M., and Ojcius, D.M. (2007). ATP activates a reactive oxygen species-dependent oxidative stress response and secretion of proinflammatory cytokines in macrophages. J. Biol. Chem. 282, 2871–2879.

169. Dostert, C., Pe´trilli, V., Van Bruggen, R., Steele, C., Mossman, B.T., and Tschopp, J. (2008). Innate immune activation through Nalp3 inflammasome sensing of asbestos and silica. Science 320, 674–677.

170. Gross, O., Poeck, H., Bscheider, M., Dostert, C., Hannesschla¨ger, N., Endres, S., Hartmann, G., Tardivel, A., Schweighoffer, E., Tybulewicz, V., et al. (2009). Syk kinase signalling couples to the Nlrp3 inflammasome for anti-fungal host defence. Nature 459, 433–436.

171. Lee S, Kim SM, and Lee RT (2013) Thioredoxin and thioredoxin target proteins: from molecular mechanisms to functional significance. Antioxid Redox Signal 18: 1165–1207.

172. Zhou R, Tardivel A, Thorens B, Choi I, and Tschopp J (2010) Thioredoxin-interacting protein links oxidative stress to inflammasome activation. Nat Immunol 11: 136–140.

173. Bauernfeind F, Bartok E, Rieger A, Franchi L, Núñez G, and Hornung V (2011) Cutting edge: reactive oxygen species inhibitors block priming, but not activation, of the NLRP3 inflammasome. J Immunol 187:613–617.

174. Dinarello CA. Biologic basis for interleukin-1 in disease. Blood. 1996;87:2095–2147

175. Laliberte RE, Eggler J, Gabel CA. ATP treatment of human monocytes promotes caspase-1 maturation and externalization.J Biol Chem. 36944-51.

176. Perregaux D and Gabel CA (1994) Interleukin-1 beta maturation and release in response to ATP and nigericin. Evidence that potassium depletion mediated by these agents is a necessary and common feature of their activity. J Biol Chem 269:15195–15203.

177. Meylan, E. et al. (2006) Intracellular pattern recognition receptors in the host response. Nature 442, 39–44

178. 111. Dyall SD, Brown MT, Johnson PJ. (2004) Ancient invasions: from endosymbionts to organelles. Science. 253-7.

179. Frey TG, Mannella CA.(2000) The internal structure of mitochondria. Trends Biochem Sci. 319-24.

180. 113. Vogel F, Bornhovd C, Neupert W, Reichert AS. (2006) Dynamic subcompartmentalization of the mitochondrial inner membrane. J Cell Biol.237-47.

181. Rizzuto R, Pinton P, Carrington W, Fay FS, Fogarty KE, Lifshitz LM, (1998) Close contacts with the endoplasmic reticulum as determinants of mitochondrial Ca2+ responses. Science.1763-6.

182. Benard G, Rossignol R. (2008) Ultrastructure of the mitochondrion and its bearing on function and bioenergetics. Antioxid Redox Signal. 1313-42.

183. Cereghetti GM, Scorrano L. (2006) The many shapes of mitochondrial death. Oncogene. 4717-24.

184. Santel A, Fuller MT. (2001) Control of mitochondrial morphology by a human mitofusin. J Cell Sci. 867-74.

185. James DI, Parone PA, Mattenberger Y, Martinou JC.(2003) hFis1, a novel component of the mammalian mitochondrial fission machinery. J Biol Chem.36373-9.

186. 119. Smirnova E, Griparic L, Shurland DL, van der Bliek AM. (2001) Dynamin-related protein Drp1 is required for mitochondrial division in mammalian cells. Mol Biol Cell. 2245-56.

187. Yoon Y, Krueger EW, Oswald BJ, McNiven MA. (2003) The mitochondrial protein hFis1 regulates mitochondrial fission in mammalian cells through an interaction with the dynamin-like protein DLP1. Mol Cell Biol. 5409-20.

188. 121. Yu T, Robotham JL, Yoon Y. (2006) Increased production of reactive oxygen species in hyperglycemic conditions requires dynamic change of mitochondrial morphology. Proc Natl Acad Sci U S A. 2653-8.

189. Csordas G, Hajnoczky G. (2009) SR/ER-mitochondrial local communication: calcium and ROS. Biochim Biophys Acta. 1352-62.

190. Krebs HA.(1940) The citric acid cycle and the Szent-Gyorgyi cycle in pigeon breast muscle. Biochem J. 775-9.

191. Kennedy EP, Lehninger AL. (1949) Oxidation of fatty acids and tricarboxylic acid cycle intermediates by isolated rat liver mitochondria. J Biol Chem. 957-72.

192. 125. Lambeth DO, Tews KN, Adkins S, Frohlich D, Milavetz BI. (2004) Expression of two succinyl- CoA synthetases with different nucleotide specificities in mammalian tissues. J Biol Chem. 36621-4.

193. Amemori S, Iwakiri R, Endo H, Ootani A, Ogata S, Noda T, (2006) Oral dimethyl sulfoxide for systemic amyloid A amyloidosis complication in chronic inflammatory disease: a retrospective patient chart review. Journal of gastroenterology. 444-9.

194. Quinn PJ, Dawson RM. (1969) Interactions of cytochrome c and [14C]. Biochem J. 65-75.

195. Lenaz G, Genova ML. (2010) Structure and organization of mitochondrial respiratory complexes: a new understanding of an old subject. Antioxid Redox Signal. 961-1008.

196. Boyer PD. (2000) Catalytic site forms and controls in ATP synthase catalysis. Biochim Biophys Acta. 252-62.

197. 130. Ferguson SJ. (2010) ATP synthase: from sequence to ring size to the P/O ratio. Proc Natl Acad Sci U S A. 16755-6.

198. Kroemer G, Galluzzi L, Brenner C. (2007) Mitochondrial membrane permeabilization in cell death. Physiological reviews. 99-163.

199. Garrido C, Galluzzi L, Brunet M, Puig PE, Didelot C, Kroemer G. Mechanisms of cytochrome c release from mitochondria. (2006) Cell death and differentiation. 1423-33.

200. Hill MM, Adrain C, Martin SJ. (2003) Portrait of a killer: the mitochondrial apoptosome emerges from the shadows. Molecular interventions.19-26.

201. Ravagnan L, Roumier T, Kroemer G. (2002) Mitochondria, the killer organelles and their weapons. Journal of cellular physiology. 131-7.

202. Pinton P, Ferrari D, Rapizzi E, Di Virgilio F, Pozzan T, Rizzuto R. (2001) The Ca2+ concentration of the endoplasmic reticulum is a key determinant of ceramide-induced apoptosis: significance for the molecular mechanism of Bcl-2 action. The EMBO journal. 2690-701.

203. Youle RJ, Karbowski M. (2005) Mitochondrial fission in apoptosis. Nature reviews Molecular cell biology. 657-63.

204. Szabadkai G, Simoni AM, Chami M, Wieckowski MR, Youle RJ, Rizzuto R. (2004) Drp-1- dependent division of the mitochondrial network blocks intraorganellar Ca2+ waves and protects against Ca2+-mediated apoptosis. Molecular cell. 59-68.

205. Ricchelli F, Sileikyte J, Bernardi P. (2011) Shedding light on the mitochondrial permeability transition. Biochimica et biophysica acta. 482-90.

206. Baines CP, Kaiser RA, Purcell NH, Blair NS, Osinska H, Hambleton MA, (2005) Loss of cyclophilin D reveals a critical role for mitochondrial permeability transition in cell death. Nature. 658-62.

207. Basso E, Fante L, Fowlkes J, Petronilli V, Forte MA, Bernardi P.(2005) Properties of the permeability transition pore in mitochondria devoid of Cyclophilin D. The Journal of biological chemistry. 18558-61.

208. Nakagawa Y, Suzuki T, Kamimura H, Nagai F.(2006) Role of mitochondrial membrane permeability transition in N-nitrosofenfluramine-induced cell injury in rat hepatocytes. European journal of pharmacology. 33-9.

209. Burnstock, G. (2007) Physiology and pathophysiology of purinergic neurotransmission. Physiol. Rev. 87, 659–797

210. Mariathasan, S., Weiss, D. S., Newton, K., McBride, J., O'Rourke, K., Roose-Girma, M., Lee, W. P., Weinrauch, Y., Monack, D. M., and Dixit, V. M. (2006) Cryopyrin activates the inflammasome in response to toxins and ATP. Nature 440, 228–232

211. Di Virgilio, F. (2013) The therapeutic potential of modifying inflammasomes and NOD-like receptors. Pharmacol. Rev. 65, 872– 905

212. Ferrari, D., Villalba, M., Chiozzi, P., Falzoni, S., Ricciardi-Castagnoli, P., and Di Virgilio, F. (1996) Mouse microglial cells express a plasma membrane pore gated by extracellular ATP. J. Immunol. 156, 1531–1539

213. Lamkanfi, M., and Dixit, V. M. (2014) Mechanisms and functions of inflammasomes. Cell 157, 1013–1022

214. Schroder, K., and Tschopp, J. (2010) The inflammasomes. Cell 140, 821–832

215. Di Virgilio, F. (2013) The therapeutic potential of modifying inflammasomes and NOD-like receptors. Pharmacol. Rev. 65, 872– 905

216. Haneklaus, M., O'Neill, L. A., and Coll, R. C. (2013) Modulatory mechanisms controlling the NLRP3 inflammasome in inflam- mation: recent developments. Curr. Opin. Immunol. 25, 40–45

217. Di Virgilio, F. (2007) Liaisons dangereuses: P2X(7) and the inflammasome. Trends Pharmacol. Sci. 28, 465–472

218. Mariathasan, S., Weiss, D. S., Newton, K., McBride, J., O'Rourke, K., Roose-Girma, M., Lee, W. P., Weinrauch, Y., Monack, D. M., and Dixit, V. M. (2006) Cryopyrin activates the inflammasome in response to toxins and ATP. Nature 440, 228–232

219. Rayah, A., Kanellopoulos, J. M., and Di Virgilio, F. (2012) P2 receptors and immunity. Microbes Infect. 14, 1254–1262

220. Burnstock, G. (2007) Physiology and pathophysiology of purinergic neurotransmission. Physiol. Rev. 87, 659–797

221. Steinberg, T. H., Newman, A. S., Swanson, J. A., and Silverstein, S. C. (1987) ATP4- permeabilizes the plasma membrane of mouse macrophages to fluorescent dyes. J. Biol. Chem. 262, 8884–8888

222. Pelegrin, P., and Surprenant, A. (2006) Pannexin-1 mediates large pore formation and interleukin-1beta release by the ATP- gated P2X7 receptor. EMBO J. 25, 5071–5082

223. Huggett, J. F., Foy, C. A., Benes, V., Emslie, K., Garson, J. A., Haynes, R., Hellemans, J., Kubista, M., Mueller, R. D., Nolan, T., Pfaffl, M. W., Shipley, G. L., Vandesompele, J., Wittwer, C. T., and Bustin, S. A. (2013) The digital MIQE guidelines: Minimum Information for Publication of Quantitative Digital PCR Experi- ments. Clin. Chem. 59, 892–902

224. Di Virgilio, F., Bronte, V., Collavo, D., and Zanovello, P. (1989) Responses of mouse lymphocytes to extracellular adenosine 59-triphosphate (ATP). Lymphocytes with cytotoxic activity are resistant to the permeabilizing effects of ATP. J. Immunol. 143, 1955–1960

225. Di Virgilio, F. (1995) The P2Z purinoceptor: an intriguing role in immunity, inflammation and cell death. Immunol. Today 16, 524–528

226. Di Virgilio, F., Ferrari, D., and Adinolfi, E. (2009) P2X(7): a growth-promoting receptor-implications for cancer. Purinergic Signal. 5, 251–256

227. Bours, M. J., Dagnelie, P. C., Giuliani, A. L., Wesselius, A., Di Virgilio, F. (2011) P2 receptors and extracellular ATP: a novel homeostatic pathway in inflammation. Front. Biosci. (Schol. Ed.) 3, 1443–1456

228. Franchi, L., Kanneganti, T. D., Dubyak, G. R., and Nuñez, G. (2007) Differential requirement of P2X7 receptor and intracellular K+ for caspase-1 activation induced by in- tracellular and extracellular bacteria. J. Biol. Chem. 282, 18810–18818

229. Harder, J., Franchi, L., Muñoz-Planillo, R., Park, J. H., Reimer, T., and Nuñez, G. (2009) Activation of the Nlrp3 inflammasome by Streptococcus pyogenes requires streptolysin O and NF-kappa B activation but proceeds independently of TLR signaling and P2X7 receptor. J. Immunol. 183, 5823–5829

230. Muñoz-Planillo, R., Kuffa, P., Martınez-Colon, G., Smith, B. L., Rajendiran, T. M., and Nuñez, G. (2013) K+ efflux is the common trigger of NLRP3 inflammasome activation by bacterial toxins and particulate matter. Immunity 38, 1142–1153

231. Martinon, F., Burns, K., and Tschopp, J. (2002) The inflammasome: a molecular platform triggering activation of inflammatory caspases and processing of proIL-beta. Mol. Cell 10, 417–426

232. Wieckowski MR, Giorgi C, Lebiedzinska M, Duszynski J, Pinton P. (2009) Isolation of mitochondria-associated membranes and mitochondria from animal tissues and cells. Nat Protoc. 1582-90.

233. Bartlett R., Stokes L., Sluyter R. (2014). The P2X7 receptor channel: recent developments and the use of P2X7 antagonists in models of disease. Pharmacol. Rev. 66, 638–675.

234. Murphy, M. P. (2009). How mitochondria produce reactive oxygen species. Biochem. J. 417, 1-13.

235. Hurd T.R., DeGennaro M., Lehmann R. Redox regulation of cell migration and adhesion. Trends Cell Biol. 2012;22:107–115

236. Heerdt BG, Houston MA, Augenlicht LH (2006) Growth properties of colonic tumor cells are a function of the intrinsic mitochondrial membrane potential. Cancer Res 66: 1591–1596.